Concawe
Environmental Science
for European Refining

Report

Report no. 13/20

Detailed Evaluation of Natural Source Zone Depletion at a Paved Former Petrol Station

ISBN 978-2-87567-125-7

Detailed Evaluation of Natural Source Zone Depletion at a Paved Former Petrol Station

B. Scholtissek (Concawe Science Executive)

This report was prepared by:

B. Beuthe (Concawe STF-33)
L. Barreales (BP Remediation Management)
M. Marti (AECOM)
A. Sayas (AECOM)
J. Smith (AECOM)

Under the supervision of:

B. Scholtissek (Concawe Science Executive)

At the request of:

Concawe Special Task Force on Soil and Groundwater (STF-33)

Brussels
July 2020

ABSTRACT

This report presents the results of an investigation that was carried out to demonstrate Natural Source Zone Depletion (NSZD) occurred under a paved site and compare various monitoring measurement methods in that context. The site is considered typical of many services stations in Europe, as a paved surface is present and extends beyond the boundaries of the site. Below the pavement and surface fill, native unconsolidated material comprising pebbles and gravels in a fine sand to clayey matrix extends down to a perched water table at 8 - 12 m depth. Two plumes exist at the site; a dissolved phase gasoline plume and a diesel light non-aqueous phase liquid (LNAPL) plume, both extending in a south-easterly direction.

Three well-documented monitoring methods were utilized to assess NSZD at the site:

- CO_2 Traps, which involve measurement of CO_2 efflux from the soil at ground surface;
- The soil gas concentration gradient method, based on measurement of subsurface O_2 and CO_2 concentration profiles; and
- The biogenic heat method based on subsurface temperature measurements.

The use of multiple monitoring measurement methods provided insights into the conceptual site model and allowed for identification of site-specific interferences between some of the measurements. Complex soil gas concentration profiles and near-surface CO_2 contributions in some areas of the site presented data interpretation challenges. However, all data indicate ongoing biodegradation near the interface of LNAPL and water table.

KEYWORDS

Paved sites, NSZD Natural Source Zone Depletion, LNAPL, soil gas, NAPL, remediation, petrol site, CO_2 flux, subsurface temperature, biodegradation

INTERNET

This report is available as an Adobe pdf file on the Concawe website (www.concawe.org).

CONTENTS

SUMMARY

Background

Natural Source Zone Depletion (NSZD) is a concept that is used to describe the degradation processes of a Light Non-Aqueous Phase Liquid (LNAPL) contamination in the subsurface (ITRC 2009). NSZD quantifies the LNAPL degradation processes as an additional tool in the management and remediation of contaminated sites. Sometimes, NSZD can constitute the remedy itself. NSZD characterization has been subject to a theoretical and practical development in recent years. Several institutions have published guidance and information regarding NSZD in different parts of the world (ITRC 2009; API 2017; CRC CARE 2018; CL:AIRE 2019).

While the concept of natural attenuation of dissolved hydrocarbons in groundwater was well-documented by the early 1990s (NRC 1993; Rice et al. 1995), there was a common perception that natural attenuation did not significantly influence the LNAPL in source zones (Lyman et al, 1992; Newell et al., 1995). However, recent studies have demonstrated the importance of biodegradation within petroleum-affected sites, indicating that microorganisms not only survive, but thrive in LNAPL source areas.

Research on NSZD rates at petroleum LNAPL sites (e.g., Johnson et al., 2006; Garg et al., 2017) has demonstrated that the rate of natural depletion is often on the order of thousands to tens of thousands of litres of LNAPL per hectare, per year. The observation of natural depletion rates of this magnitude has elevated the role of NSZD in LNAPL conceptual site model (LCSM) development and site management decision making. At sites where LNAPL-related impacts are stable and potential receptors are not at risk, a compelling case can be made against continuing or implementing active remediation on the grounds of sustainability. NSZD measurements can also be used to improve our understanding of LNAPL distribution and stability (Mahler et al., 2012; Lundy 2014) and as a baseline for evaluating the relative benefit of active remediation (ITRC 2009, 2018).

Objectives

This report presents the results of an investigation that was carried out to assess NSZD rates at a paved petrol station (retail site / service station) and compare various monitoring measurement methods in that context. This work addresses two of the data gaps identified in the CL:AIRE (2019) technical bulletin which are:

1. assesses how pavement may limit downward vertical diffusion of oxygen and the influence on NSZD rates at paved sites
2. comparison of different monitoring methods.

Site Details and Methods

The site is considered typical of many services stations in Europe, as a paved surface is present and extends beyond the boundaries of the site. Below the pavement and surface fill, native unconsolidated material comprising pebbles and gravels in a fine sand to clayey matrix extends down to a perched water table at 8 - 12 m depth. Two plumes exist at the site; a dissolved phase gasoline plume and a diesel LNAPL plume.

Three well-documented methods were utilized to assess NSZD at the site:

- Measurement of CO_2 efflux from the soil at ground surface during two periods (October 2017 and April 2018) using CO_2 traps designed for application at sites with impervious ground cover conditions;
- Quarterly measurements of subsurface O_2 and CO_2 concentration profiles from soil gas probes and existing monitoring wells screened within the vadose zone to estimate NSZD rates using the soil gas concentration gradient method; and
- Quarterly subsurface temperature measurements (15 wells) and continuous subsurface temperature measurements in 3 wells to support analysis using the biogenic heat method.

The assessment included measurements for each method in background areas as well as in the gasoline and diesel source areas. The use of multiple measurement methods provided insights into the conceptual site model and allowed for identification of site-specific interferences for some of the measurements.

Results

Complex soil gas concentration profiles in soil gas probes indicated that lateral soil gas transport was occurring beneath the pavement (**Figure A**). This assumption was further supported by the observation of relatively high CO_2 efflux in an upgradient, background area located approximately 15 meters from an area where shallow impacts were identified.

Figure A. Comparison of soil gas composition profiles for simple, 1-dimensional gas diffusion (left) to study site conditions (right)

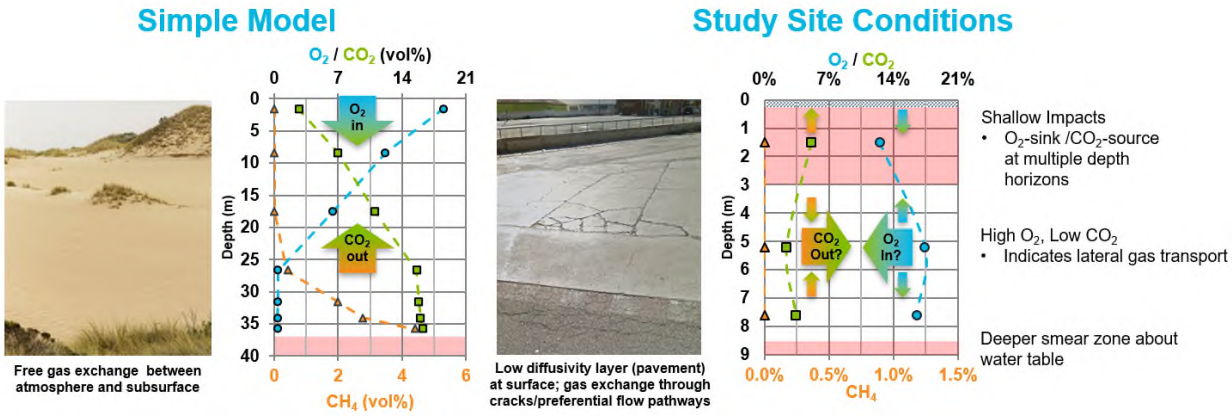

Average NSZD rates by monitoring method are presented in **Table A**, below. Key results from the study indicate:

- Pavement does not impede the flow of oxygen into the subsurface to a degree where it limits NSZD from occurring:
  - Rate estimates vary, but results obtained from monitoring methods that include subsurface measurements closer to the LNAPL and water table are relatively consistent.
  - Surface monitoring methods may underestimate NSZD and are applicable only when gas transport is predominantly vertical

- Monitoring wells are suitable for soil gas and temperature profiling measurements
  - Measurements in monitoring wells provide flexibility/adaptability to adjust and optimize depth intervals and data density depending on site conditions.
  - Fixed-depth readings from dedicated soil gas probes may miss the biodegradation zone and yield NSZD rates that are biased low.
- Soil gas concentration gradients document biodegradation and may help to identify intervals where gas transport is dominated by one-dimensional diffusion.
- Temperature gradients for NSZD calculation should be focused near the biodegradation zone.
  - Quarterly profiles or annual monitoring results yielded equivalent gradients
  - Empirical determination of thermal conductivity provides more accurate NSZD estimates

Table A. Average NSZD Results by Monitoring Measurement Method

NSZD Monitoring Measurement Method	Gasoline Area (L/ha/yr)	Diesel Area (L/ha/yr)
Gradient Method - Soil gas probes: quarterly O_2 & CO_2 profiles	**260**	**930**
Gradient Method - Monitoring wells: quarterly O_2 & CO_2 profiles	**1,100**	**1,100**
Biogenic Heat Method: quarterly manual temperature data collection	**2,500**	**2,700**
Biogenic Heat Method: continuous temperature data using loggers	**3,000**	**3,200**
CO_2 traps: Deployed October 2017 and April 2018	**54,000**	**460**

Notes:
O_2 Oxygen
CO_2 Carbon Dioxide
L/ha/yr Litres per hectare per year

1. INTRODUCTION

1.1. BACKGROUND

'Natural source zone depletion' (NSZD) describes the naturally occurring processes that collectively result in the depletion of chemical contaminant mass from a Light Non-Aqueous Phase Liquid (LNAPL) source zone (ITRC 2018). These processes include physical mass transfer by dissolution and vaporization of chemical constituents to the aqueous (groundwater) and gaseous (soil gas) phases, and biodegradation of LNAPL constituents by microorganisms. Research has been ongoing to assess NSZD in various settings and quantify its rate.

Biodegradation of LNAPL constituents can occur through a number of microbially-facilitated reactions, depending on the availability of terminal electron acceptors (TEAs) such as oxygen, nitrate, manganese and iron oxides, and sulfate. Within LNAPL source zones, where hydrocarbon concentrations and electron acceptor demand is high, the above TEAs are depleted and methanogenesis often becomes the dominant degradation pathway (Garg et al., 2017). During each of these 33biodegradation reactions, essentially all of the carbon present in LNAPL is converted to carbon dioxide and methane, which partition into the gas phase and migrate upward into the vadose zone.

In the vadose zone, LNAPL constituents may volatilize and redistribute into soil gas along with methane and carbon dioxide generated through biodegradation. As these gases migrate upward in the soil column through diffusive or advective transport processes and come into contact with higher concentrations of atmospheric oxygen, methane and volatilized LNAPL constituents are aerobically degraded, and carbon transfer is dominated by the flux of carbon dioxide from the subsurface to atmosphere (Sihota et al., 2011; McCoy et al., 2014).

The increased focus on NSZD in recent years has led to the development of guidance on data collection and interpretation approaches by several institutions around the world (ITRC 2009; ITRC 2018; API 2017; CRC CARE 2018; CL:AIRE 2019). The prevailing methods for quantifying NSZD rates rely on mass and/or energy balance approaches by measuring the flux of electron acceptors (e.g., oxygen) into the source zone (Johnson et al., 2006), and/or measuring the flux of petroleum degradation products such as carbon dioxide (Sihota et al., 2011; McCoy et al., 2014) or excess heat (Sweeney and Ririe, 2014; Warren and Bekins, 2015) out of the LNAPL source zone. Alternative approaches for estimating NSZD rates based on changes in the composition of the remaining LNAPL over time have also been described recently (Lundy, 2014; Devaull and Rhodes, 2018; CRC CARE 2018).

1.2. OBJECTIVES

NSZD is increasingly being recognized as an important process that influences LNAPL thickness and composition. However, its application across Europe is still limited. The 2019 CL:AIRE NSZD technical bulletin provided a comprehensive overview of the state of science regarding NSZD and also identified research needs to more fully develop our understanding of NSZD and its potential relevance to LNAPL site management. The current work aims to address the knowledge gaps identified by CL:AIRE (2019) which resulted in the following objectives:

- Provide a side-by-side comparison of different NSZD measurement methods at real sites with varying geological complexity that will help site owners to select the best method for their site.

- Assess the influence of short-term variability due to seasonal changes in soil moisture and temperature on NSZD rates to provide guidelines on how to deploy the NSZD measurement methods.
- Assess the influence of impervious ground cover, that may restrict vertical gas movement at the surface, on NSZD rates.

2. METHODS

2.1. SITE DESCRIPTION

This site was formerly occupied by a Petrol Station built in 1966 and decommissioned in 2009. The above-ground equipment and buildings were removed as part of decommissioning. The underground infrastructure was left in place, but filled with solid foam (piping) and grout (tanks).

The Petrol Station stored fuel in nine underground tanks of 20,000 liters each. The entire surface of the site is paved. The pavement is currently in poor condition with a large number of holes and cracks.

In addition, it should be noted that the Petrol Station formerly used a groundwater well to supply a car washing operation located adjacent to the eastern border of the site. The well is not accessible (it was paved over) and the current status of the well is unknown.

Figure 1. Former petrol station structures.

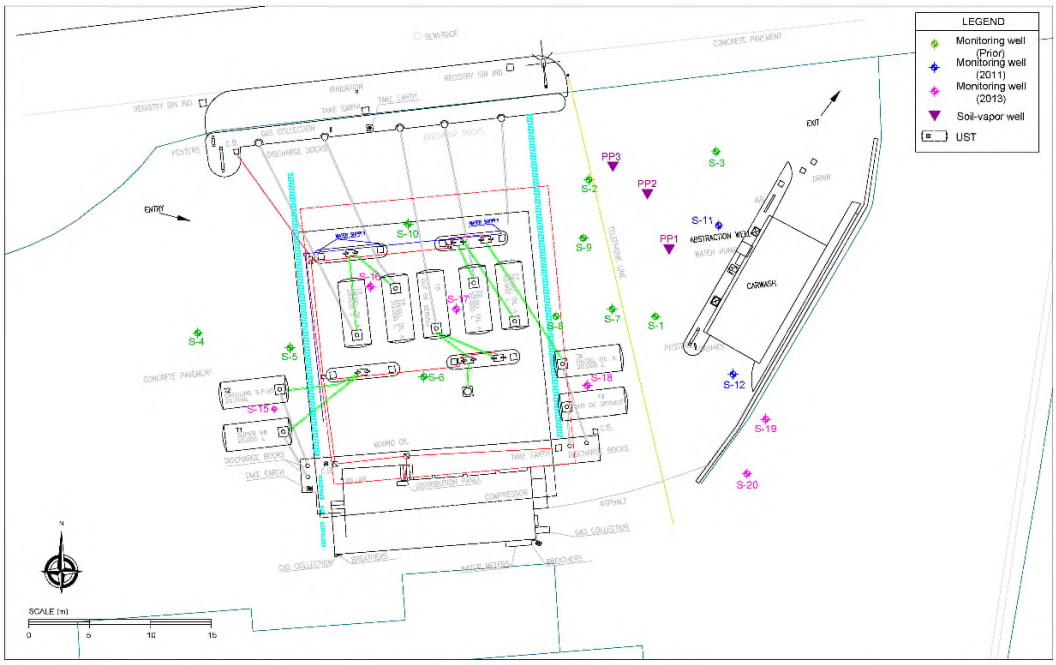

2.2. NSZD SCOPE OF WORK

Three NSZD measurement techniques were applied at the site:

- The gradient method (Davis et al., 2009; Johnson et al., 2006), based on measurement of O_2 and CO_2 concentration profiles in either:
  - Designated multilevel soil-vapour probes, or;
  - Monitoring wells using methods described by Sweeney and Ririe (2017).
- The thermal approach (Mohr and Merz, 1995; Subramanian et al., 2011; Ririe et al., 2013; Sweeney and Ririe, 2014; Warren and Bekins, 2015; Askarani et al., 2018), that quantifies NSZD rates based on heat generation in the source

zone related to biodegradation of petroleum hydrocarbons. The methodology regarding this approach can be applied using either:

  - One-time manual temperature measurements registered using a thermistor, or;
  - Continuous and automatic temperature measurements using data logger sensors.

- Passive CO_2 flux traps (Zimbron et al., 2011; McCoy et al., 2014) that capture CO_2 generated by microbial degradation of petroleum hydrocarbons as the CO_2 is discharged from the subsurface to the atmosphere.

The completed site work included:

- Advancing soil borings, which were used to both support the NSZD study and to collect complementary data to refine the conceptual site model.
- Two annual groundwater sampling events; the first event established baseline conditions in the aquifer and the second event assessed conditions at the end of the study period.
- Five quarterly O_2 and CO_2 soil gas monitoring rounds to assess seasonal variability in biodegradation rates at the site over a one-year period (one initial monitoring round and four additional quarterly rounds.
- Continuous subsurface temperature monitoring with temperature data loggers during a one-year period and five rounds of quarterly manual monitoring.
- A carbon-14 (^{14}C) isotope study to develop a baseline prior to deploying CO_2 efflux traps.
- Deployment of CO_2 efflux traps in September/October 2017 and April/May 2018.

These works are detailed in the following sections.

2.3. INSTALLATION OF NEW MONITORING DEVICES

Implementation of the NSZD monitoring plan included advancement of soil borings, construction of seven monitoring wells (S21, T1A, T1B, T1C, T2A, T2B, T2C), installation of five multi-level soil gas probes (SV1 to SV5), and installation of five CO_2 efflux trap vaults (C1 to C5) equipped with sub-slab vents designed to limit preferential (chimney) flow. The locations of soil gas probes, monitoring wells, and CO_2 efflux traps are shown on **Figure 2**.

Figure 2. Updated site map.

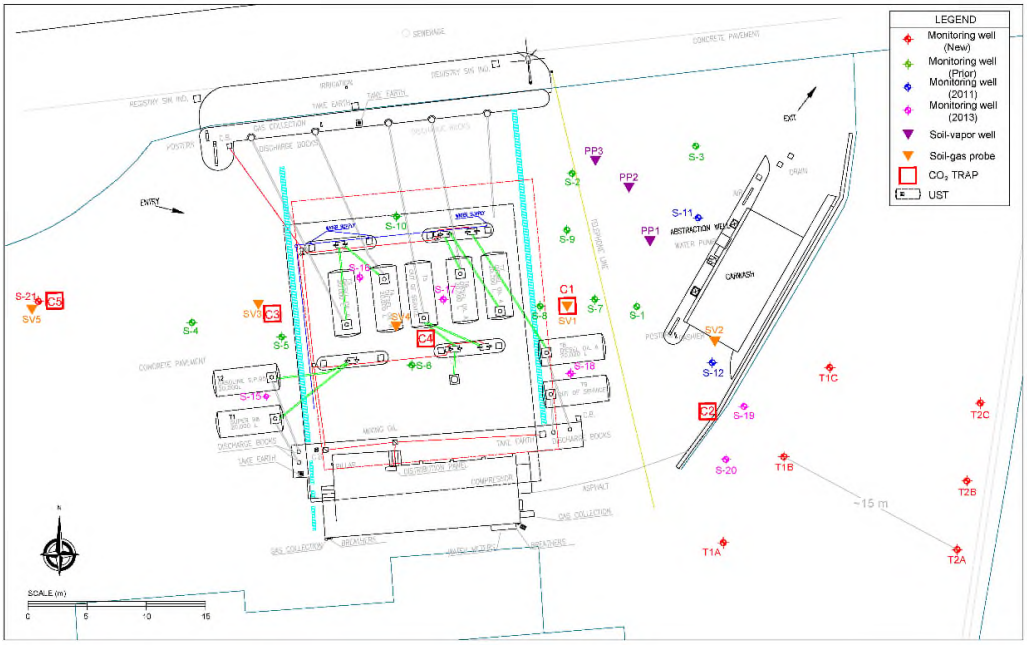

Advancement of soil borings and construction of monitoring wells and soil vapour probes were completed between June the 6th and the 27th of 2017. These activities were performed by the subcontractors Geotecnia e Ingeniería del Terreno S.L. and Testi Control System S.L. under AECOM´s supervision.

In October 2017, a borehole was drilled to reinstall a soil vapour probe (SV1 bis) in replacement of the existing probe SV1. SV1 was damaged by a heavy vehicle and was no longer operative. The drilling works were performed by the subcontractor *Perforaciones y Sondeos Jaren S.L.* under AECOM´s supervision.

13 soil borings (SV1 to SV5, S21, T1A, T1B, T1C, T2A, T2B and T2C) were completed at the site. The soil boring depth ranged from 7.7 to 16.4 m below ground surface (bgs). The installation of each borehole was determined on the basis of the monitoring objective and location within the site.

Table 1 below, shows the exact depth and other installation details of the new monitoring devices. The boring logs and well construction details are included in **Annex C**. Photographs of the soil cores are presented in **Annex D**.

Table 1. 2017 Soil boring and installation details.

Location ID	Type	Total borehole depth (m)	Installed piezometers			Soil probes		
			Total well depth (m)	Plain section (m)	Screened section (m)	Upper probe depth (m)	Middle probe depth (m)	Bottom probe depth (m)
SV1	Soil gas probe	10.9	-	-	-	1.2	5.2	8.2
SV1 bis		8.5	-	-	-	1.2	5.2	8.2
SV2		10.7	-	-	-	1.2	5.2	10.0
SV3		9.5	-	-	-	1.2	4.8	6.8
SV4		7.7	-	-	-	1.5	5.2	7.6
SV5		8.2	-	-	-	1.2	5.0	8.0
S21	Monitoring well	10.6	10.5	0 - 5.0	5.0 - 10.5	-	-	-
T1A		16.0	15.7	0 - 5.5	5.5 - 15.7	-	-	-
T1B		16.2	16.0	0 - 6.0	6.0 - 16.0	-	-	-
T1C		16.3	16.2	0 - 6.0	6.0 - 16.2	-	-	-
T2A		16.3	16.2	0 - 5.6	5.6 - 16.2	-	-	-
T2B		16.3	16.2	0 - 5.0	5.0 - 16.2	-	-	-
T2C		16.4	16.3	0 - 5.0	5.0 - 16.3	-	-	-

Rotary drilling was used with a diameter of 79 to 101 mm. No fluids were used during borehole drilling except tap water during asphalt cover removal. Temporary casing was used to avoid borehole collapse while drilling in unsaturated soil strata with little geologic strength or while drilling in the saturated zone.

Soil samples were collected at regular depths (every 0,5 – 1m) in order to evaluate soil contamination by means of *Head-Space* tests. Soil samples for further laboratory analysis were selected based on these data (see attached procedure "Soil sampling", **Annex F**).

An AECOM expert supervised the bore drilling and recorded the description of the extracted materials in a lithologic log, which is presented in **Annex C**.

2.3.1. Installation of new monitoring wells

Transects

A series of new wells was arranged in two transects. The intent of establishing transects was to observe mass flux and contaminant migration at the South East end of the site (downgradient), that will be later used to assess the following:

- The spatial change in petroleum hydrocarbon discharge along the direction of groundwater flow.
- The temporal change in petroleum hydrocarbon discharge from the source zone.

Thus, boreholes T1A, T1B, T1C, T2A, T2B and T2C were located along two lines perpendicular to the groundwater flow direction and spaced 15 meters apart from one another (see **Figure 2** and **Figure 1** in **Annex A**).

These monitoring wells were installed with 2''-diameter PVC risers and were screened using 10-slot PVC screen from the base of the permeable deposits to approximately 16 m bgs. The annular space was filled with a silica gravel pack and a bentonite seal. The wellheads were completed with traffic-rated watertight metal protective caps at ground surface.

The new monitoring wells were drilled down to 16 meters depth in the eastern part of the site, leaving the water table at least 3 meters above the borehole bottom.

Background well

A background well was installed to provide baseline data for assessing NSZD. The background well, S21, was drilled approximately 15 meters to the West of S4, on the Western limit of the former petrol station, which is far from the influence of the site source area.

2.3.2. Installation of soil vapour probes

Multi-level soil vapour probes (SVPs) were constructed in five soil borings, SV1 to SV5, to measure petroleum hydrocarbon concentrations and O_2, CO_2 and CH_4 content in soil gas.

Three soil vapour sampling points were installed in each SVP location. The elevations of the sampling points were selected for each location depending on the water table elevation and sub-surface structures at each location, as shown in **Table 1**.

The intent of including these SVPs in the monitoring program was to characterize the vertical profile of the hydrocarbons and other compounds (O_2, CO_2 and CH_4) that will be used to assess biodegradation processes (volatilization and biodegradation).

Figure 3. Scheme of measurements to evaluate NSZD (Johnson et al., 2006; ITRC, 2009).

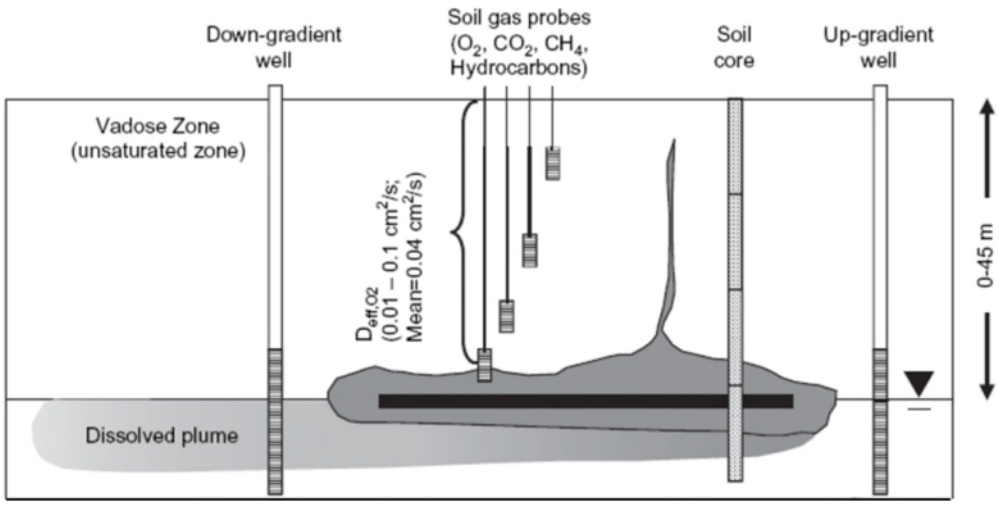

Five locations for the SVPs were chosen, both in the source zones and the new background area, placed close to existing monitoring wells for comparison purposes:

- SV-1 and SV-2 located in the Eastern zone (where diesel impacts are present), next to S7 and S12, respectively.

- SV-3 and SV-4 located in the central area of the site, adjacent to wells S-5 and S-6, respectively, where the gasoline impacts were identified. SV-4 was drilled within the containment structure of the underground storage tanks.
- SV-5 in a non-impacted area, next to S21, which was considered a background location (see point 3.1.1.).

The installation of the SVPs followed the procedure shown in **Figure 4**:

- At the end of the probe, a stainless-steel vapour inlet shaft was installed, protected by a geo-textile to minimize dust or humidity entering the probe.
- Each probe was connected to the surface with Teflon tubing.
- The filter pack material had a thickness of 15 to 20 cm, comprised of gravel to allow unrestricted gas flow through the filter pack.
- A layer of sand (10 cm) was emplaced above the gravel filter pack to prevent contact between the gravel and the bentonite slurry used to seal the wells.
- Above the sand, a bentonite seal was placed between the probes to vertically isolate the probes and seal the annulus.

Figure 4. Scheme of soil vapour probes and monitoring points to evaluate NSZD.

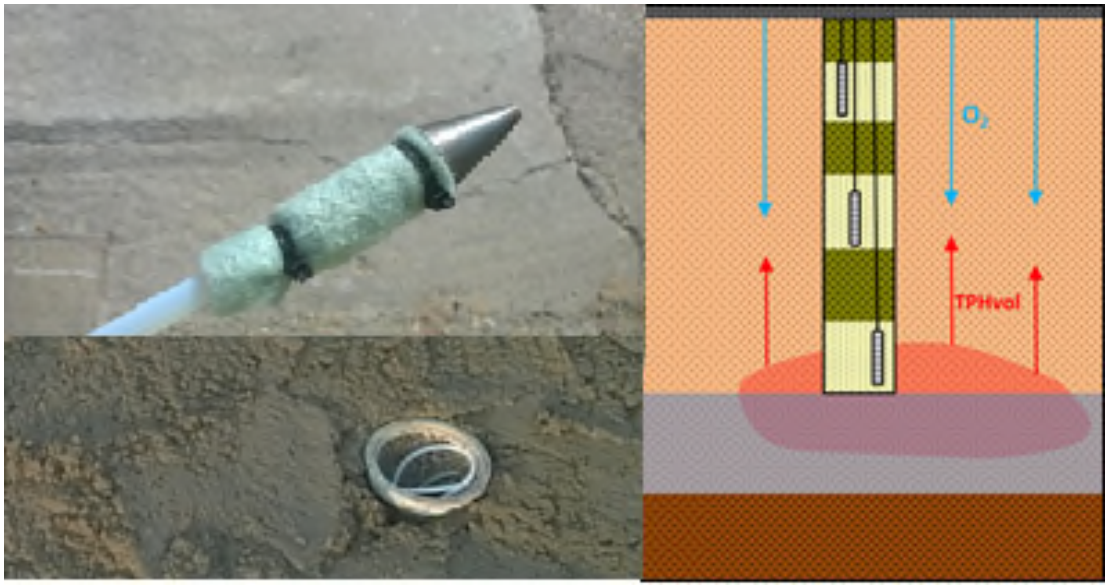

Table 2 shows specific information regarding the location of the multilevel SVPs.

Table 2. Soil vapour probe installation details

Location ID	Site source zone	Reference MW	Lithology		
			Upper probe	Middle probe	Bottom probe
SV1	Diesel	S7	Silt	Gravels-sand	Gravels-sand
SV1 bis		S7	Silt	Gravel (sand matrix)	Gravel (sand matrix)
SV2		S12	Silt	Gravels (sand matrix)	Gravels (semi-lithified)
SV3	Gasoline	S5	Gravels (silt matrix)	Gravel (sand matrix)	Gravel (sand matrix)
SV4		S6	tank filling	Gravel (sand matrix)	Gravel (semi-lithified)
SV5	Background	S21	Gravels (sand/silt matrix)	Gravels (sand/silt matrix)	Gravel (semi-lithified)

Further installation details and specifications are shown in **Annex C**.

2.3.3. Installation of CO_2 traps

Five CO_2 traps were installed at the site next to the SVPs and piezometers to complement the soil gas NSZD data (see Figure 2 and Figure 1 in **Annex A**).

CO_2 traps were supplied by E-FLUX, the inventors of the CO_2 trap method for NSZD rate measurement. AECOM worked with E-FLUX to develop an installation method specific for this site. A common problem for CO_2 flux measurement at sites that are covered by pavement is that the puncture in the pavement for trap installation becomes a preferential path for gas migration out of the subsurface because the trap has a higher pneumatic conductivity and gas diffusivity than the pavement. This method developed by E-FLUX prevents the stack (chimney) effect in the CO_2 flux by installing the traps inside a vault and connecting the top of the traps to the soil under the concrete with a vapour pin to equalize pressure conditions. The creation of a closed system ensures that the trap is exposed to natural gas flux and does not become a pathway for advective flow of gas into or out of the subsurface. **Figure 5** shows the installation scheme of CO_2 traps.

Figure 5. CO_2 trap installation scheme.

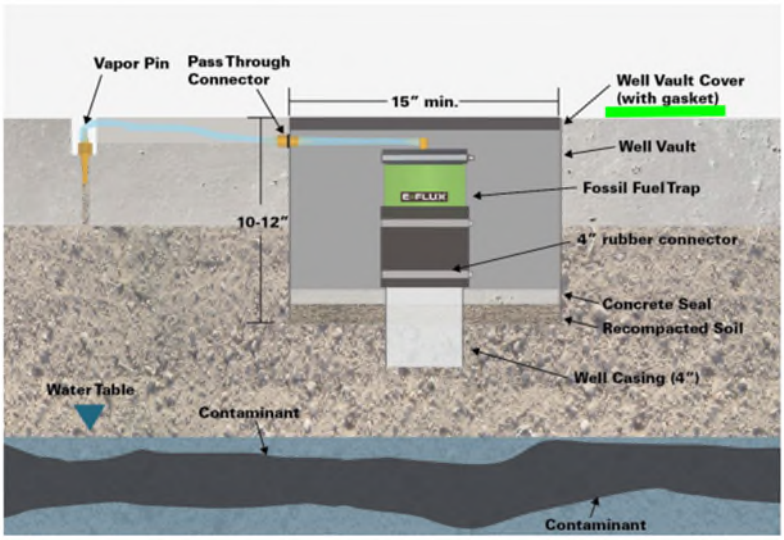

Five pits were excavated in order to install vaults to protect the CO_2 traps from atmospheric conditions and heavy load traffic. Each pit, of approximately 1 m^2 of surface area and a depth of 0.8 m, was dug to fit inside a concrete manhole well vault (see **Figure 6**). The bottom of the well vault was covered with a concrete seal, leaving a 4" PVC well casing installed several centimeters into the natural soil (receiver pipe). The manhole was covered with a screened metallic lid to protect traps from any tampering, since the area is open to the public and heavy vehicles.

A flexible pipe was installed from the inside to the outside of the manhole to connect the CO_2 trap with soil beneath the site pavement. To complete this connection, the pipe was brought through by cutting the pavement and drilling a 16-mm vertical hole across the concrete pavement and into the natural soil where the vapour pin was installed. The pavement cut line was sealed afterwards with flexible cement. Finally, the whole installation was covered with metallic plates during 14 days to protect them from heavy load traffic until the concrete had dried and hardened.

Figure 6. CO_2 traps pre-installation.

2.3.4. Topographical survey

After the installation of the new monitoring devices, the location coordinates and elevation of every existing monitoring point were surveyed using precise GPS equipment and a total station.

The topographic survey was conducted by the subcontractor *David Goñi Topografía S.L.* under AECOM´s supervision.

The location (UTM ETRS89 co-ordinates) of all the monitoring points included in the survey are shown in **Table I** of **Annex B**.

2.4. FIELD DATA COLLECTION

2.4.1. Soil characterization

During the soil boring campaign, several samples were collected at different depths in order to support four different characterization efforts:

- General characterization of soil impact - contaminants of concern (CoCs) related to the identified gasoline and diesel impacts. The increased monitoring network to the southeast has allowed for a wider understanding of the impact extension.
- Detailed hydrocarbon profile analysis - conducted to acquire a more accurate understanding of the vertical hydrocarbon distribution in the source areas within the most impacted horizon (smear zone and upper saturated zone).
- Effective gas diffusivity related parameters - samples were selected with the objective of determining site-specific soil parameters related to vapour transport in the vadose zone.
- ^{14}C isotope content - soil samples were collected in the background and source areas to evaluate the feasibility of utilizing ^{14}C-corrected CO_2 traps for estimating biodegradation rates at this particular site.

Table 3 summarizes the soil samples collected, their depths and purpose of analysis.

Table 3. Soil samples collected during June 2017 soil boring campaign.

Location ID	General impact characterization		HC soil detailed characterization		^{14}C dating study	Effective diffusivity related parameters
	CoCs - Shallow (depth ≤ 1,5 m)	CoCs (depth > 1,5 m)	Undisturbed sample (Geochem)	Discretized sample (Analytico)	Undisturbed sample (University of Groningen)	Undisturbed sample (CEPASA)
SV1	C1 (1.5)	SV1 (2.2)	SV1 (9.1-9.7)	-	SV1 (8.2)	fail
		SV1 (5)	SV1 (9.7-10.3)	-	-	-
		SV1 (8.7)	SV1 (10.3-10.9)	-		SV1 (6.8-7.4)
SV1 bis	SV1bis(1.5)		-	-	-	-
SV2	C2 (1.5)	SV2 (10.0)	-	-	-	-
		SV2 (10.5)				
SV3	C3 (1.5)	SV3 (2.0)	-	SV3 (8.1-8.25)	SV3 (6.8)	SV3 (2.2-2.6)
			-	SV3 (8.25-8.45)		SV3 (4.9-5.3)
		SV3 (4.8)	-	SV3 (8.5-8.7)		-
				SV3 (8.9-9.1)		
		SV3 (6.8)		SV3 (9.1-9.3)		
				SV3 (9.3-9.5)		
SV4	C4 (1.5)	SV4 (3.5)	-	-	-	-
		SV4 (5.2)	-	-		-
		SV4 (7.5)	-	-		-
SV5	C5 (1.5)		-	-	SV5 (8.0)	-
S21	-	S21 (8.9)	-	-	-	-
T1A	-	T1A (8.9)	-	-	-	-
		T1A (12.5)	-	-	-	-
		T1A (13.0)	-	-	-	-
T1B	-	T1B (12.0)	-	-	-	-
T1C	-	T1C (10.5)	-	-	-	-
T2A	-	T2A (13.0)	-	-	-	-
T2B	-	T2B (13.4)	-	-	-	-
T2C	-	T2C (12.0)	-	-	-	-

General characterization of soil impact

Samples were collected from each of the new boreholes in order to achieve a better understanding of the petroleum hydrocarbon impacts throughout the site.

The soil samples were collected at different depths and lithological units taking into consideration organoleptic observations (odor, color) and headspace PID readings (VOCs). **Table 3** shows the totality of the 26 samples collected from Vadose Zone in the new boreholes and excavated pits.

The analytical program included TPH C_6-C_{16}, BTEX, PAHs, MTBE and ETBE. All analysis were carried out at Eurofins Analytico facilities in Barneveld (The Netherlands).

Detailed hydrocarbon profile analysis

A detailed understanding of vertical hydrocarbon distribution in the subsurface is considered to be a key aspect for NZSD assessment[1]. Therefore, collection of a series of continuous undisturbed samples at both source areas was included in the drilling campaign to assess the distribution and composition of the LNAPL in the vadose zone.

The undisturbed cores were planned to be collected in one borehole per source area (SV1 – diesel zone and SV3 – gasoline zone), using a SPT device[2] mounted over the drilling rig, at the depths where hydrocarbon impacts were identified during previous investigation campaigns. A PVC pipe was installed inside the rig and introduced by percussion, which drove soil inside the pipe.

Figure 7. Detailed hydrocarbon sampling.

The undisturbed sample lengths varied from 10 to 60 cm. Due to the presence of coarse-grained lithology, complete soil cores were difficult to recover from the target locations.

A 1,5-meter length of undisturbed soil core was successfully collected from borehole SV1. After collection the sealed, undisturbed cores from SV1 (see **Figure 7**) were flash frozen using dry ice in order to prevent changes to the hydrocarbon distribution within the cores during shipping to the laboratory (**Figure 8**).

Upon arrival at the laboratory (*CE Geochem*, United Kingdom), frozen samples were split in several 10 cm long subsamples for hydrocarbon analyses.

[1] ITRC (2009)

[2] Standard test method for Standard Penetration Test

Figure 8. Preservation using dry ice and shipping of the undisturbed soil cores.

Continuous undisturbed soil cores could not be retrieved from borehole SV3. Six consecutive disturbed soil samples were collected in place of the undisturbed cores to resemble a continuous profile from 8 to 9.5 m below grade. These samples were analyzed at Eurofins Analytico facilities in Hoogvliet (The Netherlands).

The analytical scope for all samples was TPH C_6-C_{40} Aliphatic/Aromatic split, BTEX, and PAHs.

Table 3 shows the specific sampled depths (see *HC soil detailed characterization* section of the table), which slightly deviated from the initial scope due to the aforementioned drilling difficulties.

Effective diffusivity related parameters

Soil properties are an essential factor in soil gas transport processes. Therefore, in order to determine the hydrocarbon biodegradation rate using vapour concentration profiles, geotechnical properties of the soil were determined from undisturbed soil samples.

Following the same methodology as described in the detailed soil characterization section above, cores were collected from SV1 and SV3 boreholes at depths shown in **Table 4.**

Table 4. Undisturbed samples for soil parameters vs. lithology.

Effective diffusivity related parameters		
Location ID	**Undisturbed sample (CEPASA)**	**Lithology**
SV1	Fail	-
	SV1(6.8-7.4)	Gravels in sand matrix
SV3	SV3(2.2-2.6)	Sand and gravels
	SV3(4.9-5.3)	Gravels in sand matrix

The soil samples were sent to the Spanish laboratory *CEPASA Ensayos Geotécnicos* to determine grain size, bulk density, porosity, and, moisture content. Based on these measurements the vapour and total porosities needed to calculate the effective diffusivity of the soil were obtained.

Supplemental 14C isotope study

Carbon-14 (^{14}C) isotope analysis allows for classification of carbon sources based on the fact that living organisms actively exchange carbon with the atmosphere. ^{14}C is naturally produced through interactions between cosmic neutrons and nitrogen atoms in the upper atmosphere, and is subsequently oxidized to radioactive carbon dioxide ($^{14}CO_2$) and assimilated into living organisms. When organisms cease to live, they no longer exchange carbon with the atmosphere, and the ^{14}C content in the remaining biomass decays with a half-life of approximately 5,730 (±40) years (Aelion et al., 2010). Given the relatively short half-life of ^{14}C, the proportion of ^{14}C isotopes in carbon dioxide evolved from biological degradation of petroleum hydrocarbons is negligible (non-detect). By contrast, the ^{14}C content of carbon dioxide produced through degradation of naturally occurring organic matter in near surface environments where organic matter has more recently been in equilibrium with the atmosphere will reflect the mean age of the organic material being degraded.

Based on BP Remediation previous experience, unexpectedly high rates of NSZD have been obtained from CO_2 efflux traps set in background locations. At these sites, the NSZD rates were calculated from ^{14}C concentrations using a two end-member mixing model, assuming that all CO_2 captured by the traps represents a combination of petroleum hydrocarbon degradation and degradation of organic matter that has recently been in equilibrium with the atmosphere. The assumption that all carbon sources other than petroleum hydrocarbons contain ^{14}C concentrations near modern atmospheric levels will over-predict the percentage of petroleum-derived CO_2 for sites with buried organic materials of sufficient age to have a lost a significant fraction of ^{14}C isotopes (Lundegard et al., 2000).

Thus, to further differentiate between carbon dioxide generated through biological degradation of naturally occurring soil organic matter and degradation of LNAPL constituents, concentrations of ^{14}C and carbon-13 (^{13}C) isotopes in soil-gas CO_2, soil, and LNAPL were collected at the site. Concentrations of both isotopes in soil-gas CO_2 can be compared to the composition of potential source materials to evaluate provenance of the carbon dioxide.

Undisturbed soil samples were collected using a SPT device from the most impacted horizon at both source areas, i.e. the smear zone, to assess the content of modern carbon associated with combustible fuel additives and / or natural organic carbon.

Additionally, a sample was taken from the same horizon in the background location, which was assumed to be a non-impacted area, for comparison purposes.

The specific depths at which samples were collected are included in **Table 3**. These samples were sent to the *Centre for Isotope Research of the University of Groningen* for ^{14}C dating analysis.

2.4.2. Groundwater baseline and monitoring program

Groundwater baseline

Once the new piezometers were developed and purged, groundwater samples were collected from all the available piezometers in the site. The aim of this initial campaign was to establish a groundwater quality baseline as a reference for further monitoring campaigns.

Prior to groundwater sample collection, water table depth and in-well NAPL thicknesses, if present, were measured in all available piezometers using an interface probe. Piezometers where NAPL phase was detected were not sampled, except for monitoring well S7, which was sampled as part of the ^{14}C isotope study conducted at the site.

Groundwater samples were collected by using a peristaltic pump or bailer, purging groundwater until pH and conductivity stabilized. At this point, appropriate bottles were filled and labeled and placed on ice until reception at the laboratory.

All non-disposable equipment that came in contact with groundwater was decontaminated between each sampling location.

The analytical program for groundwater comprised:

- TPH C_6-C_{16}, BTEX, ETBE, MTBE and PAHs (collectively referred to as CoCs).

  CoCs were determined in all collected samples. These samples were analyzed by Eurofins Analytico Laboratories, in Barneveld (The Netherlands).

- MNA parameters (Sulphate, Nitrate, Methane, Total Alkalinity, Iron II, Manganese II)

  MNA parameters were analyzed in the backgrounds (S21 and S11), the diesel source zone (S9 and S20) and the downgradient transects (T1B and T2B). This configuration was initially assumed to reproduce aquifer conditions along the groundwater flux direction.

  These samples were analyzed in Exova – Jones Environmental Laboratories, in the United Kingdom.

- Detergents (anionic, cationic, non-ionic).

  Detergents were identified in the past in monitoring well S12, close to the former car wash. The potential current presence of detergents could affect the results of the conducted studies concerning carbon dating. Thus, anionic, cationic and non-ionic detergent content in S12 was updated at Agrolab Al-West laboratories, in Deventer (The Netherlands).

The performed analytical program for 19 piezometers sampled is summarized in **Table 5**.

Table 5. Groundwater analytical program -Baseline.

Location ID	GW			Free Phase
	COCs	MNA	Detergents	^{14}C
S1				
S2				
S3	X			
S4				
S5	X			
S6	X			
S7				X
S8				
S9		X		
S10	X			
S11	X	X		
S12			X	
S15	X			
S16	X			
S18	X			
S19				
S20	X	X		
S21	X	X		
T1A	X			
T1B	X	X		
T1C	X			
T2A	X			
T2B	X	X		
T2C	X			

Groundwater monitoring program

On a semi-annual basis (in January and July 2018) the monitoring program has included the following parameters and wells:

- The monitoring wells available in the Southeastern area of the site (S20 and transects T1 A/B/C and T2 A/B/C) were sampled to determine contaminants of concern. The aim of these sampling rounds has been to identify any contaminant migration downgradient from the site.
- MNA parameters were analyzed in the background area, the diesel source zone and the downgradient transects to evaluate biodegradation in dissolved phase.

Additionally, a complete groundwater monitoring round was conducted in July 2018, a year after the set-up of this study, which included the sampling of every well available without NAPL phase to monitor groundwater quality at the site. The monitoring program comprised *in situ* measurements of temperature, dissolved oxygen, electric conductivity, pH and ORP, as well as analytical determination of the contaminants of concern in the collected groundwater samples.

2.4.3. Vapor monitoring and sampling

The vapour phase in the vadose zone is the third field data component of this study, after the soil and the groundwater.

The soil vapour monitoring study was designed to accurately measure the vertical distributions of O_2 and CO_2 concentrations in order to estimate biodegradation rates across the site, following the gradient approach described by Davis et al. (2009) and Johnson et al. (2006).

For such purpose, soil gas profiles were measured at both monitoring wells and designated soil vapour probes. The comparison between both methods during a one-year monitoring period was intended to determine whether specific soil gas monitoring probes are required for NSZD assessment, or if representative soil gas composition data could be obtained using existing monitoring wells instead.

For the monitoring well method, profiles were measured with and without the use of a packer in order to determine if a packer is needed for use in NSZD studies. In addition, a vapour profile was measured at 1 m intervals within the screened section of the well to determine the O_2/CO_2 gradients within that interval of the vadose zone. These results were used to determined the best methodology for application to NSZD studies.

Soil-gas samples were also collected from monitoring wells and soil vapour probes to analytically determine COC's concentration in the laboratory.

Vapor profiles at multilevel designated probes

Five quarterly vapour profiling campaigns were performed in June 2017 (baseline), October 2017 (first quarter), January 2018 (second quarter), April 2018 (third quarter) and July 2018 (fourth quarter).

The field sampling program included measuring O_2, CO_2, LEL(CH_4) and H_2S with a multigas detector[3] and COVs with a photoionization detector (PID), at each of the three different elevations where vapour probes (SV1/SV1bis to SV5) were installed. The three depths, upper, intermediate and lower, were measured consecutively to avoid interference while purging probes.

Figure 9. Vapor profiling methodology in SVPs

[3] MSA Safety Services Altair 5X. The accuracy of this instrument is ± 0.7% vol. for 0 – 30% O_2 and ± 0.01 % vol. for 0 – 10% CO_2.

The soil gas sampling points were purged until the monitored values were stabilized and the stabilized values were recorded.

Vapor profiles at monitoring wells

Vapor profiling at monitoring wells was also performed during the five quarterly campaigns (baseline: from the 26th to the 30th of June 2017; first quarter: from the 16th to the 19th of October 2017; second quarter: from the 17th to the 23rd of January 2018; third quarter: from the 17th to the 26th of April 2018 and; fourth quarter: from the 9th to the 17th of July 2018).

The field sampling program included measuring O_2, CO_2, LEL (CH_4) and H_2S with a multigas detector and COVs with a photoionization detector (PID), at multiple depths in all the available piezometers of the site.

The vapour sampling from the monitoring wells started at the top of the well screen and continued down to the smear zone, in one meter intervals. The depths were soil gas data were collected from the piezonmeters were matched to the SVP depths, to the extent practical, for comparison purposes.

For the 2'' monitoring wells, a double reading was collected to determine the benefit of using a packer (**Figure 10**) to isolate sections of the screened interval (this methodology has been modified after Jewell and Wilson, 2011).

Sampling of monitoring wells and soil vapor probes

Vapor samples were collected from monitoring wells and soil vapour probes during the five sampling campaigns.

Table 6 lists the depths in the monitoring wells and SVPs where vapour was analyzed in the study. The monitoring points were intended to be representative of the gasoline source area (SV3 and S5), the diesel source area (SV1 and S7) and background conditions (SV5). However, after installation, soil vapour probe SV1 was damaged and could not be sampled at the deepest elevation during the baseline monitoring round. A multilevel soil vapour probe was installed to replace SV1 (SV1 bis) and samples were collected from this location at the three designated depths during the following four quarterly monitoring rounds.

Figure 10. Vapor profiling methodology in piezometers.

Soil gas samples were collected with sorbent tubes (granular activated carbon and amberlite) by pumping (extracting) soil gas at a pre-established flow rate.

The sampling points were purged prior to sampling to assure that a representative sample was collected. COVs, O_2, CO_2, LEL(CH_4) and H_2S were monitored during the purge to verify parameter stabilization before sampling.

Table 6. Vapor samples record.

	Location ID	BASELINE	1st QUARTER	2nd QUARTER	3rd QUARTER	4th QUARTER
		June 2017	October 2017	January 2018	April 2018	July 2018
Diesel zone	*SV1*	SV1(1)	-			
		SV1(5)	-			
	SV1bis	-	SV1(1)	SV1(1)	SV1(1)	SV1(1)
		-	SV1 (5)	SV1 (5)	SV1 (5)	SV1 (5)
		-	SV1 (8)	SV1 (8)	SV1 (8)	SV1 (8)
	S7	S7(8)	S7(8)	S7(8)	S7(8)	S7(8)
		S7(9.5)	S7(9.5)	S7(9.5)	S7(9.5)	S7(9.0)
	SV2	SV2(1)	-			
		SV2(5)	-			
		SV2(10)	-			
	S12	S12(8)	-			
		S12(10)	-			
Gasoline zone	*SV3*	SV3(1)	SV3(1)	SV3(1)	SV3(1)	SV3(1)
		SV3(4.8)	SV3(4.8)	SV3(4.8)	SV3(4.8)	SV3(4.8)
		SV3(6.8)	SV3(6.8)	SV3(6.8)	SV3(6.8)	SV3(6.8)
	S5	S5(7)	S5(7)	S5(7)	S5(7)	S5(7)
		S5(8)	S5(8)	S5(8)	S5(8)	S5(8)
Background	*SV5*	-	SV5(1.2)			
		-	SV5(5.2)			
		-	SV5(8)			

All samples were labeled and kept refrigerated until the samples were received by the laboratory.

The analyses were performed by the laboratories Agrolab and Alcontrol. **Annex E** includes the laboratory certificates.

Supplemental 14C isotope study

Based on the O_2 and CO_2 data collected from the SVPs during the baseline monitoring round (the 27th of June of 2017), soil gas samples were collected for ^{14}C analysis from the SVPs at the depth where the maximum concentration of CO_2 was observed (see **Table 7**).

Table 7. ^{14}C study vapour samples record.

Location ID	Depth (m)	Max. CO_2 reading (%)
SV1	5,0	4,30
SV2	10,0	7,00
SV3	6,8	2,50
SV4	1,5	5,10
SV5	1,2	1,44

The ^{14}C analysis required two *Tedlar bags* of one litre volume each. These samples were collected using a vacuum chamber.

Figure 11. Sampling methodology (Tedlar bags).

The vacuum chamber was sealed with the Tedlar bag inside and connected to an external pump (see **Figure 11**). The vacuum inside the chamber induced soil gas flow from the vadose zone into the Tedlar bag. This set up prevented soil vapour from coming into contact with any sampling material other than single-use disposable tubing and the sampling bag itself. Thus, cross contamination of samples is not considered to be a concern. Prior to the sampling, the soil gas sampling points were purged to assure representativeness.

All of the samples were packed in a refrigerated box and sent to the *Center for Isotope Research* at Groningen University (The Netherlands).

2.4.4. Temperature monitoring

Subsurface temperatures were measured by two methods, as suggested by Subramanian et al. (2011), Ririe et al. (2013), and Sweeney and Ririe (2014), using the following devices:

i) A thermistor was used to measure instantaneous temperature profiles on a quarterly basis;

ii) Temperature data loggers were used to record temperature profiles continuously throughout a one-year period.

Manual temperature profiles in monitoring wells

Five manual temperature profiling campaigns were conducted at all available monitoring wells in the source areas and in the background location. The temperature profile data were collected in June 2017 (baseline), October 2017 (first quarter), January 2018 (second quarter), April 2018 (third quarter) and July 2018 (fourth quarter). Temperature measurements were recorded in one-meter increments from the surface, following the instructions of the "*BP Standard Operating Procedure Temperature Sampling to Document Hydrocarbon Biodegradation (October 2016)*". The thermistor used had an accuracy of ± 0.3°C degrees.

Installation of Temperature sensors

The temperature data loggers were installed to collect temperature data at one-hour intervals. The high-frequency temperature data was used to: 1) calibrate subsoil thermal properties of the soil (thermal diffusivity); and 2) document seasonal variability in NSZD rates. The temperature sensors had an accuracy of ± 0.5°C degrees.

A total of 36 temperature sensors/data loggers were installed, including twelve in the background well S21, eleven in the gasoline impacted well S5, and thirteen in the diesel impacted well S7. The data loggers were installed at one-meter intervals from the surface to the bottom of the wells. An additional sensor/data logger was installed under a canopy at a nearby hotel, with no direct exposure to sunlight or wind, in order to record the ambient temperature at the site.

The temperature sensors under the water table level and within the smear zone were installed inside waterproofing capsules, as shown in **Figure 12**.

Figure 12. Temperature sensor installation.

Several temperature sensor failures occurred during the course of the study. The sensors that were installed without waterproofing capsules were coated with silicon grease to decrease the potential for further failures. However, some temperature sensors both inside waterproofing capsules and with silicon grease coating failed, some of which were replaced during the course of the study.

2.4.5. CO_2 traps

As described in section 3.1.3, CO_2 traps were included as part of the monitoring program to estimate biodegradation rates. The intent of performing this surface technique was to establish another line of evidence that NSZD is occurring at the site. The CO_2 trap data will additionally be compared to the other NSZD assessment methods implemented at the site.

Figure 13 shows a visual scheme of the traps capturing CO_2, that is later identified as modern or fossil carbon based on the ^{14}C value.

Figure 13. Scheme of CO_2 traps

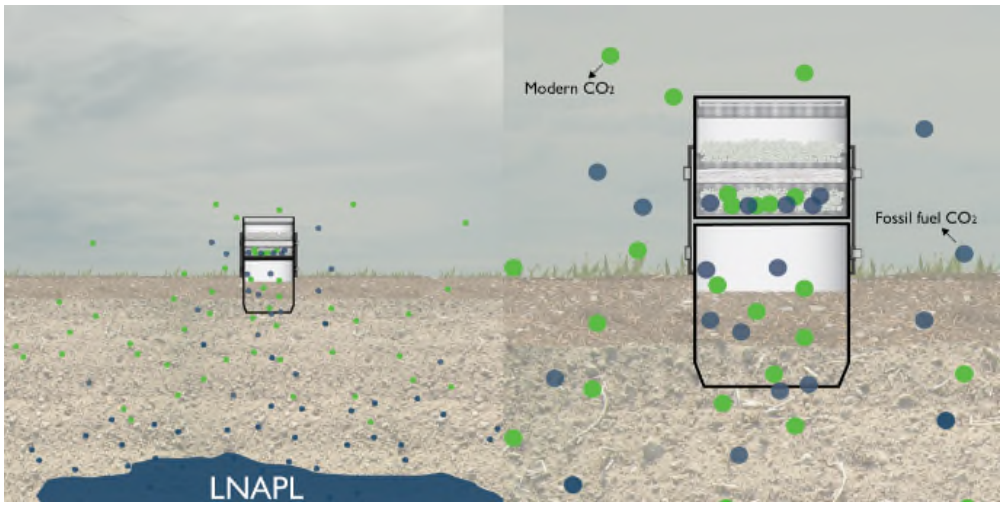

The CO_2 traps were placed five locations (see **Figure 2** in section 3.1 and **Figure 1** in **Annex A**):

- C1 and C2 in the diesel source area, at the east of the site.
- C3 and C4 in the gasoline zone, at the center and west of the site.
- C5 in the background area, next to monitoring well S21 and soil vapour probe SV5.

Because the site is paved, the permeability of the pavement as compared to the CO_2 trap sorbent material can result in a stack effect that magnifies the CO_2 flux from the subsurface into the trap, leading to an overestimation of the biodegradation rates (API 2017). Hence, as described in section 3.1.3, the CO_2 traps were installed following the specific methodology developed by the supplier for paved sites to avoid the stack effect.

The bottom of the traps were connected to previously installed receiver pipes using rubber connectors (see **Figure 14**). Traps were covered with a rubber cap connected to the vapour pin.

Figure 14. CO_2 trap installation.

In the first CO_2 trap monitoring round conducted in September/October 2017, the traps were collected after a 9-day deployment period, as shown in **Table 8**, and sent to the supplier for analysis. The deployment period in the second monitoring round conducted in April/May 2018 was 13 days, as shown in **Table 9**.

Table 8. CO_2 traps installation periods - First monitoring round September / October 2017.

Location ID	Area	CO_2 Traps			
		Installation		Retrieve	
		Date	Hour	Date	Hour
C1	Diesel	28/09/2017	16:45	06/10/2017	10:12
C2		28/09/2017	17:24	06/10/2017	10:18
C3	Gasoline	28/09/2017	15:56	06/10/2017	9:56
C4		28/09/2017	16:29	06/10/2017	10:04
C5	Background	28/09/2017	15:35	06/10/2017	9:50

Table 9. CO_2 traps installation periods - Second monitoring round April / May 2018.

Location ID	Area	CO_2 Traps			
		Installation		Retrieve	
		Date	Hour	Date	Hour
C1	Diesel	20/04/2018	11:42	03/05/2018	13:58
C2		20/04/2018	11:32	03/05/2018	13:55
C3	Gasoline	20/04/2018	11:18	03/05/2018	13:45
C4		20/04/2018	11:25	03/05/2018	13:50
C5	Background	20/04/2018	11:05	03/05/2018	13:40

3. RESULTS

3.1. SOIL RESULTS

Tables II and III in **Annex B** show the analytical results of contaminants of concern for the soil samples collected during the drilling campaign.

Figure 15 presents a geological cross section for the site including recent and historical TPH C_5-C_{40} concentration data (in red, in mg/kg), PAHs (in purple, in mg/kg) and head space PID measurements (in black, in ppm) of the soil samples. All new monitoring wells and soil vapour probes installed as part of this study are depicted in light blue whereas existing monitoring wells are in black.

Figure 15. Site cross section

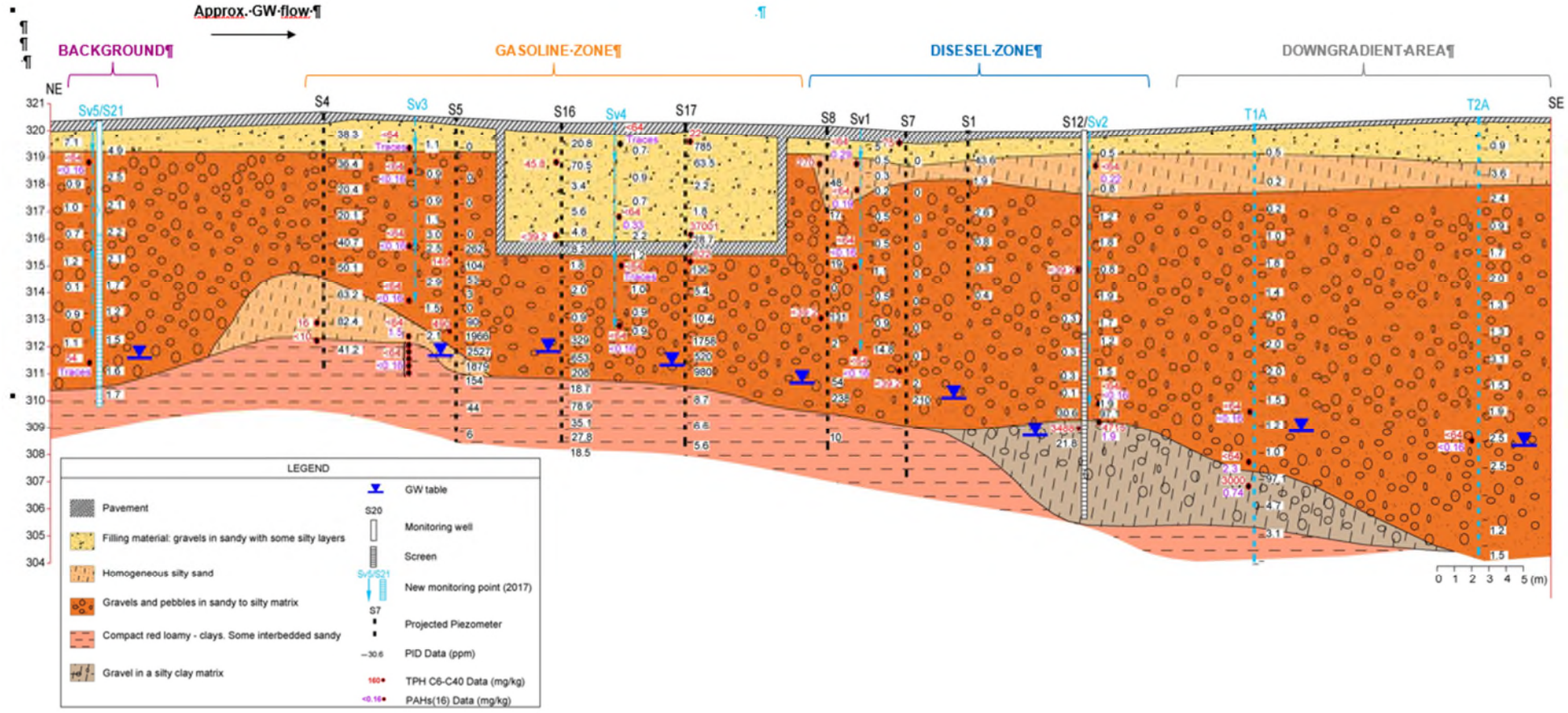

With regards to soil quaility, the main findings of the subsurface investigation carried out in 2017 are the following:

- **Shallow soil** (from surface to approximately 3 to 4 meters)
  - During the drilling works, no organoleptic sign of impact was observed in shallow soil in any of the investigated locations, nor was any significant COV concentration measured with the PID instrument. This fact suggests that TPH detected in a soil sample collected 1 m bgs at the southeast end of the site, during the soil-gas survey performed in 2016 (sample SG-T), may be a localized *hot spot* within the fill, since no impact was observed in the shallow soil within nearby boreholes. The low O_2 and high CO_2 concentrations measured in 2016 in that area were initially considered indicative of potential shallow petroleum impact present in this part of the site. The findings of the recent field disproves this hypothesis.
  - Shallow soil samples were collected in the five locations (C1 to C5) where "surface techniques", such as CO_2 traps, were deployed and no contaminants of concern were detected, apart from low levels of PAHs in the diesel source area below 0.3 ppm.
- Smear zone (groundwater related impact)
  - The soil at the smear zone in the background location (S21) was slightly impacted with low concentrations of aliphatic compounds (carbon range of C_{10}-C_{21}) and traces of PAHs. Based on the nature of the impact and the affected depth, it is presumed to be a representative of impacted groundwater within the soil sample rather than evidence of source-area soil impacts.
  - All reported results for hydrocarbons were below the detection limit for soil samples collected from boreholes drilled in the gasoline source area (SV3 and SV4), except for negligible levels of PAHs and MTBE/ETBE detected at the smear zone and upper saturated zone and within the UST secondary containment.
  - As for borehole SV2 located in the diesel zone, the sample collected at 10.5 m bgs shows similar results to that obtained in 2011 for S12 (next to SV2) at approximately the same depth. Comparing the aliphatic composition profile of both samples (**Graph 1**), it is apparent that over the six years between sampling at S12 and SV2, the composition was enriched in the heavier fractions. This suggests that natural attenuation processes are taking place (volatilization and biodegradation of lighter hydrocarbons).
  - Among the down-gradient transect boreholes (T1A-T1C and T2A-T2C), hydrocarbon impacts were only been identified in T1A at a depth of 13 m bgs. The composition profile for the sample collected at 13 m bgs from borehole T1A resembles the composition observed in the diesel source area, in SV-2 (**Graph 2**). None of the other boreholes have shown any sign of impact nor has hydrocarbon been detected in the samples collected from them.

Graph 1. Total Petroleum Hydrocarbon fraction distribution.

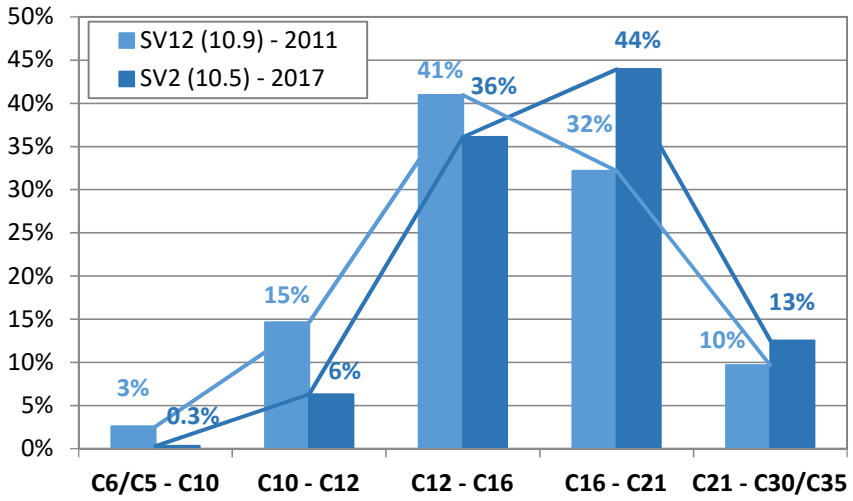

Graph 2. Total Petroleum Hydrocarbon fraction distribution.

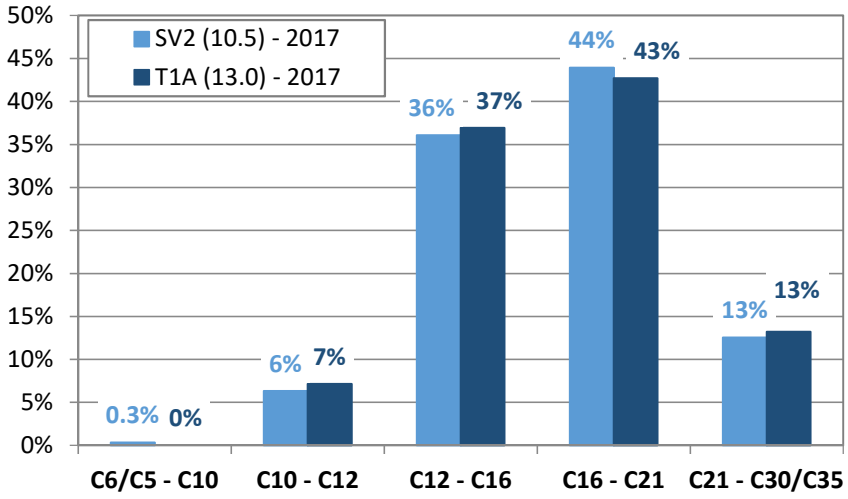

Figure 16 shows the detailed hydrocarbon profile of SV1 (diesel source area), where a description of the lithology and organoleptic observations (odour, colour) together with soil core photographs and the detected concentration of contaminants of concern were logged with depth in the boring.

Detailed analysis of the lithology and TPH concentration was conducted at the most impacted horizon of SV1 (diesel source area). This analysis confirmed that the highest concentrations of TPH (over 5.000 mg/kg) were located within a 20 to 30 cm layer coincident with the smear zone and upper saturated zone. Hydrocarbon concentrations increase with depth corresponding to a greater proportion of fine material. The maximum concentration of hydrocarbon, 24.000 mg/kg was detected in a 5-cm interval of gravelly medium sand. No PAHs were detected in the studied horizon (9 to 10.5 m bgs).

Figure 16. Detailed hydrocarbon profile analysis of SV1 soil core (9 to 10.5 m bgs)

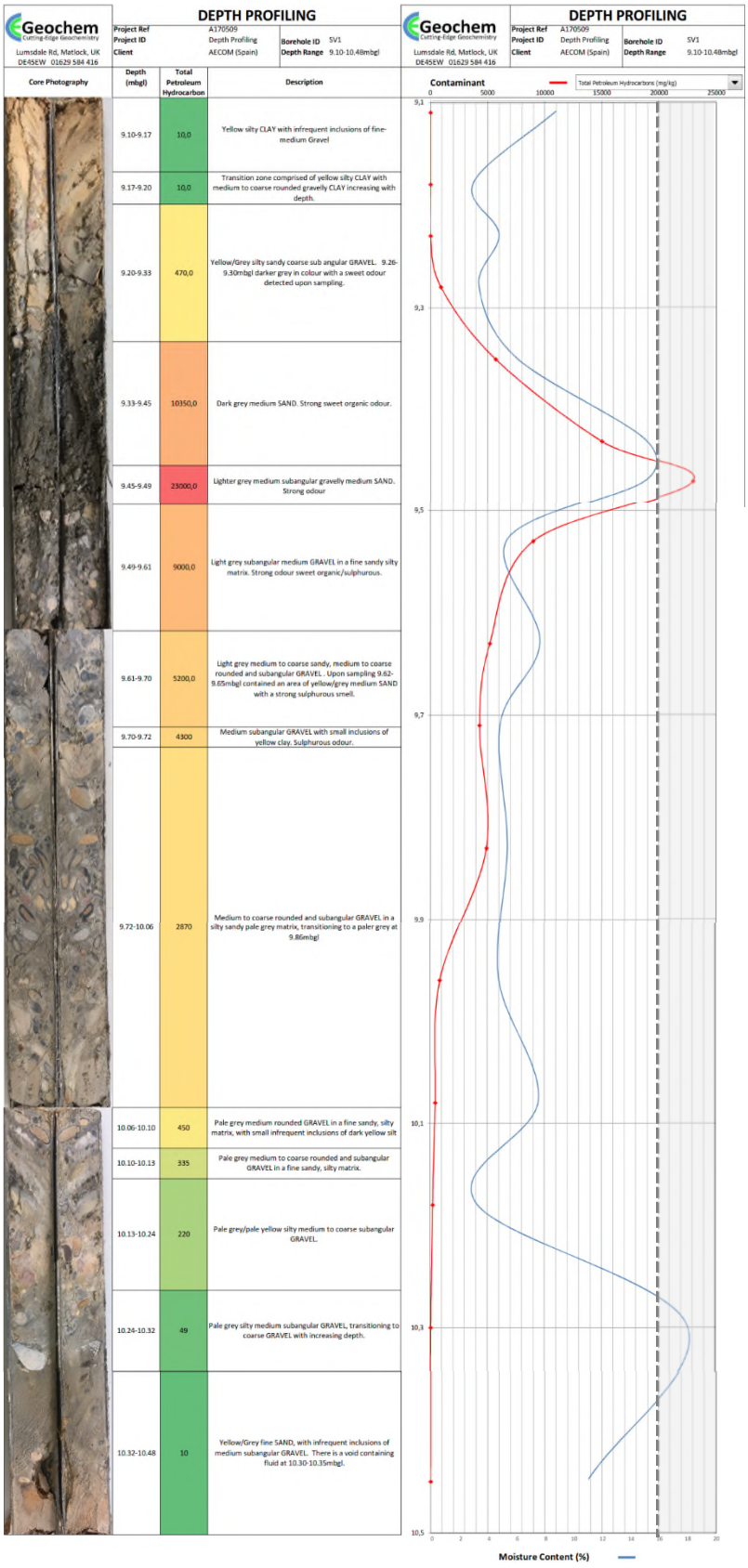

3.1.1. Site Specific Oxygen Diffusion Coefficient Calculation

Consumption of O_2 and production of CH_4 and CO_2 from natural depletion of petroleum LNAPL creates concentration gradients that drive diffusive gas flux within the vadose zone. Soil gas concentrations measured from monitoring wells and SVPs coupled with knowledge of gas diffusion coefficients for subsurface materials, can be applied to calculate rates of O_2 ingress and utilization and/or CO_2 efflux as described by Johnson et al. (2006) and ITRC (2009, 2018). **Table 10** shows geotechnical parameters (moisture, porosity, bulk density, etc.), determined for the samples collected in the vadose zone of both the Gasoline Source Area and the Diesel Source area. These data were used to estimate gas diffusivity of the vadose zone soil.

Table 10. Diffusivity related parameters results

		Gasoline area		Diesel area
		SV3	SV3	SV1
Depth	m	2.20 - 2.60	4.90 - 5.30	6.80 - 7.40
Wet mass	g	1,133.93	1,139.35	1.248.26
Dry mass	g	1,091.26	1,107.13	1.204.65
Sample volume	cm^3	511.85	496.47	534.69
Moisture	%	3.91	2.91	3.62
Dry density	g/cm^3	2.132	2.23	2.253
Bulk density	g/cm^3	2,215	2.295	2.335
Specific solid mass	g/cm^3	2.688	2.747	2.678
Total Porosity	%	20.68	18.82	15.87

The granulometric distribution of the soil samples is shown in **Table 11** and **Graph 3**.

Graph 3. Granulometric distribution (sieving method).

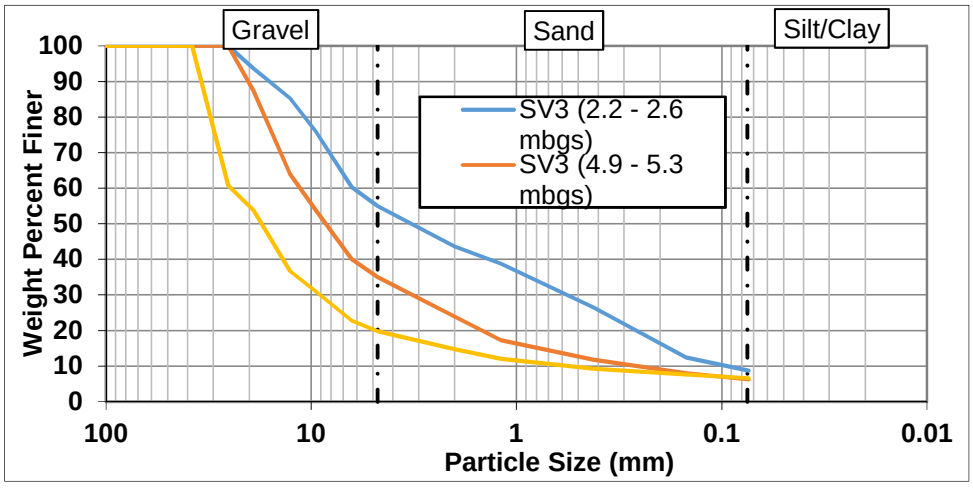

Table 11. Particle size distribution

		Gasoline area		Diesel area
Sieve diameter (mm)		SV3	SV3	SV1
Depth	m	2.20 - 2.60	4.90 - 5.30	6.80 - 7.40
101,6	%	100	100	100
76,2	%	100	100	100
63,5	%	100	100	100
50,8	%	100	100	100
38,1	%	100	100	100
25,4	%	100	100	60.73
19,1	%	93.67	87.37	53.80
12,7	%	85.25	64.00	36.73
9,52	%	75.98	53.86	31.02
6,35	%	60.26	40.02	22.71
4,75	%	54.95	34.96	19.75
2,00	%	43.61	23.88	14.77
1,19	%	38.80	17.23	12.04
0,42	%	26.45	11.75	9.25
0,149	%	12.37	7.98	7.64
0,074	%	8.72	6.26	6.61

The diffusion rate of gases (e.g., O_2 and CO_2) in soil is reduced relative to diffusion in air because the majority of space in the soil is occupied by solid particles and liquids, and the path a gas molecule follows when diffusing through soil is more tortuous.

Based on the Millington and Quirk (1961) relationship (Equation 1) the effective diffusivity (D_e) can be estimated by correcting the air diffusion coefficient with a function of the gas-filled porosity (θ_{gas}) and total porosity (θ_{total}) of soil (Davis et al., 2009).

$$D_{e,} = D_{,air} \cdot \theta_{gas}^{3.33} / \theta_{total}^{2} \qquad \textbf{Equation 1}$$

The gas-filled porosity was estimated based on the diffusivity related parameters determined for the soil samples collected (**Table 10**) as follows:

θ_{air} = *Dry pore volume / sample volume = (Pore volume - Water volume) / sample volume* *Eq.15*

where:

Pore volume = Sample volume·Total porosity

Water volume = (Wet mass - Dry mass) / Density

Table 12 shows the results of the site-specific effective diffusivity parameters compared to the literature values that were estimated using the total and air filled porosity values published by USCS for well graded sands.

Table 12. Site-specific effective diffusivity for CO_2 and O_2

		SV3	SV3	SV1	Bibliographic reference
Depth	**m**	**2,20 - 2,60**	**4,90 - 5,30**	**6,80 - 7,40**	**USCS**
Lithology as described in the boring log	-	*Fine sand with gravel*	*Sand and gravel*	*Sand and gravel*	*Clean well graded sands*
Total porosity	%	20.68	18.82	15.87	41
Gas-filled porosity	%	12.34	12.33	7.71	33
De, O_2	m^2/s	$3.9 \cdot 10^{-7}$	$4.6 \cdot 10^{-7}$	$1.4 \cdot 10^{-7}$	$2.6 \cdot 10^{-6}$
De, CO_2	m^2/s	$3.5 \cdot 10^{-7}$	$4.2 \cdot 10^{-7}$	$1.2 \cdot 10^{-7}$	$2.4 \cdot 10^{-6}$

The measured site-specific porosity and gas-filled porosity values are compared to literature values for clean, well graded sands in **Table 12**. The high dry bulk density and lower porosity values determined from the laboratory analysis are low relative to literature values, but consistent with the large range in particle sizes from sieve analysis and photos in **Figure 16**, as well as the difficult drilling conditions noted during soil core collection. The effective gas diffusion coefficient estimated using the site-specific values are approximately one order of magnitude lower than if the values published by USCS for well graded sands.

3.2. ^{14}C RESULTS

The concentration of ^{14}C isotopes values was determined for soil, soil gas, and LNAPL samples collected from the gasoline and diesel source areas. Additional soil and vapour samples from the background location were also analyzed for ^{14}C values to assess relative contributions from degradation of petroleum constituents and contributions associated with the decay of organic matter within the soil matrix.

The results of the ^{14}C analysis are reported as a fraction of modern carbon ($F^{14}C$), where modern carbon is defined relative to a 1950 baseline. The 1950 baseline reflects atmospheric conditions before the advent of widespread testing of nuclear weapons, which resulted in an approximate doubling of the $^{14}CO_2$ content in the atmosphere between 1955 and 1964 (Turnbull et al., 2017). As a result, the concentration of ^{14}C in atmospheric air continues to have a $F^{14}C$ value slightly greater than 1 (ASTM International, 2016; Turnbull et al., 2017). These results can be compared directly with the ^{14}C results obtained from the CO_2 efflux traps.

Table 13 shows the ^{14}C results for the samples of soil, soil-gas, and LNAPL collected from the background location and the source areas. For soil samples, ^{13}C values and total amount of carbon has also been reported.

Table 13. ^{14}C isotope study results

Sample ID	Area	Matrix	^{14}C isotope content $F^{14}C$	^{13}C isotope content $\delta\ ^{13}C$ (‰)	Carbon content % C
SV1 (5.2)	Diesel source area	Soil-gas	0.3503 ± 0.0010	-	-
SV2 (10.0)			0.2524 ± 0.0008	-	-
SV3 (6.8)	Gasoline source area		0.6207 ± 0.0014	-	-
SV4 (1.5)			0.1738 ± 0.0007	-	-
SV5 (1.2)	Background		0.6958 ± 0.0014	-	-
PL-ALC-S7	Diesel source area	Free phase LNAPL	0.0567 ± 0.0008	-26.01 ± 0.06	84.3
S-ALC-SV3 (6.8)	Gasoline source area	Soil	0.0036 ± 0.0002	-2.22 ± 0.06	7.8
S-ALC-SV1 (8.2)	Diesel source area		0.0033 ± 0.0002	-2.33 ± 0.05	8.2
S-ALC-SV5 (8.0)	Background		0.0065 ± 0.0003	-1.26 ± 0.05	Fail

Among the soil vapour samples collected at the site, the highest content in modern carbon is reported for the **background** SV5 (1.2 m). While this result suggests a smaller contribution from petroleum degradation in the background location, the $F^{14}C$ value measured in soil gas from the background location is much lower than the background value assumed in the standard calculations provided by E-Flux (1.05), and is very close to the $F^{14}C$ value for soil gas collected from SV3 in the **gasoline source area** (0.62). The similarity between $F^{14}C$ measured in soil gas from the background and gasoline areas suggests lateral migration of soil gas.

The $F^{14}C$ result for the 1.5 m CO_2 sample collected from SV4 (0.17), is indicative of shallow contamination (fossil carbon) within the UST secondary containment area. This surface contamination is consistent with the O_2/CO_2 profile measured in the area, as discussed in Section 4.5.

$F^{14}C$ values of 0.35 (5.2 m in SV1) and 0.25 (10 m in SV2) for the soil vapour CO_2 samples collected from the **diesel source area** are consistent with the presence of a fossil source related impact at depth in the vadose zone. The $F^{14}C$ value of 0.06 for carbon in the LNAPL sample (monitoring well S7) indicates a fossil carbon source, possibly slightly altered by additives. The ^{13}C value of the LNAPL is typical for a fuel.

Carbonates are widely present in the soil matrix of the site and, therefore, the carbon content of the soil samples collected are rather high (approximately 8% as shown in **Table 13**). Obtaining conclusive information about recent organic carbon fractions based on ^{14}C results of the soil samples is hindered by the high carbon content documented, mainly related to inorganic carbon.

According to the reported levels of ^{14}C isotope measured in the samples collected from the subsurface of the site, it is not foreseen that biodegradation rate estimations based on CO_2 traps can be drastically affected by an unexpectedly high presence of modern carbon. Consequently, CO_2 traps were further installed as described in section 3.2.5.

3.3. GROUNDWATER RESULTS

Field tasks were performed in order to define a baseline for the status of groundwater with regards to: i) presence of LNAPL; ii) CoC concentrations and; iii) biodegradation indicators concentrations.

During the one-year period of this study, fluid levels were monitored on a quarterly basis, CoC concentrations on a yearly basis and biodegradation indicators concentration on a semi-annual basis.

No LNAPL was identified in the Gasoline source area, whereas the LNAPL thickness values registered in the Diesel source area (purple shadowed area in **Figure 17**) were similar to those documented in previous monitoring campaigns and in the range from 2 to 45 cm.

3.3.1. Local hydrogeology

The depths to the water table and LNAPL were measured at all monitoring points, as well as the depth to the bottom of the piezometers during each monitoring campaign.

Six monitoring campaigns were undertaken during the one-year period of this study. All water table depth measurements and related groundwater elevation data are included in Table IV - Annex B, referred to the most recently conducted topographical survey. Based on these data, groundwater contour maps were drawn for the quarterly monitoring rounds conducted in October 2017, January 2018, April 2018 and July 2018 (see **Figure 17**).

Updated groundwater contours, including the groundwater elevation data gathered in all the recently installed monitoring wells, show that groundwater flow is consistently heading towards the southeast. The hydraulic gradient varies from 1%, in the West and East of the site, to 5% in the central area.

Figure 17. Groundwater contours, 2017 - 2018.

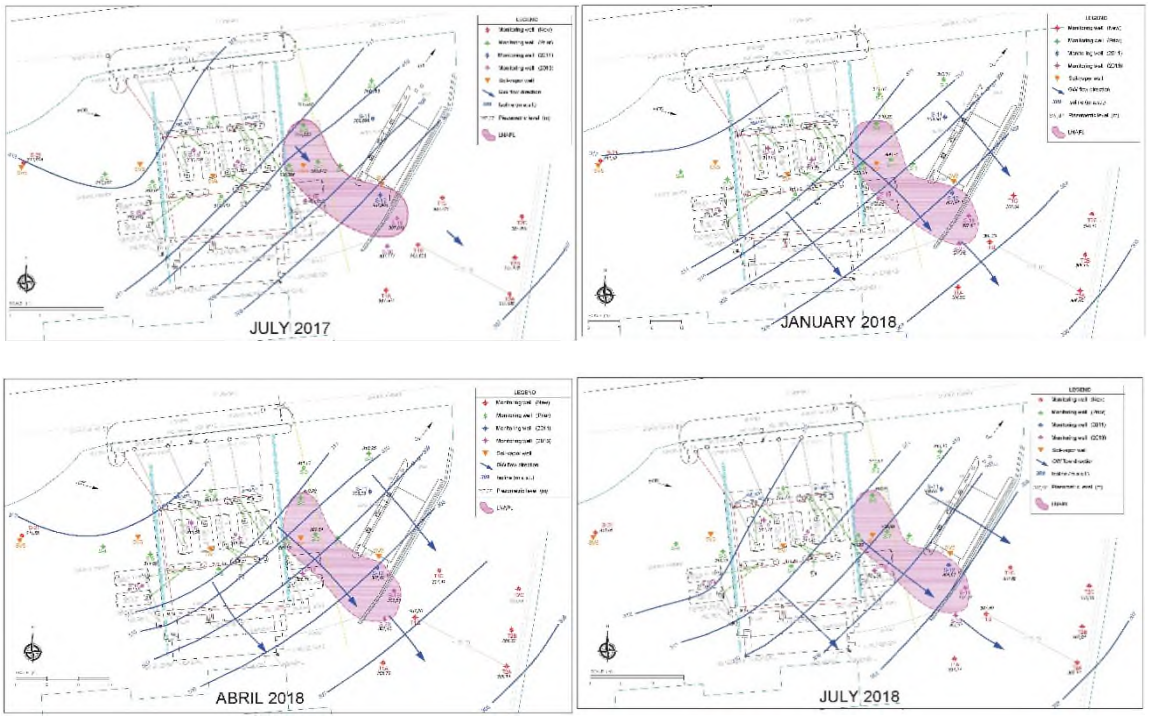

3.3.2. Contaminants of concern

All wells without LNAPL were sampled in June 2017 and July 2018. Table V in Annex B shows the detailed analytical results for BTEX, TPH C_6-C_{40}, PAHs, MTBE and ETBE. These results are summarized and presented on the site map in **Figures 18** and **19**. Complete laboratory analytical reports and tables are available in **Annex E**.

With regards to BTEX, TPH and MTBE and ETBE dissolved concentrations, the observed distribution of the contaminants is consistent with the conceptual site model (see **Figure 18**):

1. A gasoline-related impact is seen in the central area of the petrol station, where the detected concentrations of hydrocarbons (S5, S16, S17) are mainly due to the presence of the lighter fractions of TPH (C_6-C_{10}), BTEX and MTBE/ETBE (common additives of gasoline).
2. A diesel-related impact is found in the eastern area where LNAPL has been identified (blue shadowed area in **Figures 18** and **19**) and detected hydrocarbon concentrations (S18, S20, T1A and T1C) are asociated with heavier hydrocarbon fractions (C_{10}-C_{40}).

Naphthalene and other PAHs (see **Figures 20** and **21**) were found in both source areas, and most significantly in those wells showing maximum hydrocarbon concentrations, such as:

- S5 & S16 in the gasoline zone, where more than 90% of PAHs is Naphthalene and;
- S20 in the diesel zone, where Naphthalene is below the detection limit.

Figure 18. TPH groundwater baseline concentrations, June 2017.

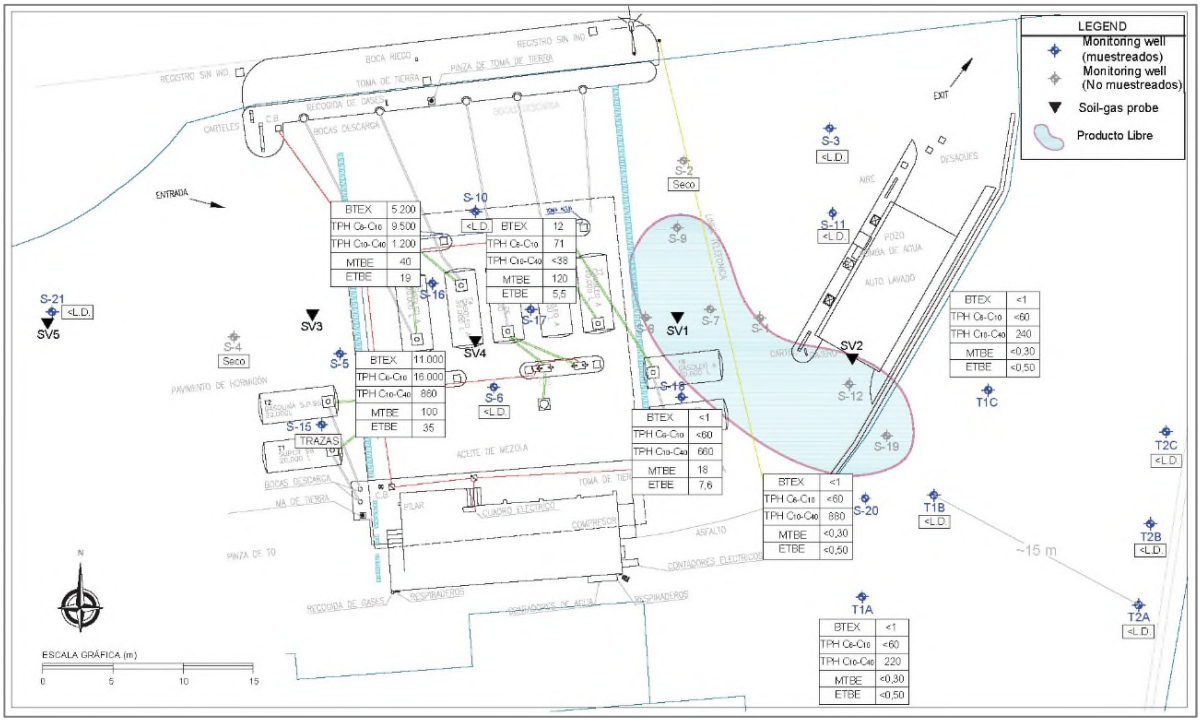

Figure 19. TPH groundwater concentrations, July 2018.

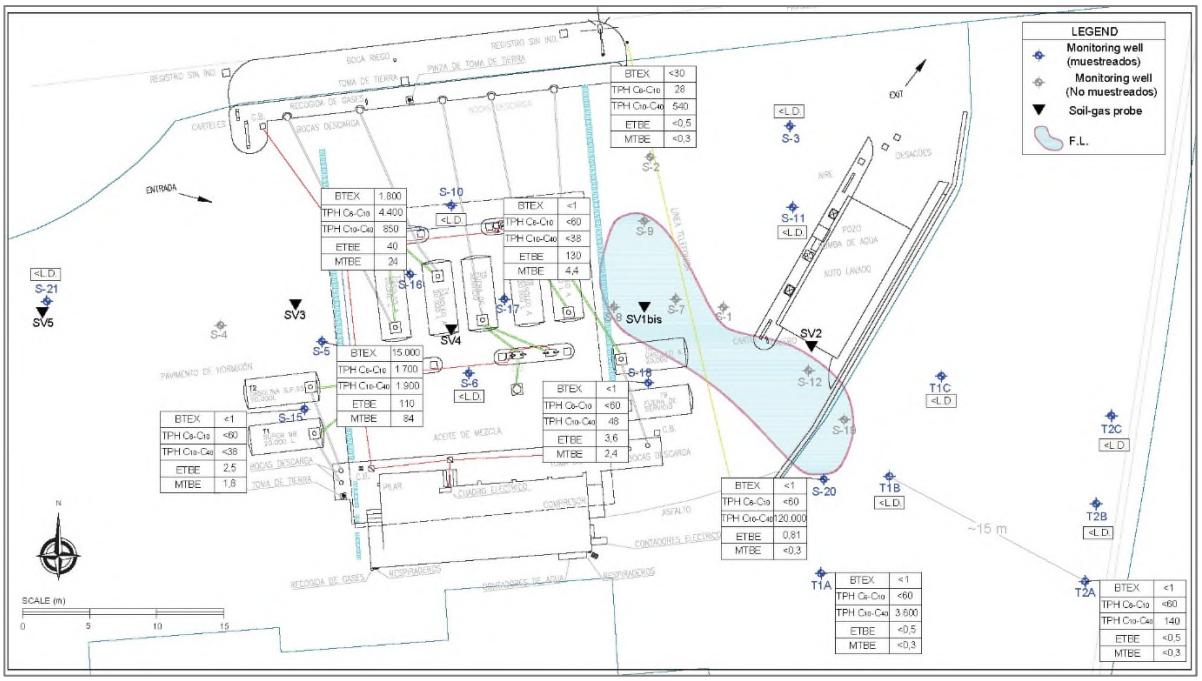

Figure 20. PAHs groundwater baseline concentrations, June 2017.

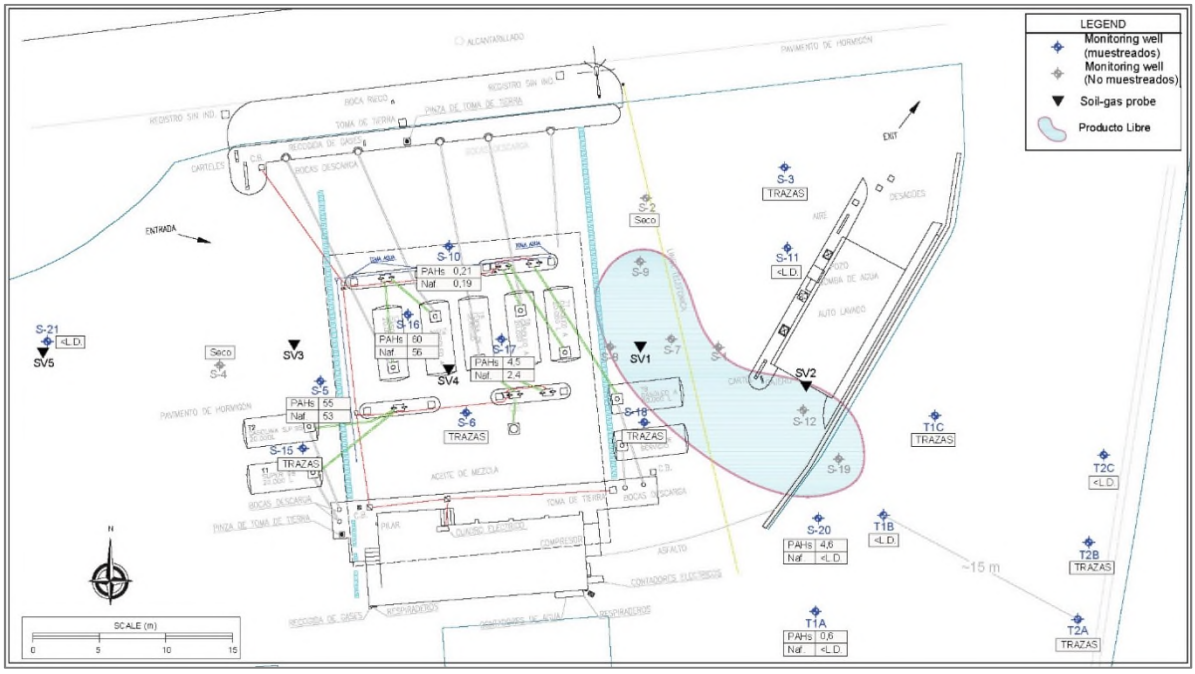

Figure 21. PAHs groundwater concentrations, July 2018.

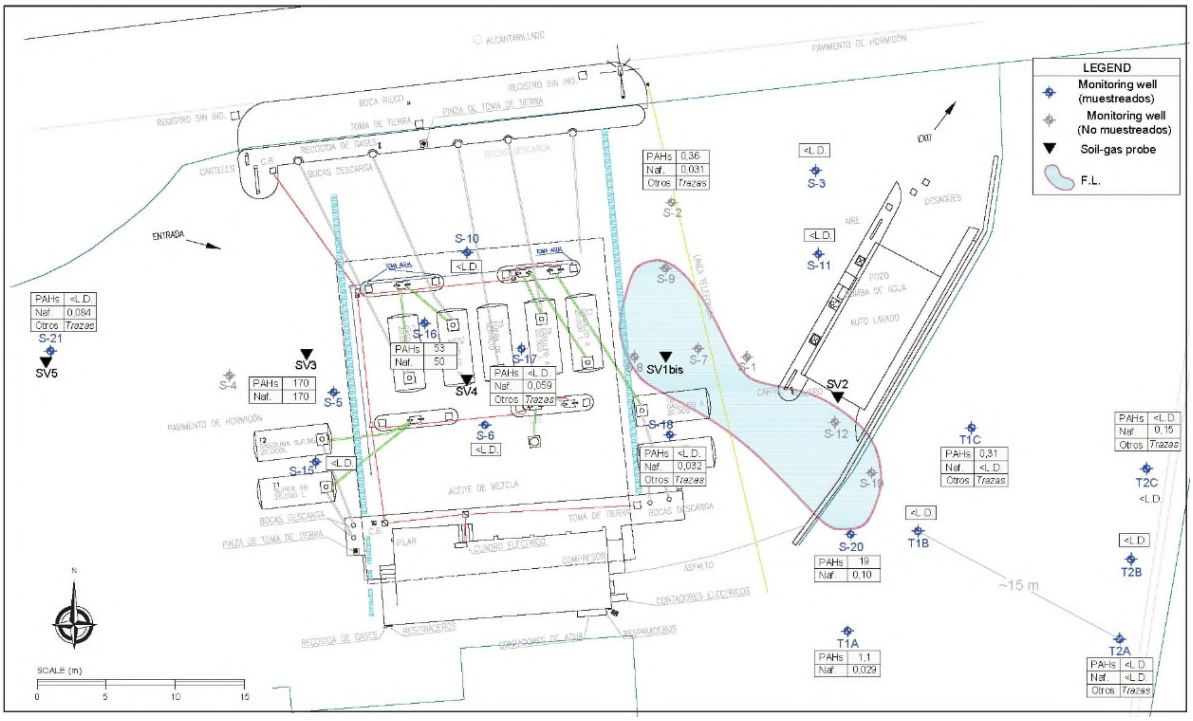

3.3.3. Natural attenuation parameters

Groundwater samples were collected from nine wells and analyzed for biogeochemical parameters in order to confirm that biodegradation of petroleum is occurring in the saturated zone of the aquifer:

- **S21 & S11**, located in non-impacted areas, up-gradient from the source zones, that are considered representative of background aquifer conditions;
- **S16 & S17**, located in the gasoline source area;
- **S9 & S20**, located in the diesel source area and;
- **T1A, T1B & T2B,** located downgradient from the edge of the eastern area of concern.

Table 14 shows the analytical results for the biogeochemical parameters and in situ dissolved oxygen and oxidation-reduction potential (ORP) measurements. The average results are also grouped by area in **Figure 22** along with dissolved petroleum hydrocarbons (TPH C_6-C_{40}) from June 2017 and July 2018 (see **Figure 18** and **19**) to compare spatial relationships between attenuation parameters.

Groundwater at the site is generally characterized by relatively high sulfate and alkalinity. Data indicate a shift in geochemical conditions between background and source area wells. However, aquifer conditions are similar to background downgradient of the petroleum-affected areas, indicating that oxidation/reduction poise recovers quickly.

Table 14. Natural attenuation parameters, 2017-2018

			Background		Gasoline Source Area		Diesel Source Area		Downgradient		
			S21	S11	S16	S17	S9	S20	T1A	T1B	T2B
June 2017	Dissolved Oxygen	mg/l	5.98	2.6	n.m.		n.m.	0,51	n.m.	0,72	0,96
	Nitrate as NO_3	mg/l	11.7	24.0	n.a.	18.2	<0.2	17,6	n.a.	21,4	23,4
	Manganese II	mg/l	0.19	0.03	n.a.	0.09	0,4	0,07	n.a.	0,04	0,25
	Dissolved Iron II	mg/l	<0.02	<0.02	n.a.	<0.02	<0.02	<0.02	n.a.	<0.02	<0.02
	Sulphate as SO_4	mg/l	1377.1	1377.5	n.a.	1701.7	922	1360,7	n.a.	1391,3	1290
	Dissolved Methane	µg/l	<1	<1	n.a.	<1	15	<1	n.a.	<1	<1
	Oxidation-reduction potential	mV	23.5	18.6	-59.2	-18.9	n.m.	13.1	n.m.	22.4	17.5
	Total Alkalinity as $CaCO_3$	mg/l	474	260	n.a.	278	500	296	n.a.	290	306
January 2018	Dissolved Oxygen	mg/l	n.m.	4.16	2.05	n.m.	n.m.	0.00	2.33	7.93	3.49
	Nitrate as NO_3	mg/l	n.a.	25.5	<0.2	n.a.	<0.2	19.3	7.8	19.5	23.2
	Manganese II	mg/l	n.a.	0.02	0.28	n.a.	0.20	0.04	0.20	0.08	0.03
	Dissolved Iron II	mg/l	n.a.	<0.02	0.04	n.a.	0.06	<0.02	0.03	<0.02	0.08
	Sulphate as SO_4	mg/l	n.a.	1494.5	202.8	n.a.	1333.1	1312.2	1352.7	1337.7	1399.9
	Dissolved Methane	µg/l	n.a.	<1	304	n.a.	33	<1	2	<1	<1
	Oxidation-reduction potential	mV	n.a.	-140.9	-355.9	n.a.	n.m.	-145.9	-148.3	-112.5	-89.8
	Bicarbonate Alkalinity as $CaCO_3$	mg/l	n.a.	289	667	n.a.	422	288	319	293	288
	Total Alkalinity as $CaCO_3$	mg/l	n.a.	289	667	n.a.	422	288	319	293	288
July 2018	Dissolved Oxygen	mg/l	n.m.	3.66	0.09	n.m.	n.m.	n.m.	n.m.	2.18	4.40
	Nitrate as NO_3	mg/l	n.a.	26.4	<0.2	n.a.	<0.2	9.0	n.a.	30.3	29.2
	Manganese II	mg/l	n.a.	<0.02	0.17	n.a.	0.15	0.31	n.a.	0.36	0.43
	Dissolved Iron II	mg/l	n.a.	<0.02	0.09	n.a.	0.04	0.88	n.a.	<0.02	<0.02
	Sulphate as SO_4	mg/l	n.a.	1382.3	180.1	n.a.	840.4	1214.5	n.a.	1420.9	1402.4
	Dissolved Methane	µg/l	n.a.	<1	308	n.a.	26	4	n.a.	<1	<1
	Oxidation-reduction potential	mV	n.a.	30.2	-246.7	n.a.	n.m.	n.m.	n.m.	-46.4	32.2
	Total Alkalinity as $CaCO_3$	mg/l	n.a.	268	606	n.a.	644	368	n.a.	558	1234.0

Notes:
n.m.: not measured
n.a.: not analyzed

Figure 22. Average Values for Geochemical Parameters by Area

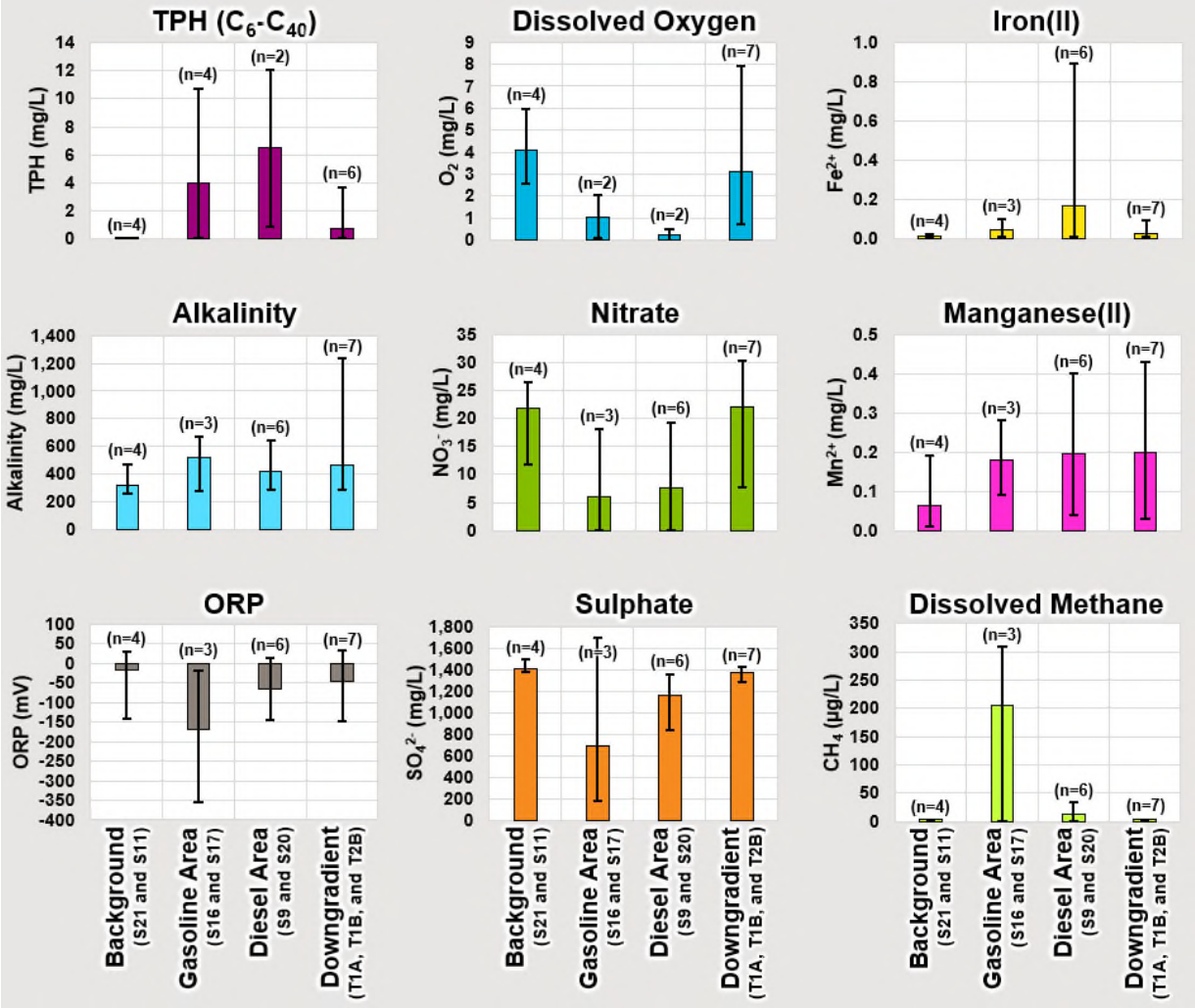

The data collected within the gasoline and diesel source areas provide qualitative evidence of biodegradation, based on the following trends:

- Decreased concentrations of electron acceptors (oxygen [O_2], nitrate [NO_3^-], and sulphate [SO_4^{2-}]) relative to background conditions, and
- Increased concentrations of metabolic by-products (ferrous iron [Fe^{2+}], manganese [Mn^{2+}]) and methane (CH_4).

Groundwater data were utilized to estimate rates of dissolution and biodegradation occurring within the groundwater saturated portion of the LNAPL zone using a lateral mass balance approach. The rate of LNAPL depletion through dissolution (R_{diss}) as groundwater moves through the source zone was estimated using **Equation 2** (Johnson et al., 2006; ITRC 2009) and the rate of LNAPL depletion through biodegradation in the submerged portion of the source zone ($R_{bio\text{-}sat}$) was estimated using **Equation 3** (Johnson et al., 1999).

$$R_{diss} = K_w \cdot i \cdot h \cdot w \cdot C_d \qquad \textbf{Equation 2}$$

$$R_{bio-sat} = K_w \cdot i \cdot h \cdot w \cdot AC \qquad \textbf{Equation 3}$$

Where,

K_w = Hydraulic conductivity (1.3 m/d)

i = Hydraulic Gradient (0.03)

h = Vertical extent of hydrocarbon impacts in the saturated zone (1.0 m)

w = Lateral extent of hydrocarbon impacts perpendicular to groundwater flow
(24 m)

C_d = Average increase in concentration of hydrocarbons in groundwater flowing through the source zone (g/m^3)

AC = Assimilative capacity, defined as the difference between upgradient and downgradient concentrations of each natural attenuation indicator species multiplied by a representative stoichiometric coefficient (g/m^3)

For this evaluation, hydraulic conductivity (K_w) was estimated based on grain size analysis results (**Table 11**) using the Kozeny-Carman formula (Carrier 2003) and stoichiometric relationships were calculated assuming octane (C_8H_{18}) as a representative LNAPL constituent. Stoichiometric coefficients for the biological oxidation reactions considered in this evaluation are presented in **Table 15**.

Table 15. Stoichiometric Coefficients for LNAPL Depletion as Octane (C_8H_{18})

Reaction	Election Acceptor	Measured Parameter	Stoichiometric Coefficient
Aerobic	O_2	O_2	0.29 kg-HC/kg-O_2
Nitrate Reduction	NO_3^-	NO_3^-	0.18 kg-HC/kg-NO_3^-
Iron Reduction	$Fe(OH)_{3(s)}$	Fe^{2+}	0.04 kg-HC/kg-Fe^{2+}
Sulfate Reduction	SO_4^{2-}	SO_4^{2-}	0.19 kg-HC/kg-SO_4^{2-}
Manganese Reduction	$MnO_{2(s)}$	Mn^{2+}	0.08 kg-HC/kg-Mn^{2+}
Methanogenesis	CO_2	CH_4	1.1 kg-HC/kg-CH_4

Notes: O_2 Oxygen; NO_3^- Nitrate; $Fe(OH)_{3(s)}$ Iron (III) oxide-hydroxide; Fe^{2+} Ferrous; SO_4^{2-} Sulfate ion; $MnO_{2(s)}$ Manganese dioxide; Mn^{2+} Manganese ion; CO_2 Carbon dioxide; CH_4 Methane; HC hydrocarbon; kg kilogram

The estimated rate of LNAPL mass depletion through dissolution (**Equation 2**) is approximately 1.6 kilograms per year (kg/yr) and the rate of LNAPL mass depletion through biodegradation in the saturated zone (**Equation 3**) is approximately 27 kg/yr.

Using an LNAPL density of 0.8 grams per cubic centimeter (g/cm^3), the total equivalent volumetric LNAPL depletion rate for dissolution and biodegradation that occurs in groundwater as it moves through the source zone is approximately 36 liters per year (L/yr). The combined gasoline and diesel source zone footprint at the site is approximately 0.1 hectare (ha) giving an estimated depletion rate of approximately 350 L/ha/yr.

The above approach, based on changes in groundwater parameters as it moves through the source zone, only captures a small fraction of the total LNAPL losses with as much as 99 percent of losses occurring vertically through the vadose zone (Lundegard and Johnson, 2006; Suthersan et al., 2015). Additionally, electron acceptor processes evaluated using the aqueous phase mass budget approach can be subject to interferences that may be difficult to identify. For example, reduced iron and manganese may be immobilized on sediments through precipitation of sulfide and carbonate minerals (Ng et al., 2014) or may remain bound to insoluble oxyhydroxide coatings in soil (Beck and Mann, 2010). This can result in significant underestimation of iron-reducing and manganese-reducing biodegradation reactions as the immobilized reduction byproducts are not measurable in groundwater within and downgradient of the submerged source zone.

3.3.4. Detergents

Detergents were previously found in site groundwater. The suspected source of the detergents is the former car wash facility that was previously operated at the site. During the baseline campaign, a groundwater sample was collected from S12, the closest monitoring well to the former car tunnel wash system, in for detergent analysis.

Table 16 below shows that non-ionic detergents are still present in this monitoring well, but have decreased significantly from the 5,4 mg/l concentration registered back in May 2015..

Table 16. Laboratory results for detergents

Parameters		S12
Anionic detergents	mg/l	<0.1
Cationic detergents	mg/l	0.2
Non-ionic detergents	mg/l	1.7

While the detergents identified in well S12 area have been attributed to the former carwash due to proximity, microbial breakdown products of diesel could be potentially contributing to the detected concentrations.

3.4. CO_2 TRAPS STUDY

During the quarterly campaigns of October 2017 and April 2018, CO_2 traps where installed in the five locations investigated in this study: the background location (C5), the gasoline source area (C3 and C4) and the diesel source area (C1 and C2).

The raw results of CO_2 flux obtained for both monitoring rounds are shown in **Table 17**. The results are corrected according to the travel blanks and the ^{14}C isotope determinations, and are shown in **Table 18**. The laboratory reports, included in the **Annex**, describe the CO_2 flux estimation method and the corrections made to determine the equivalent fossil fuel component used in the calculation of the NSZD rates. Additionally, ^{13}C isotope results for the CO_2 from the traps are listed for the April 2018 campaign. **Figure 22** shows the distribution of NSZD rates distributed across the site.

Table 17. Raw results for CO_2 traps and ^{13}C isotope results

Site Area	Date	Location	Dry sorbent mass (g)	Number of replicates[1]	Average CO_2[2] (%)	Coefficient of variation CO_2[3] (%)	^{13}C results
-	October 2017	Travel blank	42.421	2	0.93	0.83	-
	April 2018	Travel blank 1	41.454	2	1.36	2.50	4
		Travel blank 2	42.351	2	1.55	4.74	-3
		Travel blank average	41.903	2	1.45	-	0
Diesel Source Area	October 2017	C1	40.636	2	1.10	1.30	-
		C2	42.096	2	1.36	0.01	-
	April 2018	C1	41.119	2	1.83	0.77	-9
		C2	40.879	2	1.33	2.29	-24
Gasoline Source area	October 2017	C3	44.358	2	10.40	1.91	-
		C4	45.141	2	14.85	2.34	-
	April 2018	C3	42.457	2	5.67	2.62	-25
		C4	37.869	2	5.17	4.87	-21
Background	October 2017	C5	44.467	2	5.53	0.83	-
	April 2018	C5	42.340	2	3.56	1.83	-16

Table 18. CO_2 trap results corrected according to travel blanks and ^{14}C isotope determinations

Site Area	Date	Location	Carbon content		CO_2[4] flux	Modern carbon	Standard deviation	Modern CO_2[4] flux	Adjusted fossil fuel carbon	Fossil fuel CO_2 mass	Fossil fuel CO_2 flux	Equivalent Fossil Fuel based NAPL loss rate[7]	
			%	(g)	(µmol/m²s)	%	%	(µmol/m²s)	%	(g)	(µmol/m²s)	(gallons/acre yr)	(L/ha· yr)
-	October 2017	Travel blank	-	-	-	79.9	0.24	-	23.9	-	-	-	-
	April 2018	Travel blank 1	-0.09	-0.04	-	68.1	0.36	-	35.2	-0.02	-	-	-
		Travel blank 2	0.09	0.04	-	67.0	0.25	-	36.2	0.02	-	-	-
		Travel blank average	0.00	0.00	-	67.6	0.31	-	35.7	0.00	-	-	-
Diesel Source Area	October 2017	C1	0.2	0.07	0.3	77.1	0.25	0.2	26.6	0.03	0.1	74	690
		C2	0.4	0.18	0.8	80.4	0.32	0.6	23.4	0.04	0.2	108	1,000
	April 2018	C1	0.38	0.16	0.38	73.8	0.25	0.36	29.7	0.01	0.03	16	150
		C2	-	-	-	65.7	0.43	-	37.4	-	-	-	-
Gasoline Source area	October 2017	C3	9.5	4.20	17.6	32.2	0.17	4.6	69.4	3.10	13.0	8113	76,000
		C4	13.9	6.28	26.4	21.8	0.14	4.5	79.2	5.21	21.9	13663	130,000
	April 2018	C3	4.22	1.79	4.44	43.4	0.17	1.48	58.7	1.19	2.96	1848	17,000
		C4	3.71	1.41	3.48	30.7	0.18	0.54	70.7	1.19	2.94	1839	17,000
Background	October 2017	C5	4.6	2.05	8.6	68.0	0.23	5.3	35.2	0.77	3.2	2006	19,000
	April 2018	C5	2.10	0.89	2.20	64.2	0.23	1.30	38.8	0.37	0.90	566	5,300

Notes

1- The carbon analyses were replicated when the coefficient of variation was ≤ 5%.
2- Percentage of CO_2 in the dry sorbent mass prior to travel blank corrections.
3- The coefficient of variation expresses the relation between the standard deviation and the average.
4- The transversal area of the traps is $8.11x10^{-3}$ m² (equivalent to a 4" pipe).
5- Percentage of modern carbon according to 1950's standard.
6- Adjusted fossil fuel carbon content according to ^{14}C isotope estimations based on modern carbon percentages (1950's standard).
7- Equivalent Fossil Fuel based NAPL loss rate have been estimated based on the Fossil fuel CO2 flux assuming the formula C_8H_{18} and a hydrocarbon density of 0.77 g/mL.

Figure 23. CO_2 trap results (L/ha/yr) distributed across the site.

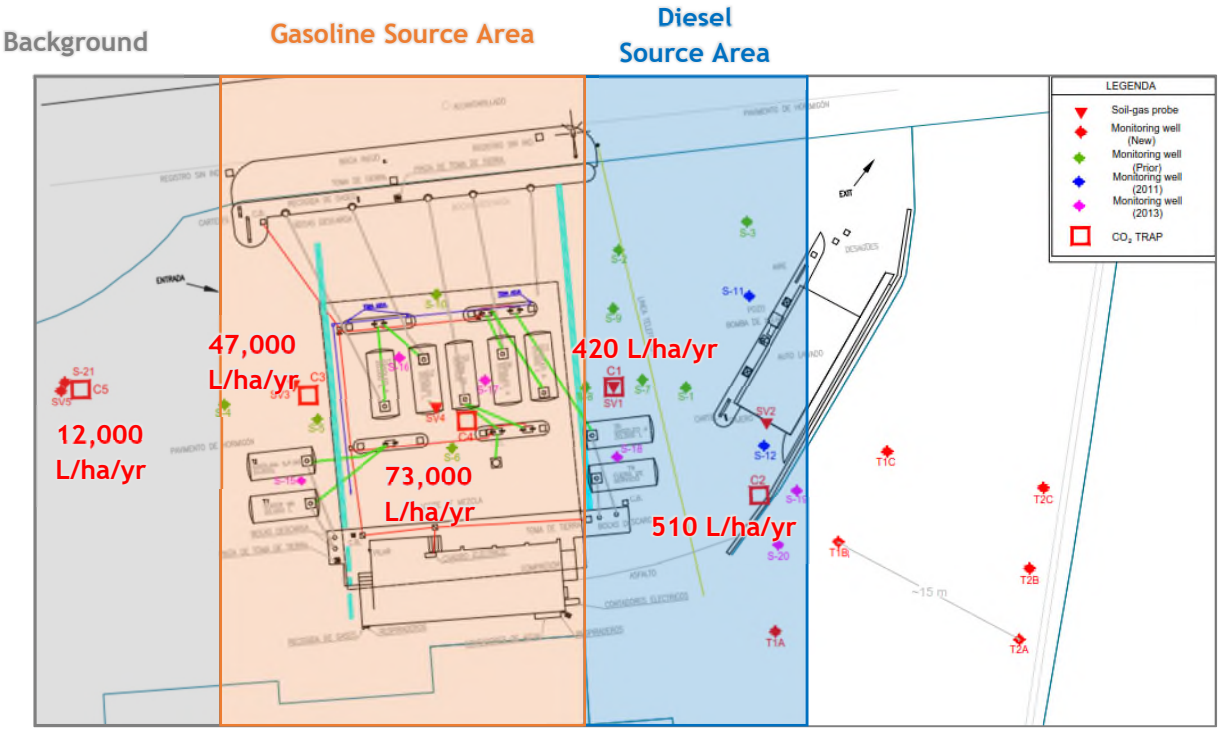

According to the location of results in **Figure 22**, the maximum biodegradation rates are present in the gasoline source area, whereas the minimum rates are observed within the diesel source area. Moreover, the biodegradation rates related to the background location are high compared to the diesel source area.

The standard assumptions for interpreting CO_2 flux results assume uniform, vertical gas exchange between the vadose zone and atmosphere. As noted previously, the entire site is paved, with asphalt pavement present in the western portion of the site (background and western portion of the gasoline area), and concrete pavement present in the central and eastern portion of the site. Gas phase diffusivity of the pavement materials at the site were not measured directly, however, Peng et al. (2012) report an estimate for oxygen diffusivity of intact, competent asphalt pavement less than 9.8×10^{-9} m^2/sec (more than an order of magnitude lower than the average oxygen diffusivity estimated for site soils). Estimated oxygen diffusion coefficients for intact concrete in the literature generally range from 5×10^{-9} m^2/sec to 1×10^{-7} m^2/sec (Comité Euro-International du Béton, 1990; Peng et al., 2012; Yoon et al., 2018). While gas diffusivity in competent asphalt and concrete pavement may be of similar magnitude, cracks and fissures appear to be more abundant in the concrete pavement areas, and thus there is likely greater exchange of gases between the subsurface and atmosphere in these areas. This may explain why there is evidence of significant lateral diffusion of petroleum-derived CO_2 at the background trap location (where asphalt pavement is present), but not at the CO_2 traps located in the diesel area.

Additionally, the presence of inorganic carbon in the form of carbonates in soil may also complicate the interpretation of the CO_2 trap results, as CO_2 produced from biodegradation of petroleum hydrocarbons at depth may react and go into solution within a bicarbonate-buffered system. Under these circumstances, CO_2 traps

provide results that need to be evaluated on the basis of site-specific conditions, where:

- The higher biodegradation rates in the gasoline area likely represent degradation of shallow contamination immediately below the paved surface
- The low biodegradation rate in the diesel area may be due to lateral off-set of CO_2 diffusing upward from the source, or reactions between CO_2 produced at depth with carbonate minerals in soil and pore water.
- The higher biodegradation rates observed at the background location are likely the result of lateral vapour transport from areas of the site where hydrocarbon impacts are present.

It appears that the CO_2 trap deployment method using the vapour pins to equilibrate pressure and avoid the stack or chimney effect that often results due to the contrast in gas diffusivity between soil and pavement was effective. Other than the high CO_2 flux measured at location C4 in the gasoline area in October 2017, the measured NSZD rates results do not appear to be biased high relative to NSZD rates reported in literature (e.g., Garg et al., 2017). However, while the approach appears to have mitigated the stack effect, the CO_2 trap method includes a simplifying assumption of one-dimensional gas transport, i.e. it is assumed that the CO_2 measured at the surface is derived from petroleum present in the subsurface directly below the trap. In reality there is likely lateral transport of CO_2 to fissures in the pavement. Under these circumstances and for this particular site, CO_2 traps apparently provide results that do not account for all the vapour transport pathways. Thus, the possible existence of a significant lateral flow undermines the reliability of CO_2 traps for quantifying NSZD at the site. However, the observation that petroleum-derived CO_2 is being produced is a direct line of evidence that NSZD is occurring.

3.5. SOIL-GAS PROFILING STUDY

This soil gas profiling study was conducted not only to quantify biodegradation rates in the source areas, but also to assess whether existing monitoring wells can provide reliable vapour profiles compared to multi-level soil vapour probes specifically installed for NSZD evaluation.

3.5.1. Soil-gas profiles using designated probes

O_2 and CO_2 concentrations have been measured at three depths from each probe location during the NSZD monitoring program. **Figures 23** to **27** show the distribution of results from the baseline (June 2017) and the four quarterly monitoring rounds conducted throughout the study period (October 2017, January 2018, April 2018 and July 2018).

Figure 24. Results of CO_2 and O_2 in soil vapour probes – Baseline June 2017.

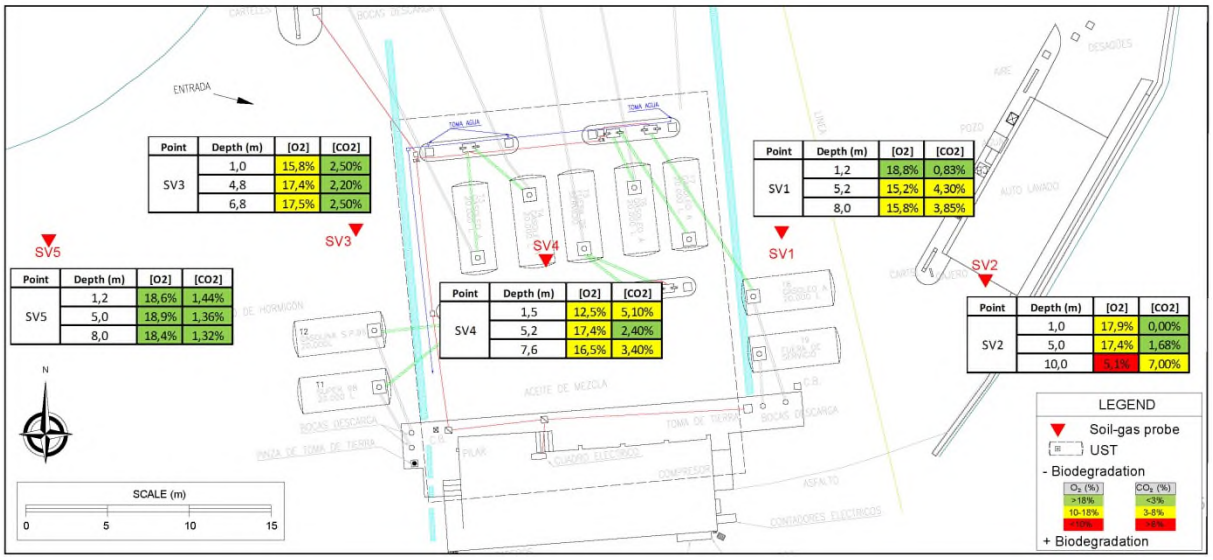

Figure 25. Results of CO_2 and O_2 in soil vapour probes – First quarter October 2017.

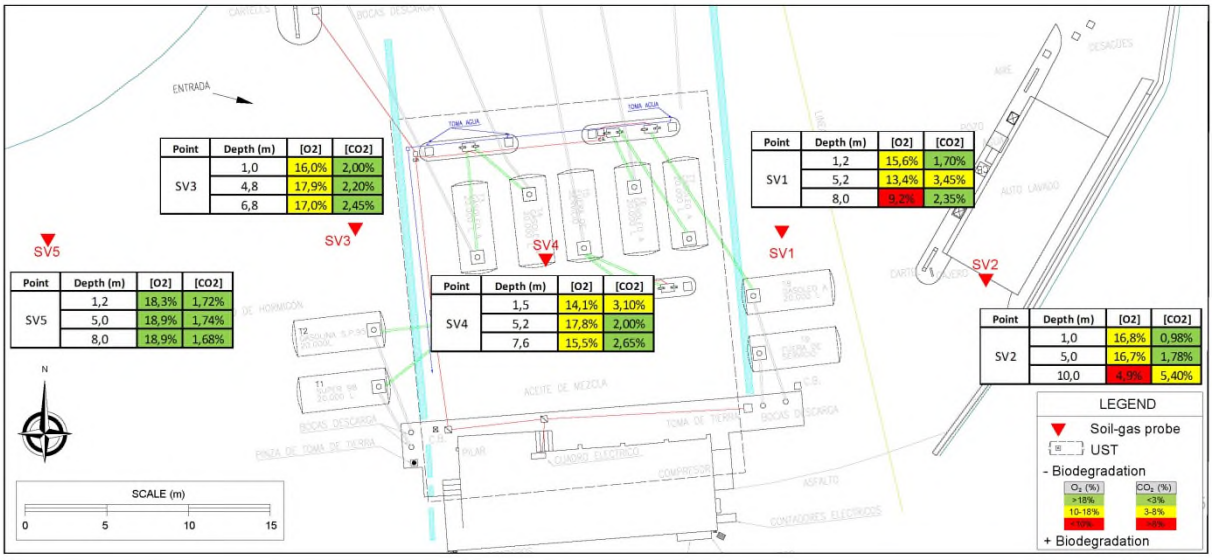

Figure 26. Results of CO_2 and O_2 in soil vapour probes – Second quarter January 2018.

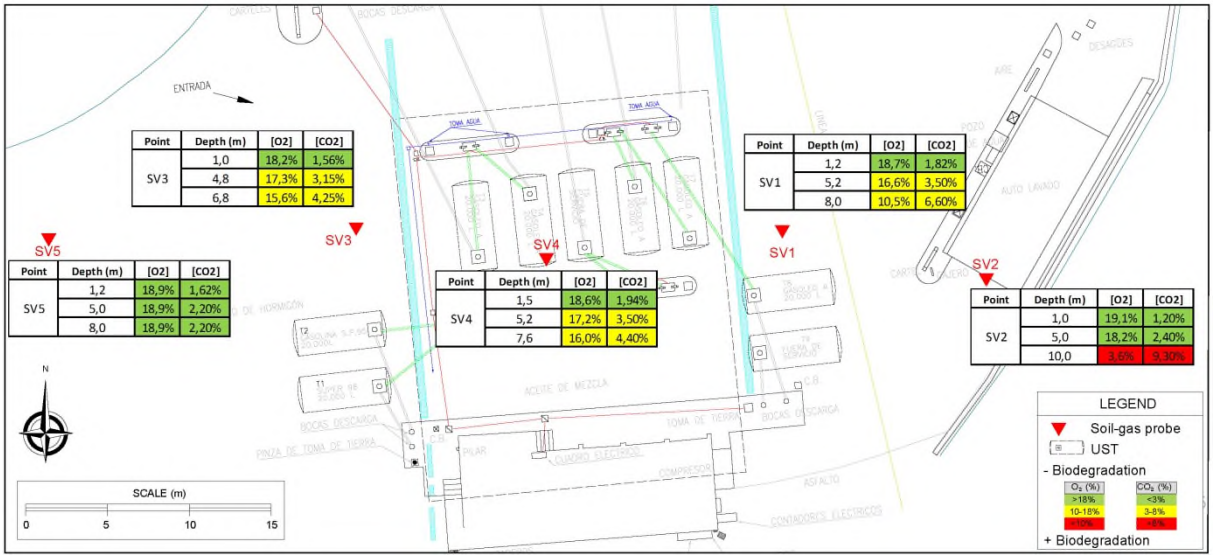

Point	Depth (m)	[O2]	[CO2]
SV3	1,0	18,2%	1,56%
	4,8	17,3%	3,15%
	6,8	15,6%	4,25%

Point	Depth (m)	[O2]	[CO2]
SV5	1,2	18,9%	1,62%
	5,0	18,9%	2,20%
	8,0	18,9%	2,20%

Point	Depth (m)	[O2]	[CO2]
SV4	1,5	18,6%	1,94%
	5,2	17,2%	3,50%
	7,6	16,0%	4,40%

Point	Depth (m)	[O2]	[CO2]
SV1	1,2	18,7%	1,82%
	5,2	16,6%	3,50%
	8,0	10,5%	6,60%

Point	Depth (m)	[O2]	[CO2]
SV2	1,0	19,1%	1,20%
	5,0	18,2%	2,40%
	10,0	3,6%	9,30%

Figure 27. Results of CO_2 and O_2 in soil vapour probes – Third quarter April 2018.

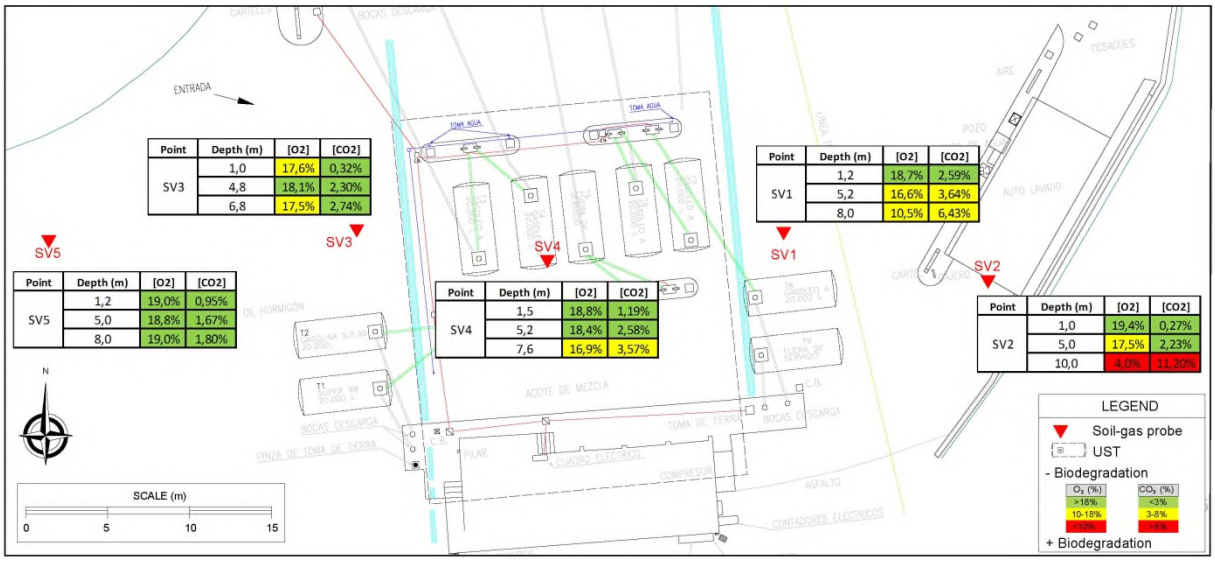

Point	Depth (m)	[O2]	[CO2]
SV3	1,0	17,6%	0,32%
	4,8	18,1%	2,30%
	6,8	17,5%	2,74%

Point	Depth (m)	[O2]	[CO2]
SV5	1,2	19,0%	0,95%
	5,0	18,8%	1,67%
	8,0	19,0%	1,80%

Point	Depth (m)	[O2]	[CO2]
SV4	1,5	18,8%	1,19%
	5,2	18,4%	2,58%
	7,6	16,9%	3,57%

Point	Depth (m)	[O2]	[CO2]
SV1	1,2	18,7%	2,59%
	5,2	16,6%	3,64%
	8,0	10,5%	6,43%

Point	Depth (m)	[O2]	[CO2]
SV2	1,0	19,4%	0,27%
	5,0	17,5%	2,23%
	10,0	4,0%	11,20%

Figure 28. Results of CO_2 and O_2 in soil vapour probes – Fourth quarter July 2018.

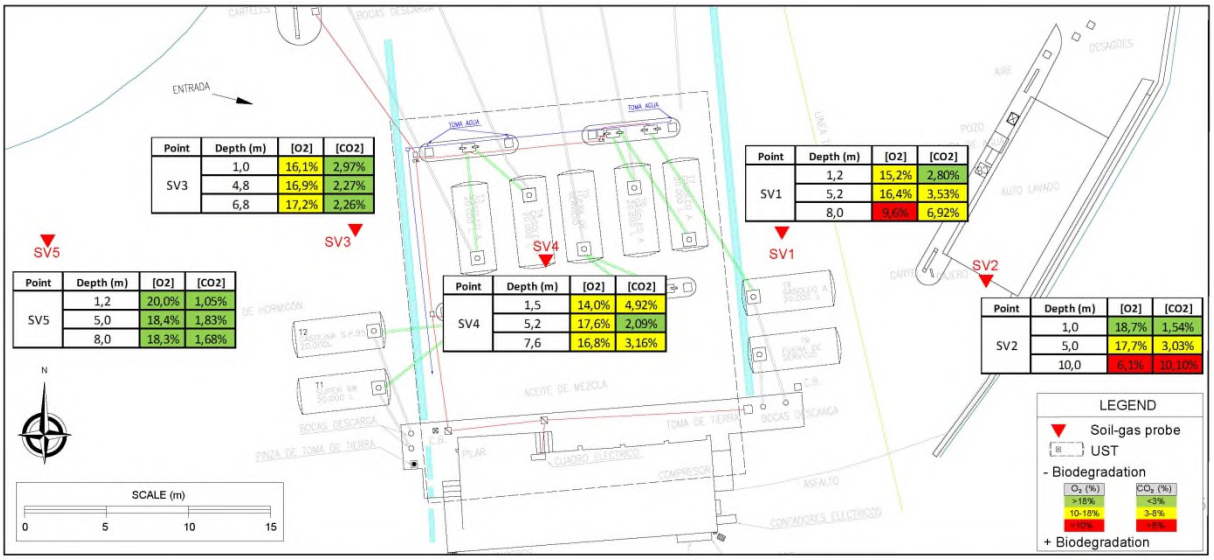

Generally, the O_2 and CO_2 profile data from soil gas probes indicate:

- Relative to the background location, lower concentrations of O_2 and higher concentrations of CO_2 are generally present in the gasoline and diesel area, with the lowest O_2 and highest CO_2 concentrations generally observed at the deepest soil gas probes.
- Minor depletion of O_2 and low CO_2 content in soil gas collected from the background location (SV5); the presence of percent levels of CO_2 in soil gas at the background location further suggests that lateral gas transport is occurring.
- Biodegradation processes predominantly taking place in the smear zone of the diesel source area (SV1 and SV2), evidenced by the lower O_2 and higher CO_2 content near the base of the vadose zone. In June 2017, soil gas profiles from SV1 indicate increasing O_2 and decreasing CO_2 with depth between the probes installed at 5.2 and 8.0 mbgs, which suggests lateral gas transport.
- The presence of shallow impacts within the UST secondary containment of the central area of the site (SV4), as suggested by the lower O_2 and higher CO_2 content detected in the shallow probe, when compared to the deeper probes, in three of the quarterly monitoring rounds conducted (baseline, first quarter and fourth quarter). The observation of increasing O_2 and/or decreasing CO_2 with depth at SV4 in June 2017, October 2017, and July 2018 suggest lateral soil gas transport is occurring within the upper 5 to 6 meters of the vadose zone.
- As with SV4, soil gas profiles collected from SV3 in June 2017, October 2017, April 2018, and July 2018 indicate increased concentrations of O_2 between the upper probe at 1 mbgs and the probe installed at 4.8 mbgs, indicating lateral transport of soil gas within the upper 5 meters of the vadose zone. The fact that ^{14}C results for the soil vapour sample collected from SV3's bottom probe were similar to those of the background (see section 4.2) provides an additional line of evidence for lateral gas transport.

The observation of depleted O_2 and higher CO_2 levels in the source zone locations relative to background provides evidence that NSZD is occurring. Given that there are multiple lines of evidence indicating lateral soil gas transport in the upper 5 to 6 meters of the vadose zone, the standard assumption of vertical (1-dimensional) soil gas transport at the site is not realistic. Soil gas data collected from monitoring wells screened across the water table (see Section 4.5.2), suggest a transition to a vertical transport regime near the base of the vadose zone. Using the data collected from the lower two probes (approximately 5 and 8 m bgs) to define vertical concentration gradients for O_2 and CO_2, biodegradation rates were estimated using the following equation (Davis et al., 2009):

$$H_{bio;HC}\ (g/m^2 \cdot day) = dC / dz * De / CF \qquad \textbf{Equation 1}$$

Where:

dC/dz = O_2 or CO_2 concentration gradient (g/m^4)

De = effective diffusion coefficient calculated on basis of air filled porosity and total porosity values published by USCS for well graded sands.

CF = stoichiometric conversion factor (mass rate) for biodegradation reaction – O_2 / HC or CO_2 / HC

Mass loss rates calculated using Equation 1 have also been converted to equivalent volumetric LNAPL depletion rate units using a density of 0.77 grams per cubic centimeter (g/cm^3) for gasoline and 0.85 g/cm^3 for diesel. The following spreadsheets (**Figures 28** to **32**) list the field data used, and the step-by-step determination of the biodegradation rate for each SVP per monitoring round. The annual average biodegradation rates in the gasoline area (85 - 490 L/ha/yr) are lower than those obtained in the diesel area (460 – 1,500 L/ha/yr), with the biodegradation rate in the background area being negligible.

Special attention should be paid to the fact that average biodegradation rates based on O_2 and CO_2 profiles yield comparable values (**Figures 28** to **32**). However, rates estimated from O_2 gradients are generally higher than those measured from CO_2 gradients. On average, rates estimated from O_2 gradients using SVPs are approximately 46 percent higher than rates estimated from CO_2 gradients in the diesel area, and 20 percent higher in the gasoline area.

As indicated above, these calculations assume that gas transport is vertical, whereas data from the soil gas probes suggests lateral soil gas transport within the upper 5 to 6 meters of the vadose zone. It is acknowledged that the limited number of vertical sampling points at each SVP location do not provide sufficient resolution within the vertical transport regime at the base of the vadose zone, and thus NSZD rate estimates obtained from the soil gas probes are likely biased low.

While the presence of methane in soil gas is a line of evidence for anaerobic degradation of hydrocarbons, the accuracy of the measurement is not as critical as that for O_2 or CO_2 for quantifying NSZD rates. Therefore, two different lower quality methods were used in the study. The 'explosivity' measurement was used during the baseline (June 2017) and the following two quarterly monitoring rounds (October 2017 and January 2018). Direct methane measurement was used for the third and fourth quarterly monitoring rounds (April and July 2018). Both methods showed that methane concentration in the soil vapour is <1 %. The low levels of CH_4 detected in soil gas, along with the observation of O_2 at concentrations greater than 5 vol% at many of the SVPs suggests that either much of the depletion at the site is

occurring through direct aerobic oxidation of hydrocarbons within the smear zone, or that methanogenesis dominates within a very thin interval that may be difficult to resolve through conventional soil gas sampling techniques.

As observed in (**Figures 28** to **32**), CH_4, O_2 and CO_2 profiles show different trends depending on location:

- SV5 shows little change in O_2 and CO_2 concentration with depth in the vadose zone, indicating that limited biodegradation is occurring at the background location.
- Vapor probes in gasoline area (SV3 and SV4) exhibit an inverted profile in the upper 5 meters of the vadose zone with lower O_2 and higher CO_2 in the shallowest probes. At both locations, shallow impacts were identified during investigation campaigns.
- Soil gas profiling results from the diesel area vapour probes (SV1bis and SV2) generally exhibit decreasing O_2 and increasing CO_2 with depth, and detections of CH_4 in the lower-most probes (fall and winter of 2018 at SV1bis, and in all monitoring events except summer 2018 at SV2). However, instances where O_2 increases with depth (July 2018) and CO_2 decreases with depth (October 2017) at SV1 are observed. Additionally, there are several cases where the relative decrease in O_2 and increase in CO_2 between the upper two probes at SV2 do not match those predicted by aerobic hydrocarbon oxidation stoichiometry (June 2017, October 2017, January 2018, and July 2018). In each of these instances, CO_2 production with depth is lower than would be predicted using the observed O_2 depletion by a factor of two.

The above observations are consistent with the CO_2 trap results. The inversions in O_2 and CO_2 trends with depth suggest that there is significant lateral gas transport is occurring at the site, while the relative difference in the rate of O_2 depletion and CO_2 production with depth suggests that carbonate minerals in soil may be acting as a CO_2 sink that may reduce the magnitude of CO_2 flux to the atmosphere.

Figure 29. O_2 and CO_2 Profiles in Multi-level Soil Gas Probes - Baseline (June 2017)

Gas Measurements in Soil-Gas Probes	Background location				Gasoline zone								Diesel zone							
	SV5	SV5	SV5	SV5	SV3	SV3	SV3	SV3	SV4	SV4	SV4	SV4	SV1	SV1	SV1	SV1	SV2	SV2	SV2	SV2
	Depth (m)	[O2]%	[CO2]%	[CH4]%	Depth (m)	[O2]%	[CO2]%	[CH4]%	Depth (m)	[O2]%	[CO2]%	[CH4]%	Depth (m)	[O2]%	[CO2]%	[CH4%	Depth (m)	[O2]%	[CO2]%	[CH4%
	1.2	18.6%	1.44%	0.00%	1.0	15.8%	2.50%	0.00%	1.5	12.5%	5.10%	0.00%	1.2	18.8%	0.83%	0.00%	1.0	17.9%	0.00%	0.00%
	5.0	18.9%	1.36%	0.00%	4.8	17.4%	2.20%	0.00%	5.2	17.4%	2.40%	0.00%	5.2	15.2%	4.30%	0.00%	5.0	17.4%	1.68%	0.00%
	8.0	18.4%	1.32%	0.00%	6.8	17.5%	2.50%	0.00%	7.6	16.5%	3.40%	0.00%	8.0	15.8%	3.85%	0.00%	10.0	5.1%	7.00%	0.50%
%O2 %CO2 %CH4	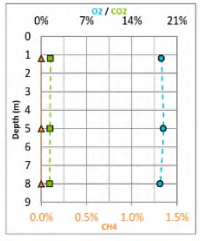				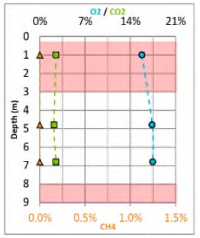				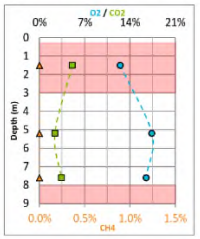				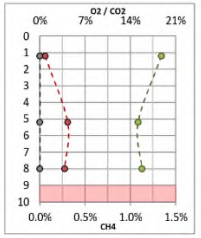				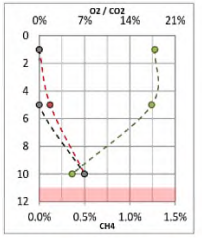			
Impacted or potentially impacted soil																				
dC/dZ %O_2 or CO_2/m		0.02%	-0.02%			-0.05%	0.15%			0.37%	0.42%			0.90%	0.87%			2.46%	1.06%	
dC/dZ g/m^4		0.3	-0.3			-0.7	2.8			5.1	7.8			12.2	16.1			33.3	19.8	
F g/m^2-day		0.0	0.0			0.0	0.1			0.1	0.2			0.3	0.4			0.9	0.5	
Stoichiometric Coefficient g-O_2 or g-CO_2/gHC		3.33	3.19			3.33	3.19			3.33	3.19			3.40	3.32			3.40	3.32	
$Hbio_{HC}$ (Average) gHC/m^2-day		**0.0**	**0.0**			**0.0**	**0.0**			**0.0**	**0.1**			**0.1**	**0.1**			**0.3**	**0.1**	
NSZD Rate (gal/acre/yr)		**1**	**-1**			**-3**	**11**			**21**	**30**			**49**	**60**			**133**	**74**	
NSZD Rate (L/ha/yr)		**13**	**-12**			**-26**	**102**			**194**	**282**			**455**	**564**			**1,244**	**692**	

Figure 30. O_2 and CO_2 Profiles in Multilevel Soil Gas Probes - October 2017

Gas Measurements in Soil-Gas Probes	Background location				Gasoline zone								Diesel zone							
	SV5	SV5	SV5	SV5	SV3	SV3	SV3	SV3	SV4	SV4	SV4	SV4	SV1 bis	SV1 bis	SV1 bis	SV1 bis	SV2	SV2	SV2	SV2
	Depth (m)	[O2]%	[CO2]%	[CH4]%	Depth (m)	[O2]%	[CO2]%	[CH4]%	Depth (m)	[O2]%	[CO2]%	[CH4]%	Depth (m)	[O2]%	[CO2]%	[CH4%	Depth (m)	[O2]%	[CO2]%	[CH4%
	1.2	18.3%	1.72%	0.00%	1.0	16.0%	2.00%	0.00%	1.5	14.1%	3.10%	0.00%	1.2	15.6%	1.70%	0.00%	1.0	16.8%	0.98%	0.00%
	5.0	18.9%	1.74%	0.00%	4.8	17.9%	2.20%	0.00%	5.2	17.8%	2.00%	0.00%	5.2	13.4%	3.45%	0.00%	5.0	16.7%	1.78%	0.00%
	8.0	18.9%	1.68%	0.00%	6.8	17.0%	2.45%	0.00%	7.6	15.5%	2.65%	0.00%	8.0	9.2%	2.35%	0.30%	10.0	4.9%	5.40%	0.45%
%O2 %CO2 %CH4	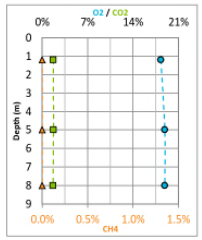				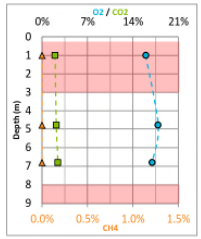				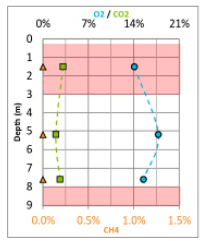				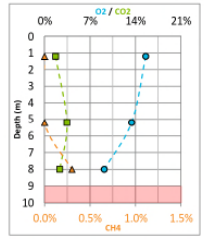				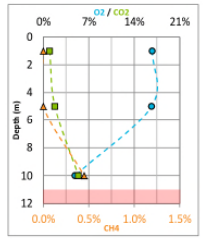			
Impacted or potentially impacted soil																				
dC/dZ %O2 or CO2/m		0.00%	-0.02%			0.45%	0.13%			0.96%	0.27%			1.50%	-0.39%			2.36%	0.72%	
dC/dZ g/m4		0.0	-0.4			6.1	2.3			13.0	5.0			20.3	-7.3			31.9	13.5	
F g/m2-day		0.0	0.0			0.2	0.1			0.3	0.1			0.5	-0.2			0.9	0.3	
Stoichiometric Coefficient g-O_2 or g-CO_2/gHC		3.33	3.19			3.33	3.19			3.33	3.19			3.40	3.32			3.40	3.32	
$Hbio_{HC}$ gHC/m2-day		**0.0**	**0.0**			**0.0**	**0.0**			**0.1**	**0.0**			**0.2**	**-0.1**			**0.3**	**0.1**	
NSZD Rate (gal/acre/yr)		**0**	**-1**			**25**	**9**			**53**	**20**			**81**	**-27**			**128**	**50**	
NSZD Rate (L/ha/yr)		**0**	**-14**			**232**	**85**			**495**	**184**			**759**	**-256**			**1,194**	**471**	

Figure 31. O_2 and CO_2 Profiles in Multi-level Soil Gas Probes - January 2018

Gas Measurements in Soil-Gas Probes	Background location				Gasoline zone								Diesel zone							
	SV5	SV5	SV5	SV5	SV3	SV3	SV3	SV3	SV4	SV4	SV4	SV4	SV1 bis	SV1 bis	SV1 bis	SV1 bis	SV2	SV2	SV2	SV2
	Depth (m)	[O2]%	[CO2]%	[CH4]%	Depth (m)	[O2]%	[CO2]%	[CH4]%	Depth (m)	[O2]%	[CO2]%	[CH4]%	Depth (m)	[O2]%	[CO2]%	[CH4%	Depth (m)	[O2]%	[CO2]%	[CH4%
	1.2	18.9%	1.62%	0.00%	1.0	18.2%	1.56%	0.30%	1.5	18.6%	1.94%	0.30%	1.2	18.7%	1.82%	0.00%	1.0	19.1%	1.20%	0.00%
	5.0	18.9%	2.20%	0.20%	4.8	17.3%	3.15%	0.40%	5.2	17.2%	3.50%	0.40%	5.2	16.6%	3.50%	0.25%	5.0	18.2%	2.40%	0.00%
	8.0	18.9%	2.20%	0.00%	6.8	15.6%	4.25%	0.50%	7.6	16.0%	4.40%	0.45%	8.0	10.5%	6.60%	0.55%	10.0	3.6%	9.30%	0.80%
%O2 %CO2 %CH4	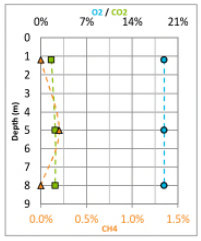				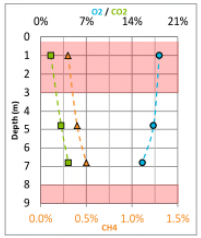				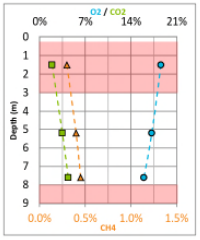				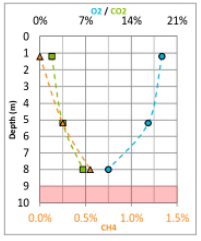				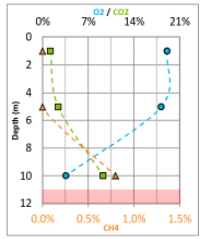			
Impacted or potentially impacted soil																				
dC/dZ %O2 or CO2/m		0.00%	0.00%			0.85%	0.55%			0.50%	0.38%			2.18%	1.11%			2.92%	1.38%	
dC/dZ g/m4		0.0	0.0			11.5	10.2			6.8	7.0			29.5	20.6			39.5	25.7	
F g/m2-day		0.0	0.0			0.3	0.3			0.2	0.2			0.8	0.5			1.1	0.6	
Stoichiometric Coefficient g-O_2 or g-CO_2/gHC		3.33	3.19			3.33	3.19			3.33	3.19			3.40	3.32			3.40	3.32	
$Hbio_{HC}$ gHC/m2-day		**0.0**	**0.0**			**0.1**	**0.1**			**0.1**	**0.1**			**0.2**	**0.2**			**0.3**	**0.2**	
NSZD Rate (gal/acre/yr)		**0**	**0**			**47**	**40**			**28**	**27**			**118**	**77**			**158**	**96**	
NSZD Rate (L/ha/yr)		**0**	**0**			**439**	**373**			**258**	**254**			**1,102**	**720**			**1,477**	**898**	

Figure 32. O_2 and CO_2 Profiles in Multi-level Soil Gas Probes - April 2018

Gas Measurements in Soil-Gas Probes	Background location				Gasoline zone								Diesel zone							
	SV5	SV5	SV5	SV5	SV3	SV3	SV3	SV3	SV4	SV4	SV4	SV4	SV1 bis	SV1 bis	SV1 bis	SV1 bis	SV2	SV2	SV2	SV2
	Depth (m)	[O2]%	[CO2]%	[CH4]%	Depth (m)	[O2]%	[CO2]%	[CH4]%	Depth (m)	[O2]%	[CO2]%	[CH4]%	Depth (m)	[O2]%	[CO2]%	[CH4%	Depth (m)	[O2]%	[CO2]%	[CH4%
	1.2	18.9%	1.62%	0.00%	1.0	18.2%	1.56%	0.30%	1.5	18.6%	1.94%	0.30%	1.2	18.7%	1.82%	0.00%	1.0	19.1%	1.20%	0.00%
	5.0	18.9%	2.20%	0.20%	4.8	17.3%	3.15%	0.40%	5.2	17.2%	3.50%	0.40%	5.2	16.6%	3.50%	0.25%	5.0	18.2%	2.40%	0.00%
	8.0	18.9%	2.20%	0.00%	6.8	15.6%	4.25%	0.50%	7.6	16.0%	4.40%	0.45%	8.0	10.5%	6.60%	0.55%	10.0	3.6%	9.30%	0.80%
%O2 %CO2 %CH4	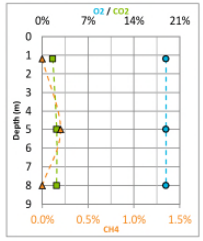				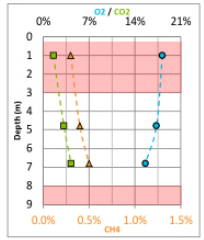				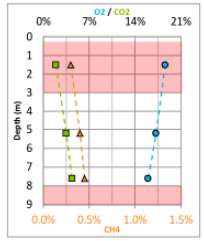				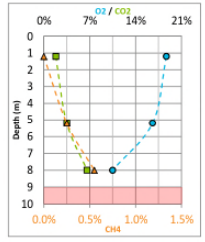				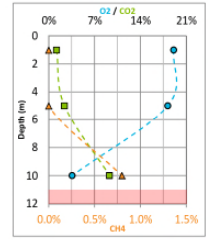			
Impacted or potentially impacted soil																				
dC/dZ %O2 or CO2/m		0.00%	0.00%			0.85%	0.55%			0.50%	0.38%			2.18%	1.11%			2.92%	1.38%	
dC/dZ g/m4		0.0	0.0			11.5	10.2			6.8	7.0			29.5	20.6			39.5	25.7	
F g/m2-day		0.0	0.0			0.3	0.3			0.2	0.2			0.8	0.5			1.1	0.6	
Stoichiometric Coefficient g-O_2 or g-CO_2/gHC		3.33	3.19			3.33	3.19			3.33	3.19			3.40	3.32			3.40	3.32	
$Hbio_{HC}$ gHC/m2-day		**0.0**	**0.0**			**0.1**	**0.1**			**0.1**	**0.1**			**0.2**	**0.2**			**0.3**	**0.2**	
NSZD Rate (gal/acre/yr)		**0**	**0**			**47**	**40**			**28**	**27**			**118**	**77**			**158**	**96**	
NSZD Rate (L/ha/yr)		**0**	**0**			**439**	**373**			**258**	**254**			**1,102**	**720**			**1,477**	**898**	

Figure 33. O_2 and CO_2 Profiles in Multi-level Soil Gas Probes - July 2018

Gas Measurements in Soil-Gas Probes	Background location				Gasoline zone								Diesel zone							
	SV5	SV5	SV5	SV5	SV3	SV3	SV3	SV3	SV4	SV4	SV4	SV4	SV1 bis	SV1 bis	SV1 bis	SV1 bis	SV2	SV2	SV2	SV2
	Depth (m)	[O2]%	[CO2]%	[CH4]%	Depth (m)	[O2]%	[CO2]%	[CH4]%	Depth (m)	[O2]%	[CO2]%	[CH4]%	Depth (m)	[O2]%	[CO2]%	[CH4%	Depth (m)	[O2]%	[CO2]%	[CH4%
	1.2	20.0%	1.05%	0.00%	1.0	16.1%	2.97%	0.00%	1.5	14.0%	4.92%	0.00%	1.2	15.2%	2.80%	0.00%	1.0	18.7%	1.54%	0.00%
	5.0	18.4%	1.83%	0.00%	4.8	16.9%	2.27%	0.00%	5.2	17.6%	2.09%	0.00%	5.2	16.4%	3.53%	0.00%	5.0	17.7%	3.03%	0.00%
	8.0	18.3%	1.68%	0.00%	6.8	17.2%	2.26%	0.00%	7.6	16.8%	3.16%	0.00%	8.0	9.6%	6.92%	0.00%	10.0	6.1%	10.10%	0.00%
%O2 %CO2 %CH4 Impacted or potentially impacted soil	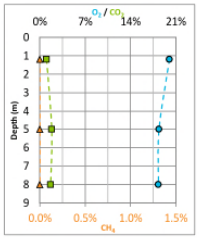				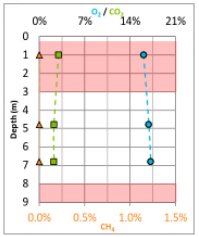				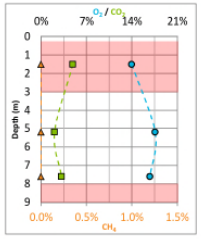				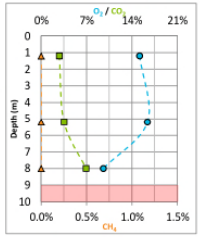				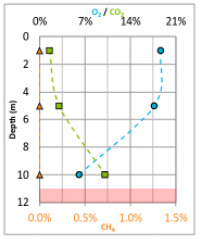			
dC/dZ %O2 or CO2/m		0.03%	-0.05%			-0.15%	-0.01%			0.33%	0.45%			2.43%	1.21%			2.32%	1.41%	
dC/dZ g/m4		0.5	-0.9			-2.0	-0.1			4.5	8.3			32.9	22.5			31.4	26.3	
F g/m2-day		0.0	0.0			-0.1	0.0			0.1	0.2			0.9	0.6			0.8	0.6	
Stoichiometric Coefficient g-O_2 or g-CO_2/gHC		3.33	3.19			3.33	3.19			3.33	3.19			3.40	3.32			3.40	3.32	
$Hbio_{HC}$ gHC/m2-day		**0.0**	**0.0**			**0.0**	**0.0**			**0.0**	**0.1**			**0.3**	**0.2**			**0.2**	**0.2**	
NSZD Rate (gal/acre/yr)		**2**	**-4**			**-8**	**0**			**18**	**32**			**131**	**84**			**125**	**98**	
NSZD Rate (L/ha/yr)		**17**	**-34**			**-77**	**-3**			**172**	**302**			**1,228**	**787**			**1,173**	**920**	

3.5.2. Soil-gas profiles in monitoring wells

O_2 and CO_2 concentrations in the vadose zone have been also measured through the screened intervals in the monitoring wells. Measurements were made at meter intervals from the smear zone up to the top of the screened section in each well. **Figures 33** to **37** show the data distributions for the five quarterly monitoring rounds conducted throughout the one-year study period.

The O_2 and CO_2 profiles measured in monitoring wells are consistent with the following interpretations:

- The background location (S21) is free of significant impact at depth, with generally similar concentrations of O_2 and CO_2 at all depths.
- NSZD is documented in the smear zone of the diesel (S7, S8, S12, S18, S19, S20) and gasoline source areas (S5, S6, S10, S16 and S17), as low O_2 and higher CO_2 concentrations exist at depths close to the water table.
- Both O_2 and CO_2 profiles indicate little biodegradation is taking place in the furthest downgradient transect (T2 A/B/C), whereas profiles in the nearest transect (T1 A/B/C) indicate biodegradation may still be occurring immediately downgradient of the LNAPL source zone, evidenced by O_2 and CO_2 content similar to that measured in the diesel source area.

Similar to the SVPs, increases in O_2 and decreases in CO_2 with depth were observed at several monitoring wells, indicating lateral soil gas transport in the upper portion of the vadose zone. However, soil gas data collected from monitoring wells generally indicate decreasing O_2 and increasing CO_2 with depth near the base of the vadose zone, within and above the LNAPL smear zone.

This spatial distributions of O_2 and CO_2 at depth in the monitoring wells are generally consistent with the detected concentrations of contaminants of concern in groundwater (see section 4.3.2).

Figure 34. Results of O_2 and CO_2 Profile Measurements in Monitoring Wells – Baseline: June 2017

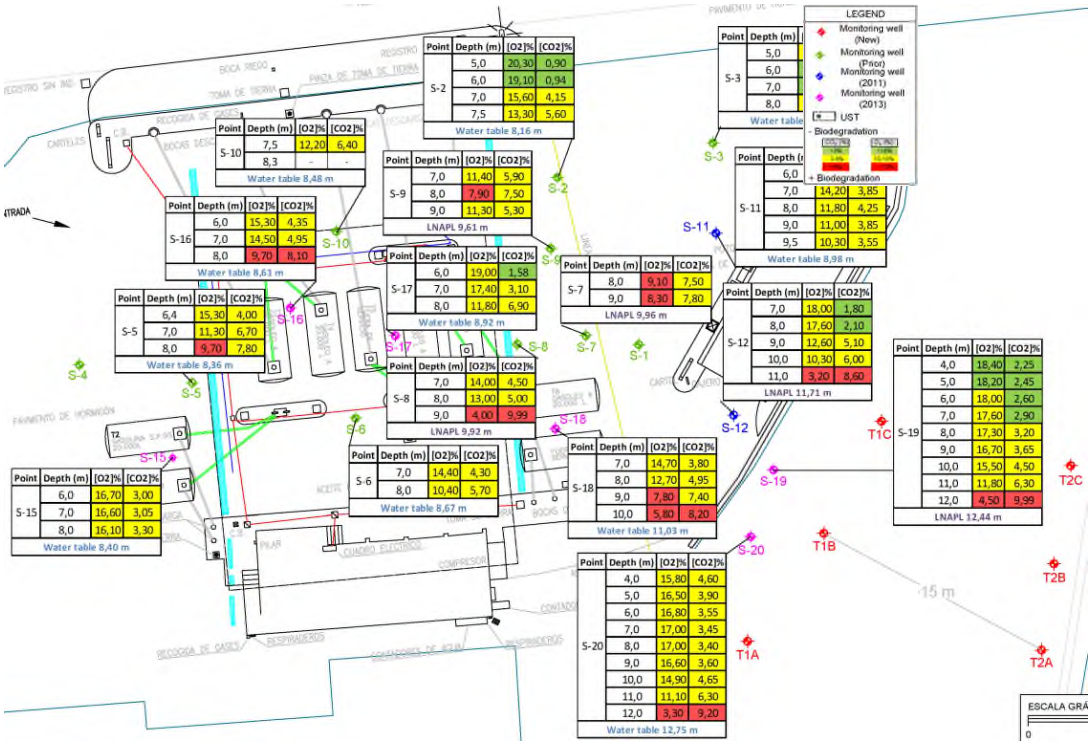

Figure 35. Results of O_2 and CO_2 Profile Measurements in Monitoring Wells - October 2017

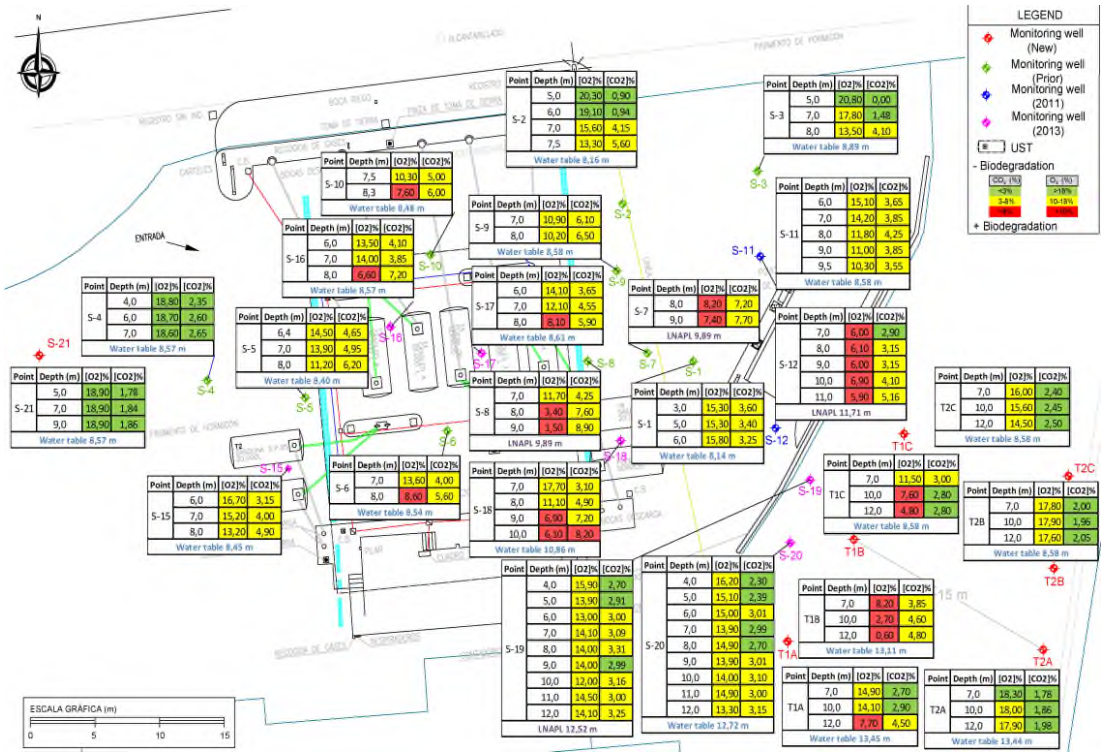

Figure 36. Results of O_2 and CO_2 Profiling in Monitoring Wells - January 2018

Figure 37. Results of O_2 and CO_2 Profiling in Monitoring Wells - April 2018

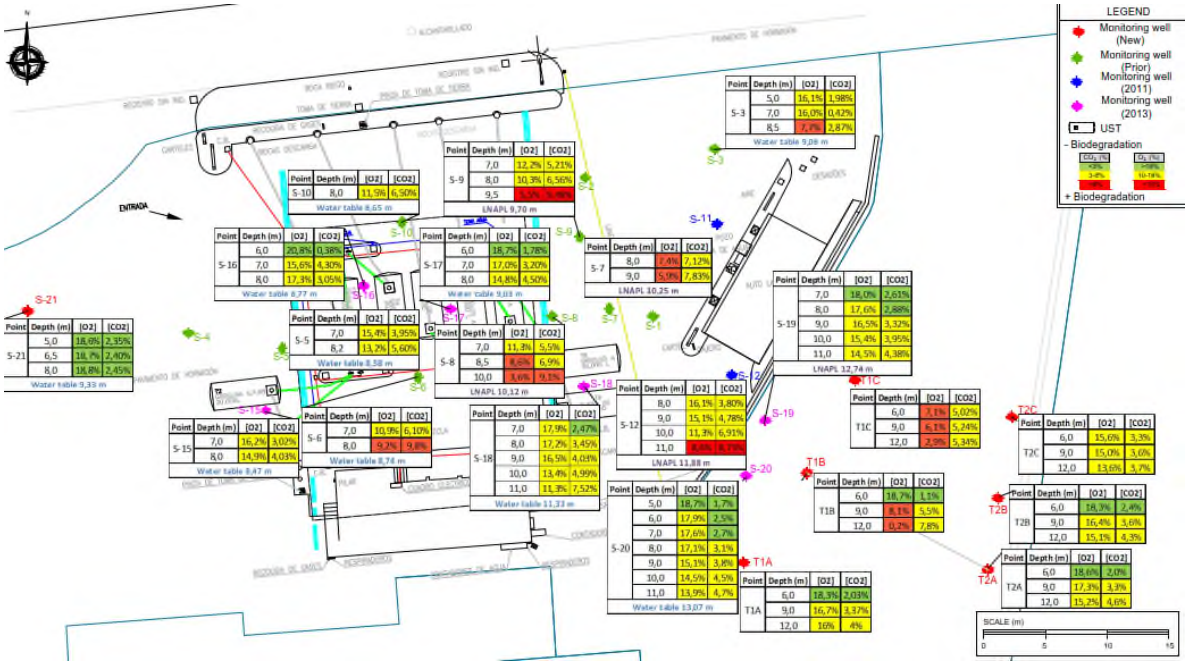

Figure 38. Results of O_2 and CO_2 Profiling in Monitoring Wells - July 2018

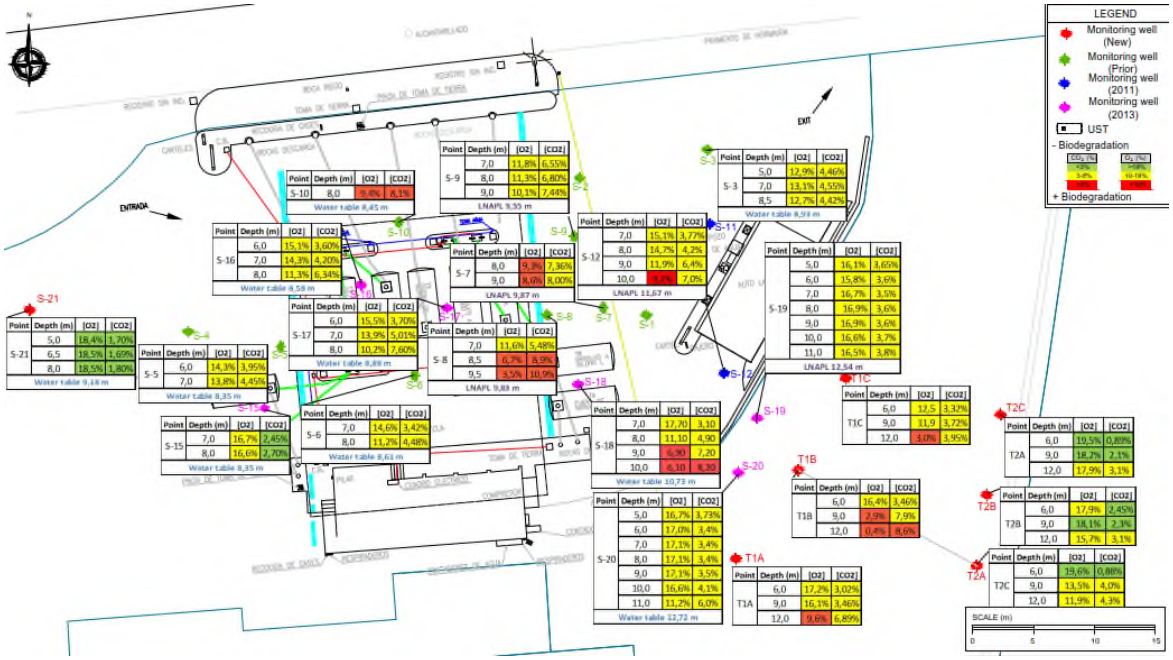

Biodegradation rates were estimated based on O_2 and CO_2 profiles using the methodology proposed by Davis et al. (Equation 1, section 4.4.1). The spreadsheets on the next pages show the field data used per quarterly monitoring round and the results for each monitoring well (**Figures 38** to **42**). O_2 and CO_2 gradients were calculated using data collected from the base of the vadose zone, where consistent trends of decreasing O_2 and increasing CO_2 with depth were observed. The annual average rates for biodegradation in the gasoline source area (52 – 2,700 L/ha/yr) are similar to those for the diesel source area (46 – 2,900 L/ha/yr, while the rates for the background area are close to zero.

In order to assess changes in soil gas composition with depth, readings collected from the shallow interval from the nearest soil gas probe are shown with the data collected from within the monitoring well screen intervals on **Figures 38** to **42**.

The NSZD rates estimated from soil gas data collected from monitoring wells are generally higher than rates estimated from soil gas probes. The higher NSZD rates determined using the monitoring well results, focused on soil gas data collected near the base of the vadose zone, are considered more realistic than the rates estimated from SVPs as the measurements from the lower vadose zone are more representative of a vertical soil gas transport regime. The ability to adjust depth intervals for soil gas data collection within monitoring wells represents a potential advantage over the fixed depth intervals from conventional soil gas probes. While soil gas probes may be suitable for sites where uniform, vertical soil gas transport dominates, data from this site demonstrates that soil gas probes installed at pre-determined depth intervals may be insufficient for resolving concentration gradients within thin reactive zones.

Figure 39. O_2 and CO_2 Profile Data from Monitoring Wells - Baseline: June 2017

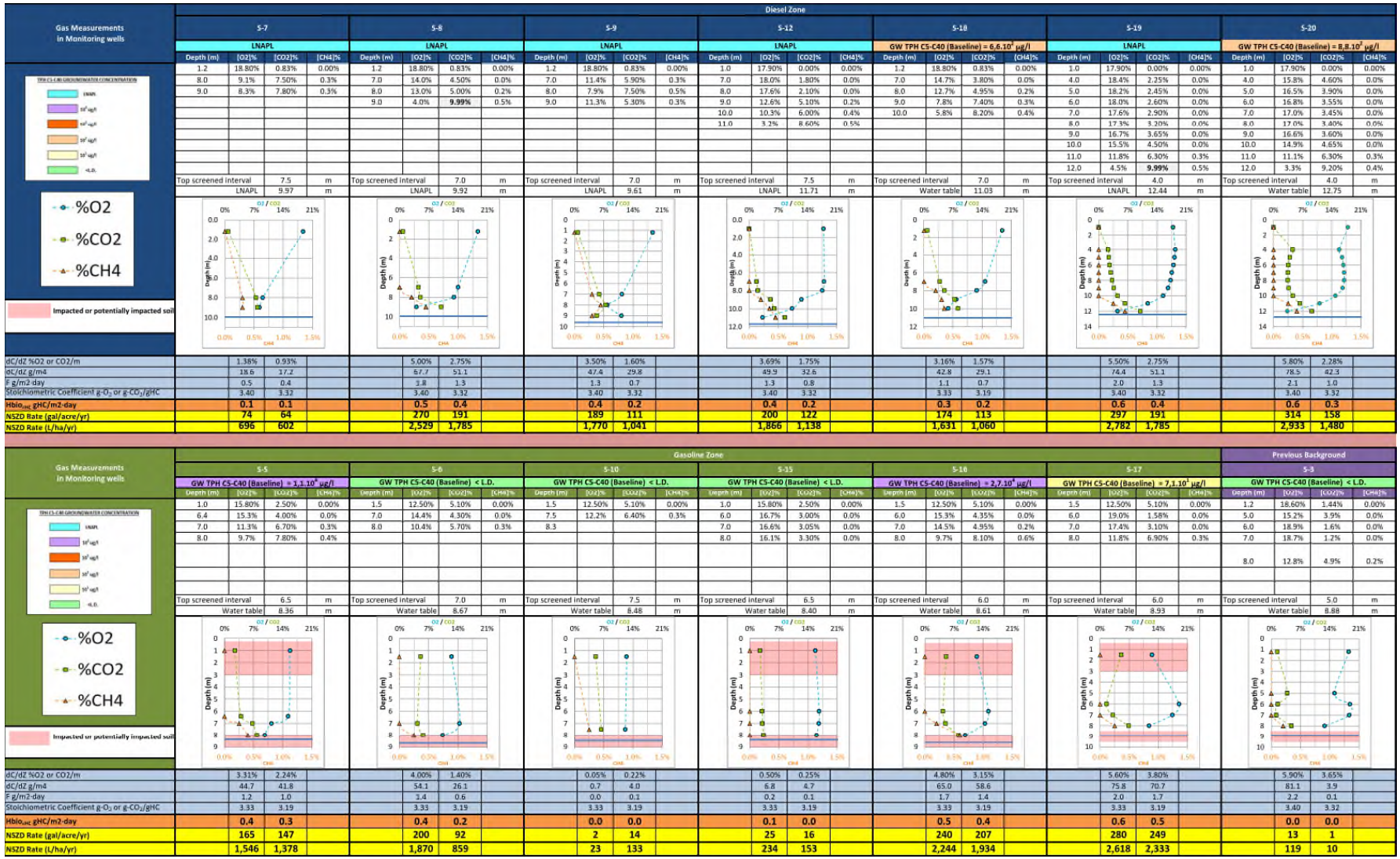

Figure 40. O_2 and CO_2 Profile Data from Monitoring Wells - October 2017

Gas Measurements in Monitoring wells	Background				Gasoline Zone																			
	S-21				S-5				S-6				S-10				S-15				S-16				S-17			
	GW TPH C5-C40 (Baseline) < L.D.				GW TPH C5-C40 (Baseline) = 1,1.10^4 µg/l				GW TPH C5-C40 (Baseline) < L.D.				GW TPH C5-C40 (Baseline) < L.D.				GW TPH C5-C40 (Baseline) < L.D.				GW TPH C5-C40 (Baseline) = 2,7.10^4 µg/l				GW TPH C5-C40 (Baseline) = 7,1.10^3 µg/l			
	Depth (m)	[O2]%	[CO2]%	[CH4]%	Depth (m)	[O2]%	[CO2]%	[CH4]%	Depth (m)	[O2]%	[CO2]%	[CH4]%	Depth (m)	[O2]%	[CO2]%	[CH4]%	Depth (m)	[O2]%	[CO2]%	[CH4]%	Depth (m)	[O2]%	[CO2]%	[CH4]%	Depth (m)	[O2]%	[CO2]%	[CH4]%
	1.2	18.3%	1.72%	0.00%	1.0	16.0%	2.00%	0.00%	1.5	14.1%	3.10%	0.00%	1.5	14.1%	3.10%	0.00%	1.0	16.0%	2.00%	0.00%	1.5	14.1%	3.10%	0.00%	1.5	14.1%	3.10%	0.00%
	6.0	18.9%	1.8%	0.0%	6.4	14.5%	4.7%	0.0%	7.0	13.6%	4.0%	0.0%	7.5	10.3%	5.0%	0.3%	6.0	16.7%	3.2%	0.0%	6.0	13.5%	4.1%	0.0%	6.0	14.1%	3.7%	0.0%
	7.0	18.9%	1.8%	0.0%	7.0	13.9%	5.0%	0.2%	8.0	8.6%	5.6%	0.3%	8.0	7.6%	6.0%	0.4%	7.0	15.2%	4.0%	0.0%	7.0	14.0%	3.9%	0.0%	7.0	12.1%	4.6%	0.2%
	9.0	18.9%	1.9%	0.0%	8.0	11.2%	6.2%	0.3%									8.0	13.2%	4.9%	0.2%	8.0	6.6%	7.2%	0.5%	8.0	8.1%	5.9%	0.4%
	Top screened interval		4.5	m	Top screened interval		6.5	m	Top screened interval		7.0	m	Top screened interval		7.5	m	Top screened interval		6.5	m	Top screened interval		6.0	m	Top screened interval		6.0	m
	Water table		9.21	m	Water table		8.40	m	Water table		8.54	m	Water table		8.44	m	Water table		8.45	m	Water table		8.57	m	Water table		8.89	m
dC/dZ %O2 or CO2/m		0.00%	0.02%			2.70%	1.25%			5.00%	1.60%			5.40%	2.00%			1.75%	0.88%			3.45%	1.55%			3.00%	1.13%	
dC/dZ g/m4		0.0	0.5			36.5	23.3			67.7	29.8			73.1	37.2			23.7	16.3			46.7	28.8			40.6	20.9	
F g/m2-day		0.0	0.0			1.0	0.6			1.8	0.7			2.0	0.9			0.6	0.4			1.3	0.7			1.1	0.5	
Stoichiometric Coefficient g-O_2 or g-CO_2/gHC		3.40	3.14			3.40	3.14			3.40	3.14			3.40	3.14			3.40	3.14			3.40	3.14			3.40	3.14	
Hbio$_{HC}$ gHC/m2-day		**0.0**	**0.0**			**0.3**	**0.2**			**0.5**	**0.2**			**0.6**	**0.3**			**0.2**	**0.1**			**0.4**	**0.2**			**0.3**	**0.2**	
NSZD Rate (gal/acre/yr)		**0**	**2**			**146**	**92**			**270**	**118**			**292**	**147**			**95**	**64**			**187**	**114**			**162**	**83**	
NSZD Rate (L/ha/yr)		**0**	**17**			**1,365**	**860**			**2,529**	**1,100**			**2,731**	**1,375**			**885**	**602**			**1,745**	**1,066**			**1,517**	**774**	

Gas Measurements in Monitoring wells	Previous Background				Diesel Zone																			
	S-3				S-7				S-8				S-9				S-12				S-18				S-19				S-20			
	GW TPH C5-C40 (Baseline) < L.D.				LNAPL				LNAPL				LNAPL				LNAPL				GW TPH C5-C40 (Baseline) = 6,6.10^3 µg/l				LNAPL				GW TPH C5-C40 (Baseline) = 8,8.10^3 µg/l			
	Depth (m)	[O2]%	[CO2]%	[CH4]%	Depth (m)	[O2]%	[CO2]%	[CH4]%	Depth (m)	[O2]%	[CO2]%	[CH4]%	Depth (m)	[O2]%	[CO2]%	[CH4]%	Depth (m)	[O2]%	[CO2]%	[CH4]%	Depth (m)	[O2]%	[CO2]%	[CH4]%	Depth (m)	[O2]%	[CO2]%	[CH4]%	Depth (m)	[O2]%	[CO2]%	[CH4]%
	1.2	18.3%	1.72%	0.00%	1.2	15.6%	1.70%	0.00%	1.2	15.6%	1.70%	0.00%	1.2	15.6%	1.70%	0.00%	1.0	16.8%	0.98%	0.00%	1.2	15.6%	1.70%	0.00%	1.0	16.8%	0.98%	0.00%	1.0	16.8%	0.98%	0.00%
	5.0	20.8%	0.0%	0.0%	8.0	8.2%	7.2%	0.4%	7.0	11.7%	4.3%	0.2%	7.0	10.9%	6.1%	0.3%	7.0	6.0%	2.9%	0.0%	7.0	17.7%	3.1%	0.0%	4.0	15.9%	2.7%	0.0%	4.0	16.2%	2.3%	0.2%
	7.0	17.8%	1.5%	0.0%	9.0	7.4%	7.7%	0.4%	8.0	3.4%	7.6%	0.5%	8.0	10.2%	6.5%	0.3%	8.0	6.1%	3.2%	0.1%	8.0	11.1%	4.9%	0.2%	5.0	13.9%	2.9%	0.2%	5.0	15.1%	2.4%	0.2%
	8.0	13.5%	4.1%	0.0%					9.0	1.5%	8.9%	0.6%					9.0	6.0%	3.2%	1.1%	9.0	6.9%	7.2%	0.4%	6.0	13.0%	3.0%	0.2%	6.0	15.0%	3.0%	0.2%
																	10.0	6.9%	4.1%	1.0%	10.0	6.1%	8.2%	0.4%	7.0	14.1%	3.1%	0.2%	7.0	13.9%	3.0%	0.3%
																	11.0	5.9%	5.2%	0.8%					8.0	14.0%	3.3%	0.3%	8.0	14.9%	2.7%	0.3%
																									9.0	14.0%	3.0%	0.2%	9.0	13.9%	3.0%	0.3%
																									10.0	12.0%	3.2%	0.2%	10.0	14.0%	3.1%	0.2%
																									11.0	14.5%	3.0%	0.2%	11.0	14.9%	3.0%	0.3%
																									12.0	14.1%	3.3%	0.2%	12.0	13.3%	3.2%	0.3%
	Top screened interval		5.0	m	Top screened interval		7.5	m	Top screened interval		7.0	m	Top screened interval		7.0	m	Top screened interval		7.5	m	Top screened interval		7.0	m	Top screened interval		4.0	m	Top screened interval		4.0	m
	Water table		8.89	m	LNAPL		9.89	m	LNAPL		9.89	m	LNAPL		9.58	m	LNAPL		11.71	m	Water table		10.86	m	LNAPL		12.52	m	Water table		12.72	m
dC/dZ %O2 or CO2/m		2.30%	1.28%			0.80%	0.50%			5.10%	2.33%			0.70%	0.40%			1.11%	0.37%			1.04%	0.69%			0.24%	0.15%			0.27%	0.17%	
dC/dZ g/m4		31.1	23.8			10.8	9.3			69.0	43.3			9.5	7.4			15.0	6.9			14.1	12.9			3.3	2.8			3.7	3.1	
F g/m2-day		0.8	0.6			0.3	0.2			1.8	1.1			0.3	0.2			0.4	0.2			0.4	0.3			0.1	0.1			0.1	0.1	
Stoichiometric Coefficient g-O_2 or g-CO_2/gHC		3.40	3.32			3.40	3.32			3.40	3.32			3.40	3.32			3.40	3.32			3.40	3.32			3.40	3.32			3.40	3.32	
Hbio$_{HC}$ gHC/m2-day		**0.2**	**0.2**			**0.1**	**0.1**			**0.5**	**0.3**			**0.1**	**0.1**			**0.1**	**0.1**			**0.1**	**0.1**			**0.0**	**0.0**			**0.0**	**0.0**	
NSZD Rate (gal/acre/yr)		**113**	**80**			**39**	**31**			**250**	**146**			**34**	**25**			**54**	**23**			**51**	**44**			**12**	**10**			**13**	**10**	
NSZD Rate (L/ha/yr)		**1,054**	**752**			**367**	**295**			**2,337**	**1,370**			**321**	**236**			**508**	**219**			**477**	**409**			**112**	**89**			**124**	**97**	

Figure 41. O_2 and CO_2 Profiles in Monitoring Wells - January 2018

Gas Measurements in Monitoring wells	Background	Gasoline Zone																			
	S-21	S-5				S-6				S-10				S-15				S-16				S-17			
	GW TPH C5-C40 (Baseline) < L.D.	GW TPH C5-C40 (Baseline) = 1,1.10^4 µg/l				GW TPH C5-C40 (Baseline) < L.D.				GW TPH C5-C40 (Baseline) < L.D.				GW TPH C5-C40 (Baseline) < L.D.				GW TPH C5-C40 (2nd Quarter) = 4,0.10^3 µg/l				GW TPH C5-C40 (Baseline) = 7,1.10^1 µg/l			
	Depth (m)	[O2]%	[CO2]%	[CH4]%	Depth (m)	[O2]%	[CO2]%	[CH4]%	Depth (m)	[O2]%	[CO2]%	[CH4]%	Depth (m)	[O2]%	[CO2]%	[CH4]%	Depth (m)	[O2]%	[CO2]%	[CH4]%	Depth (m)	[O2]%	[CO2]%	[CH4]%
	1.2	18.9%	1.62%	0.0%	1.0	18.2%	1.56%	0.3%	1.5	18.6%	1.94%	0.3%	1.5	18.6%	1.94%	0.3%	1.0	18.2%	1.56%	0.3%	1.5	18.6%	1.94%	0.3%	1.5	18.6%	1.94%	0.3%
	5.0	18.6%	2.35%	0.3%	7.0	9.1%	7.60%	0.9%	7.0	10.9%	6.10%	0.6%	8.0	11.5%	6.50%	1.0%	7.0	14.0%	4.95%	0.7%	6.0	20.8%	0.38%	0.2%	6.0	18.7%	1.78%	0.5%
	6.5	18.7%	2.40%	0.3%	8.2	8.4%	8.10%	1.1%	8.0	9.2%	9.80%	0.7%					8.0	13.3%	5.40%	0.7%	7.0	15.6%	4.30%	0.7%	7.0	17.0%	3.20%	0.6%
	8.0	18.8%	2.45%	0.3%																	8.0	17.3%	3.05%	0.6%	8.0	14.8%	4.50%	0.8%
	Top screened interval	4.5	m		Top screened interval	6.5	m		Top screened interval	7.0	m		Top screened interval	7.5	m		Top screened interval	6.5	m		Top screened interval	6.0	m		Top screened interval	6.0	m	
	Water table	9.27	m		Water table	8.45	m		Water table	8.69	m		Water table	8.52	m		Water table	8.50	m		Water table	8.65	m		Water table	8.95	m	
dC/dZ %O2 or CO2/m		-0.07%	0.03%			1.41%	0.94%			1.70%	3.70%			1.09%	0.70%			0.70%	0.45%			1.75%	1.34%			1.95%	1.36%	
dC/dZ g/m4		-0.9	0.6			19.1	17.5			23.0	68.9			14.8	13.1			9.5	8.4			23.7	24.8			26.4	25.3	
F g/m2-day		0.0	0.0			0.5	0.4			0.6	1.7			0.4	0.3			0.3	0.2			0.6	0.6			0.7	0.6	
Stoichiometric Coefficient g-O_2 or g-CO_2/gHC		3.33	3.19			3.33	3.19			3.33	3.19			3.33	3.19			3.33	3.19			3.33	3.19			3.33	3.19	
$Hbio_{net}$ gHC/m2-day		**0.0**	**0.0**			**0.2**	**0.1**			**0.2**	**0.5**			**0.1**	**0.1**			**0.1**	**0.1**			**0.2**	**0.2**			**0.2**	**0.2**	
NSZD Rate (gal/acre/yr)		**-4**	**2**			**78**	**68**			**94**	**268**			**60**	**51**			**39**	**33**			**96**	**97**			**108**	**98**	
NSZD Rate (L/ha/yr)		**-34**	**23**			**728**	**637**			**877**	**2,505**			**563**	**475**			**361**	**305**			**903**	**904**			**1,006**	**921**	

Gas Measurements in Monitoring wells	Previous Background	Diesel Zone																							
	S-3	S-7				S-8				S-9				S-12				S-18				S-19				S-20			
	GW TPH C5-C40 (Baseline) < L.D.	LNAPL				LNAPL				LNAPL				LNAPL				GW TPH C5-C40 (Baseline) = 6,6.10^2 µg/l				LNAPL				GW TPH C5-C40 (2nd Quarter) = 1,5.10^4 µg/l			
	Depth (m)	[O2]%	[CO2]%	[CH4]%	Depth (m)	[O2]%	[CO2]%	[CH4]%	Depth (m)	[O2]%	[CO2]%	[CH4]%	Depth (m)	[O2]%	[CO2]%	[CH4]%	Depth (m)	[O2]%	[CO2]%	[CH4]%	Depth (m)	[O2]%	[CO2]%	[CH4]%	Depth (m)	[O2]%	[CO2]%	[CH4]%	Depth (m)	[O2]%	[CO2]%	[CH4]%
	1.2	18.9%	1.62%	0.0%	1.2	18.7%	1.82%	0.00%	1.2	18.7%	1.82%	0.00%	1.2	18.7%	1.82%	0.0%	1.0	19.1%	1.20%	0.0%	1.2	18.7%	1.82%	0.0%	1.0	19.1%	1.20%	0.0%	1.0	19.1%	1.20%	0.0%
	5.0	16.4%	3.25%	0.2%	8.0	9.2%	6.9%	0.7%	7.0	13.4%	4.8%	0.7%	7.0	12.2%	5.30%	0.5%	8.0	13.1%	4.8%	0.9%	7.0	17.6%	2.8%	0.0%	6.0	18.3%	2.6%	0.0%	6.0	16.8%	3.6%	0.2%
	7.0	13.8%	4.20%	0.3%	9.5	2.6%	10.0%	1.1%	8.5	10.5%	6.5%	0.9%	8.0	7.7%	7.30%	0.7%	9.5	8.3%	7.4%	1.1%	8.5	11.3%	5.8%	0.5%	9.0	13.6%	4.9%	0.4%	9.0	13.4%	5.0%	0.4%
	8.5	13.1%	4.05%	0.4%					10.0	1.3%	10.0%	1.6%	9.5	0.6%	9.90%	1.4%	11.0	1.3%	9.9%	1.4%	10.0	4.9%	8.8%	0.9%	12.0	3.2%	9.9%	0.9%	12.0	2.5%	9.0%	0.9%
	Top screened interval	5.0	m		Top screened interval	7.5	m		Top screened interval	7.0	m		Top screened interval	7.0	m		Top screened interval	7.5	m		Top screened interval	7.0	m		Top screened interval	4.0	m		Top screened interval	4.0	m	
	Water table	9.02	m		LNAPL	10.12	m		LNAPL	10.08	m		LNAPL	9.68	m		LNAPL	11.80	m		Water table	11.29	m		LNAPL	12.65	m		Water table	12.97	m	
dC/dZ %O2 or CO2/m		0.96%	0.24%			4.40%	2.06%			4.03%	1.73%			4.65%	1.83%			3.93%	1.72%			4.23%	2.00%			2.52%	1.23%			2.38%	0.90%	
dC/dZ g/m4		13.0	4.5			59.6	38.3			54.6	32.2			62.9	34.1			53.2	31.9			57.3	37.2			34.1	22.8			32.3	16.7	
F g/m2-day		0.3	0.1			1.6	0.9			1.5	0.8			1.7	0.8			1.4	0.8			1.5	0.9			0.9	0.6			0.9	0.4	
Stoichiometric Coefficient g-O_2 or g-CO_2/gHC		3.40	3.32			3.40	3.32			3.40	3.32			3.40	3.32			3.40	3.32			3.40	3.32			3.40	3.32			3.40	3.32	
$Hbio_{net}$ gHC/m2-day		**0.1**	**0.0**			**0.5**	**0.3**			**0.4**	**0.2**			**0.5**	**0.3**			**0.4**	**0.2**			**0.5**	**0.3**			**0.3**	**0.2**			**0.3**	**0.1**	
NSZD Rate (gal/acre/yr)		**47**	**15**			**216**	**130**			**198**	**109**			**228**	**115**			**193**	**108**			**207**	**126**			**123**	**77**			**117**	**57**	
NSZD Rate (L/ha/yr)		**441**	**143**			**2,016**	**1,214**			**1,848**	**1,019**			**2,129**	**1,079**			**1,802**	**1,011**			**1,939**	**1,178**			**1,153**	**722**			**1,092**	**530**	

Figure 42. O_2 and CO_2 Profiles from Monitoring Wells - April 2018

Gas Measurements in Monitoring wells	Background				Gasoline Zone																			
	S-21				S-5				S-6				S-10				S-15				S-16				S-17			
	GW TPH C5-C40 (Baseline) < L.D.				GW TPH C5-C40 (Baseline) = 1,1.10^3 µg/l				GW TPH C5-C40 (Baseline) < L.D.				GW TPH C5-C40 (Baseline) < L.D.				GW TPH C5-C40 (Baseline) < L.D.				GW TPH C5-C40 (2nd Quarter) = 4,0.10^3 µg/l				GW TPH C5-C40 (Baseline) = 7,1.10^3 µg/l			
	Depth (m)	[O2]%	[CO2]%	[CH4]%	Depth (m)	[O2]%	[CO2]%	[CH4]%	Depth (m)	[O2]%	[CO2]%	[CH4]%	Depth (m)	[O2]%	[CO2]%	[CH4]%	Depth (m)	[O2]%	[CO2]%	[CH4]%	Depth (m)	[O2]%	[CO2]%	[CH4]%	Depth (m)	[O2]%	[CO2]%	[CH4]%
	1.2	19.0%	0.95%	0.01%	1.0	17.6%	0.32%	0.13%	1.5	18.8%	1.19%	0.01%	1.5	18.8%	1.19%	0.01%	1.0	17.6%	0.32%	0.13%	1.5	18.8%	1.19%	0.01%	1.5	18.8%	1.19%	0.01%
	5.0	18.6%	2.35%	0.3%	7.0	15.4%	3.95%	0.12%	7.0	10.9%	6.10%	0.07%	8.0	11.5%	6.50%	0.09%	7.0	16.2%	3.02%	0.03%	6.0	20.8%	0.38%	0.2%	6.0	18.7%	1.78%	0.5%
	6.5	18.7%	2.40%	0.3%	8.2	13.2%	5.60%	0.12%	8.0	9.2%	9.80%	0.11%					8.0	14.9%	4.03%	0.04%	7.0	15.6%	4.30%	0.7%	7.0	17.0%	3.20%	0.6%
	8.0	18.8%	2.45%	0.3%																	8.0	17.3%	3.05%	0.6%	8.0	14.8%	4.50%	0.8%
	Top screened interval		4.5	m	Top screened interval		6.5	m	Top screened interval		7.0	m	Top screened interval		7.5	m	Top screened interval		6.5	m	Top screened interval		6.0	m	Top screened interval		6.0	m
	Water table		9.33	m	Water table		8.38	m	Water table		8.74	m	Water table		8.65	m	Water table		8.47	m	Water table		8.77	m	Water table		9.03	m
	dC/dZ %O2 or CO2/m		-0.07%	0.03%			1.83%	1.38%			1.70%	3.70%			1.12%	0.82%			1.30%	1.01%			1.75%	1.34%			1.95%	1.36%
	dC/dZ g/m4		-0.9	0.6			24.8	25.6			23.0	68.9			15.2	15.2			17.6	18.8			23.7	24.8			26.4	25.3
	F g/m2-day		0.0	0.0			0.7	0.6			0.6	1.7			0.4	0.4			0.5	0.5			0.6	0.6			0.7	0.6
	Stoichiometric Coefficient g-O_2 or g-CO_2/gHC		3.33	3.19			3.33	3.19			3.33	3.19			3.33	3.19			3.33	3.19			3.33	3.19			3.33	3.19
	$Hbio_{mic}$ gHC/m2-day		**0.0**	**0.0**			**0.2**	**0.2**			**0.2**	**0.5**			**0.1**	**0.1**			**0.1**	**0.1**			**0.2**	**0.2**			**0.2**	**0.2**
	NSZD Rate (gal/acre/yr)		**-4**	**2**			**101**	**100**			**94**	**268**			**62**	**59**			**72**	**73**			**96**	**97**			**108**	**98**
	NSZD Rate (L/ha/yr)		**-34**	**23**			**946**	**931**			**877**	**2,505**			**579**	**553**			**670**	**684**			**903**	**904**			**1,006**	**921**

Gas Measurements in Monitoring wells	Previous Background				Diesel Zone																			
	S-3				S-7				S-8				S-9				S-12				S-18				S-19			
	GW TPH C5-C40 (Baseline) < L.D.				LNAPL				LNAPL				LNAPL				LNAPL				GW TPH C5-C40 (Baseline) = 6,6.10^3 µg/l				LNAPL			
	Depth (m)	[O2]%	[CO2]%	[CH4]%	Depth (m)	[O2]%	[CO2]%	[CH4]%	Depth (m)	[O2]%	[CO2]%	[CH4]%	Depth (m)	[O2]%	[CO2]%	[CH4]%	Depth (m)	[O2]%	[CO2]%	[CH4]%	Depth (m)	[O2]%	[CO2]%	[CH4]%	Depth (m)	[O2]%	[CO2]%	[CH4]%
	1.2	18.7%	2.59%	0.03%	1.2	18.7%	2.59%	0.03%	1.2	18.7%	2.59%	0.03%	1.2	18.7%	2.59%	0.03%	1.0	19.4%	0.27%	0.00%	1.2	18.7%	2.59%	0.03%	1.0	19.4%	0.27%	0.00%
	5.0	16.1%	1.98%	0.02%	8.0	7.4%	7.12%	0.04%	7.0	13.4%	4.8%	0.03%	7.0	12.2%	5.30%	0.0%	8.0	13.1%	4.8%	0.85%	7.0	17.6%	2.8%	0.0%	6.0	18.3%	2.6%	0.0%
	7.0	16.0%	0.42%	0.03%	9.0	5.9%	7.83%	0.05%	8.5	10.5%	6.5%	0.04%	8.0	7.7%	7.30%	0.0%	9.5	8.3%	7.4%	1.05%	8.5	11.3%	5.8%	0.5%	9.0	13.6%	4.9%	0.4%
	8.5	7.7%	2.87%	0.02%					10.0	1.3%	10.0%	0.06%	9.5	0.6%	9.90%	0.1%	11.0	1.3%	9.9%	1.35%	10.0	4.9%	8.8%	0.9%	12.0	3.2%	9.9%	0.9%
	Top screened interval		5.0	m	Top screened interval		7.5	m	Top screened interval		7.0	m	Top screened interval		7.0	m	Top screened interval		7.5	m	Top screened interval		7.0	m	Top screened interval		4.0	m
	Water table		9.08	m	LNAPL		10.25	m	LNAPL		10.12	m	LNAPL		9.70	m	LNAPL		11.88	m	Water table		11.33	m	LNAPL		12.74	m
	dC/dZ %O2 or CO2/m		2.27%	0.20%			1.50%	0.71%			4.03%	1.73%			4.65%	1.83%			0.90%	1.72%			4.23%	2.00%			2.52%	1.23%
	dC/dZ g/m4		30.8	3.7			20.3	13.2			54.6	32.2			62.9	34.1			12.2	31.9			57.3	37.2			34.1	22.8
	F g/m2-day		0.8	0.1			0.5	0.3			1.5	0.8			1.7	0.8			0.3	0.8			1.5	0.9			0.9	0.6
	Stoichiometric Coefficient g-O_2 or g-CO_2/gHC		3.40	3.32			3.40	3.32			3.40	3.32			3.40	3.32			3.40	3.32			3.40	3.32			3.40	3.32
	$Hbio_{mic}$ gHC/m2-day		**0.2**	**0.0**			**0.2**	**0.1**			**0.4**	**0.2**			**0.5**	**0.3**			**0.1**	**0.2**			**0.5**	**0.3**			**0.3**	**0.2**
	NSZD Rate (gal/acre/yr)		**111**	**12**			**73**	**45**			**198**	**109**			**228**	**115**			**44**	**108**			**207**	**126**			**123**	**77**
	NSZD Rate (L/ha/yr)		**1,041**	**117**			**687**	**418**			**1,848**	**1,019**			**2,129**	**1,079**			**412**	**1,011**			**1,939**	**1,178**			**1,153**	**722**

Figure 43. O_2 and CO_2 Profiles from Monitoring Wells - July 2018

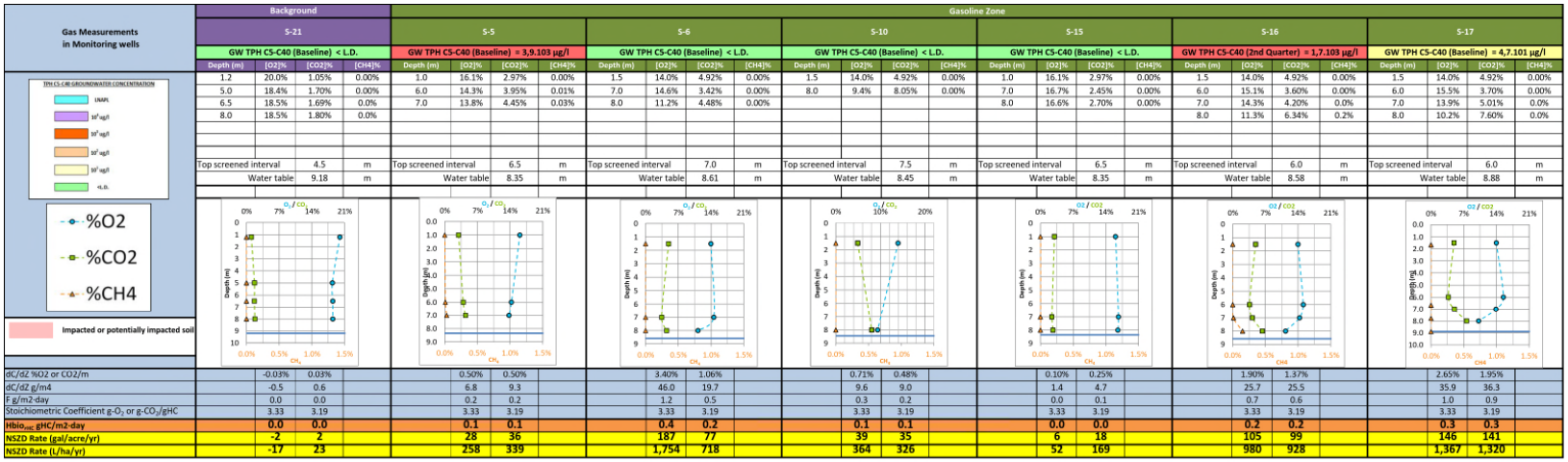

Gas Measurements in Monitoring wells	Background				Gasoline Zone																			
	S-21				S-5				S-6				S-10				S-15				S-16				S-17			
	GW TPH C5-C40 (Baseline) < L.D.				GW TPH C5-C40 (Baseline) = 3,9.103 µg/l				GW TPH C5-C40 (Baseline) < L.D.				GW TPH C5-C40 (Baseline) < L.D.				GW TPH C5-C40 (Baseline) < L.D.				GW TPH C5-C40 (2nd Quarter) = 1,7.103 µg/l				GW TPH C5-C40 (Baseline) = 4,7.101 µg/l			
	Depth (m)	[O2]%	[CO2]%	[CH4]%	Depth (m)	[O2]%	[CO2]%	[CH4]%	Depth (m)	[O2]%	[CO2]%	[CH4]%	Depth (m)	[O2]%	[CO2]%	[CH4]%	Depth (m)	[O2]%	[CO2]%	[CH4]%	Depth (m)	[O2]%	[CO2]%	[CH4]%	Depth (m)	[O2]%	[CO2]%	[CH4]%
	1.2	20.0%	1.05%	0.00%	1.0	16.1%	2.97%	0.00%	1.5	14.0%	4.92%	0.00%	1.5	14.0%	4.92%	0.00%	1.0	16.1%	2.97%	0.00%	1.5	14.0%	4.92%	0.00%	1.5	14.0%	4.92%	0.00%
	5.0	18.4%	1.70%	0.00%	6.0	14.3%	3.95%	0.01%	7.0	14.6%	3.42%	0.00%	8.0	9.4%	8.05%	0.00%	7.0	16.7%	2.45%	0.00%	6.0	15.1%	3.60%	0.00%	6.0	15.5%	3.70%	0.00%
	6.5	18.5%	1.69%	0.0%	7.0	13.8%	4.45%	0.03%	8.0	11.2%	4.48%	0.00%					8.0	16.6%	2.70%	0.00%	7.0	14.3%	4.20%	0.0%	7.0	13.9%	5.01%	0.0%
	8.0	18.5%	1.80%	0.0%																	8.0	11.3%	6.34%	0.2%	8.0	10.2%	7.60%	0.0%
	Top screened interval		4.5	m	Top screened interval		6.5	m	Top screened interval		7.0	m	Top screened interval		7.5	m	Top screened interval		6.5	m	Top screened interval		6.0	m	Top screened interval		6.0	m
	Water table		9.18	m	Water table		8.35	m	Water table		8.61	m	Water table		8.45	m	Water table		8.35	m	Water table		8.58	m	Water table		8.88	m
dC/dZ %O2 or CO2/m		-0.03%	0.03%			0.50%	0.50%			3.40%	1.06%			0.71%	0.48%			0.10%	0.25%			1.90%	1.37%			2.65%	1.95%	
dC/dZ g/m4		-0.5	0.6			6.8	9.3			46.0	19.7			9.6	9.0			1.4	4.7			25.7	25.5			35.9	36.3	
F g/m2-day		0.0	0.0			0.2	0.2			1.2	0.5			0.3	0.2			0.0	0.1			0.7	0.6			1.0	0.9	
Stoichiometric Coefficient g-O_2 or g-CO_2/gHC		3.33	3.19			3.33	3.19			3.33	3.19			3.33	3.19			3.33	3.19			3.33	3.19			3.33	3.19	
$Hbio_{soil}$ gHC/m2-day		**0.0**	**0.0**			**0.1**	**0.1**			**0.4**	**0.2**			**0.1**	**0.1**			**0.0**	**0.0**			**0.2**	**0.2**			**0.3**	**0.3**	
NSZD Rate (gal/acre/yr)		**-2**	**2**			**28**	**36**			**187**	**77**			**39**	**35**			**6**	**18**			**105**	**99**			**146**	**141**	
NSZD Rate (L/ha/yr)		**-17**	**23**			**258**	**339**			**1,754**	**718**			**364**	**326**			**52**	**169**			**980**	**928**			**1,367**	**1,320**	

Gas Measurements in Monitoring wells	Previous Background				Diesel Zone																			
	S-3				S-7				S-8				S-9				S-12				S-18				S-19				S-20			
	GW TPH C5-C40 (Baseline) < L.D.				LNAPL				LNAPL				LNAPL				LNAPL				GW TPH C5-C40 (Baseline) = 8,1.101 µg/l				LNAPL				GW TPH C5-C40 (2nd Quarter) = 24,03.104 µg/l			
	Depth (m)	[O2]%	[CO2]%	[CH4]%	Depth (m)	[O2]%	[CO2]%	[CH4]%	Depth (m)	[O2]%	[CO2]%	[CH4]%	Depth (m)	[O2]%	[CO2]%	[CH4]%	Depth (m)	[O2]%	[CO2]%	[CH4]%	Depth (m)	[O2]%	[CO2]%	[CH4]%	Depth (m)	[O2]%	[CO2]%	[CH4]%	Depth (m)	[O2]%	[CO2]%	[CH4]%
	1.2	15.2%	2.80%	0.00%	1.2	15.2%	2.80%	0.00%	1.2	15.2%	2.80%	0.00%	1.2	15.2%	2.80%	0.00%	1.0	18.7%	1.54%	0.00%	1.2	15.2%	2.80%	0.00%	1.0	18.7%	1.54%	0.00%	1.0	18.7%	1.54%	0.00%
	5.0	12.9%	4.46%	0.02%	8.0	9.3%	7.36%	0.05%	7.0	11.6%	5.48%	0.01%	7.0	11.8%	6.55%	0.03%	8.0	15.1%	3.77%	0.02%	7.0	15.5%	3.01%	0.00%	5.0	16.1%	3.65%	0.04%	5.0	16.7%	3.73%	0.01%
	7.0	13.1%	4.55%	0.03%	9.0	8.6%	8.00%	0.04%	8.5	6.7%	8.9%	0.01%	8.0	11.3%	6.80%	0.03%	9.0	14.7%	4.2%	0.02%	8.0	12.1%	4.6%	0.0%	6.0	15.8%	3.6%	0.1%	6.0	17.0%	3.4%	0.0%
	8.5	12.7%	4.42%	0.02%					9.5	3.5%	10.9%	0.03%	9.0	10.1%	7.44%	0.05%	10.0	11.9%	6.4%	0.00%	9.0	9.0%	5.7%	0.0%	7.0	16.7%	3.5%	0.0%	7.0	17.1%	3.4%	0.0%
																	11.0	9.2%	7.0%	0.01%	10.0	6.0%	7.3%	0.0%	8.0	16.9%	3.6%	0.0%	8.0	17.1%	3.4%	0.0%
																									9.0	16.9%	3.6%	0.0%	9.0	17.1%	3.5%	0.0%
																									10.0	16.6%	3.7%	0.0%	10.0	16.6%	4.1%	0.0%
																									11.0	16.5%	3.8%	0.0%	11.0	11.2%	6.0%	0.0%
	Top screened interval		5.0	m	Top screened interval		7.5	m	Top screened interval		7.0	m	Top screened interval		7.0	m	Top screened interval		7.5	m	Top screened interval		7.0	m	Top screened interval		4.0	m	Top screened interval		4.0	m
	Water table		8.93	m	LNAPL		9.87	m	LNAPL		9.83	m	LNAPL		9.55	m	LNAPL		11.67	m	Water table		10.73	m	LNAPL		12.54	m	Water table		12.72	m
dC/dZ %O2 or CO2/m		0.05%	-0.01%			0.70%	0.64%			3.24%	2.17%			1.20%	0.64%			2.05%	1.20%			3.16%	1.40%			0.15%	0.08%			2.95%	1.26%	
dC/dZ g/m4		0.7	-0.2			9.5	11.9			43.9	40.3			16.2	11.9			27.7	22.4			42.8	26.0			2.0	1.5			39.9	23.4	
F g/m2-day		0.0	0.0			0.3	0.3			1.2	1.0			0.4	0.3			0.7	0.5			1.1	0.6			0.1	0.0			1.1	0.6	
Stoichiometric Coefficient g-O_2 or g-CO_2/gHC		3.40	3.32			3.40	3.32			3.40	3.32			3.40	3.32			3.40	3.32			3.40	3.32			3.40	3.32			3.40	3.32	
$Hbio_{soil}$ gHC/m2-day		**0.0**	**0.0**			**0.1**	**0.1**			**0.3**	**0.3**			**0.1**	**0.1**			**0.2**	**0.2**			**0.3**	**0.2**			**0.0**	**0.0**			**0.3**	**0.2**	
NSZD Rate (gal/acre/yr)		**2**	**-1**			**34**	**40**			**159**	**137**			**59**	**40**			**100**	**76**			**155**	**88**			**7**	**5**			**144**	**79**	
NSZD Rate (L/ha/yr)		**22**	**-5**			**321**	**377**			**1,485**	**1,277**			**550**	**377**			**939**	**708**			**1,448**	**823**			**69**	**46**			**1,352**	**739**	

3.5.3. Soil-gas sampling results

As part of the vapour monitoring program samples were collected from a selection of both monitoring wells and soil vapour probes on a quarterly basis. Sample volumes ranged from 3.3 to 7.7 liters. **Figures 42** to **46** show the analytical results of these vapour samples over the site's cross section.

Figure 44. Results of BTEX, TPH, MTBE and ETBE in soil vapour samples – Baseline.

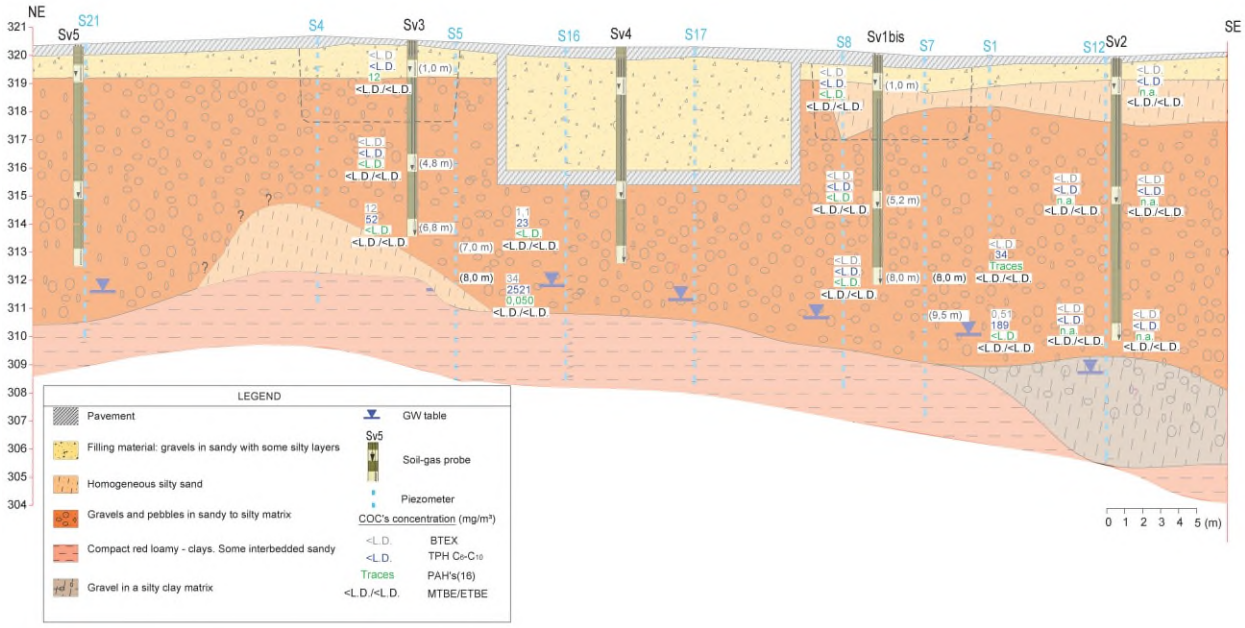

Figure 45. Results of BTEX, TPH, MTBE and ETBE in soil vapour samples – October 2017.

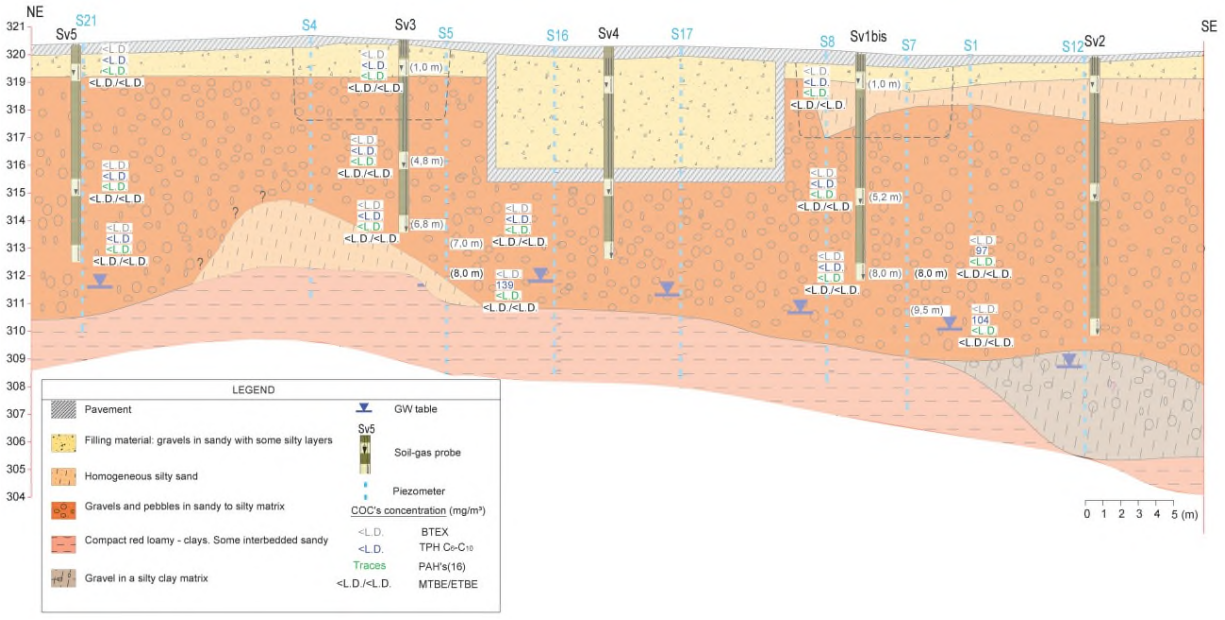

Figure 46. Results of BTEX, TPH, MTBE and ETBE in soil vapour samples – January 2018.

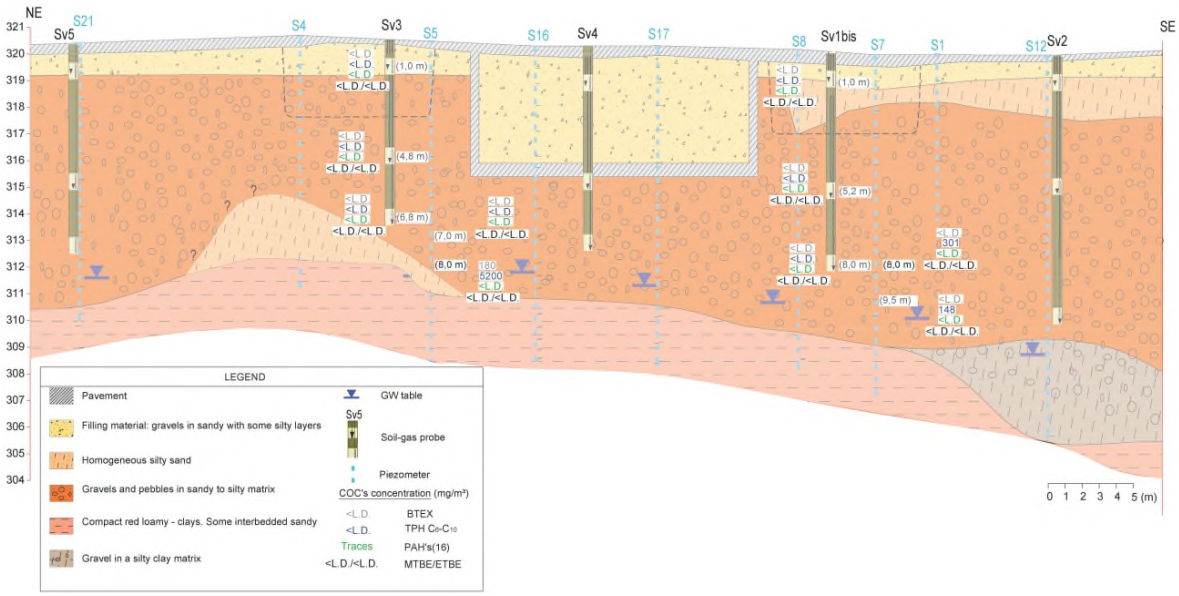

Figure 47. Results of BTEX, TPH, MTBE and ETBE in soil vapour samples – April 2018.

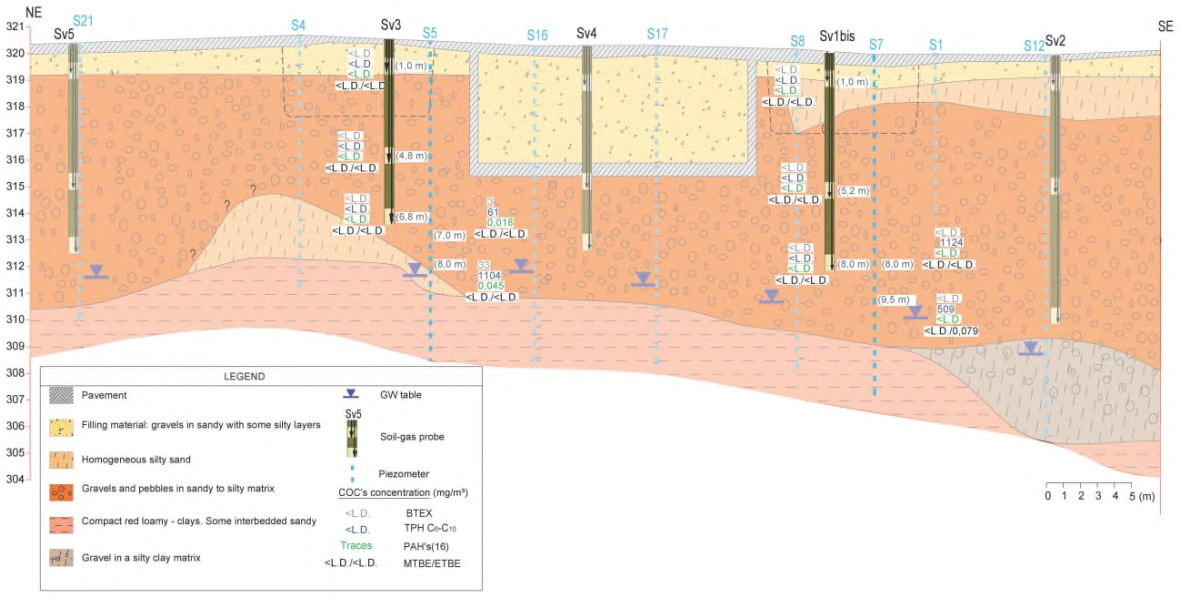

Figure 48. Results of BTEX, TPH, MTBE and ETBE in soil vapour samples – July 2018.

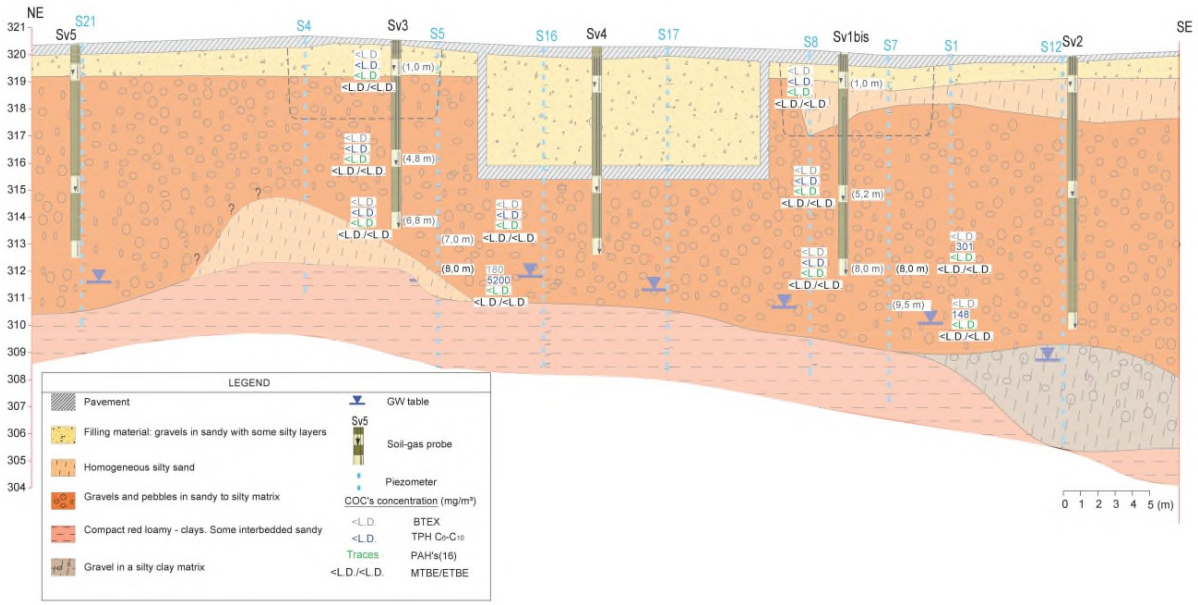

According to the analytical results, contaminants of concern have only been detected in the soil vapour sampled in the smear zone of both source areas and in monitoring wells. It is worth noting that samples collected from vapour probes nested at similar depths in the same locations (SV3 at 6.8 m vs. S5 at 7 m or SV1bis at 8 m vs. S7 at 8 m) do not yield comparable analytical results to those reported for samples collected in monitoring wells.

The most volatile compounds (TPH C_6-C_{16} and BTEX) are detected in higher concentrations in the soil vapour samples, whereas MTBE and ETBE, which have lower Henry's Law constants and partition more strongly into the aqueous phase, are present in lower concentrations and PAHs were only detected in trace levels.

None of the sampled soil probes nested at the shallow and middle depth levels (approx. 1 and 5 mgs, respectively) have shown concentrations of contaminants of concern above the laboratory analytical reporting limit, except for low concentrations of MTBE and ETBE in the middle depth probes SV1bis and SV3, respectively, in the third quarterly monitoring control conducted in April 2018.

3.6. TEMPERATURE STUDY

The biologically-mediated NSZD processes that destroy hydrocarbons and alter the composition of soil gas also release heat. The foundation for evaluating hydrocarbon biodegradation rates from measurements of increased temperature in the subsurface was established decades ago (Mohr and Merz, 1995), and has been more recently expanded as a tool for monitoring remediation performance (Subramanian et al., 2011) and NSZD (Ririe et al., 2013; Sweeney and Ririe, 2014; Warren and Bekins, 2015). The heat released from biodegradation creates temperature gradients in subsurface materials in zones where microbial degradation is occurring, and the overall heat transfer in the subsurface can be conceptualized as the superposition of heat flux from LNAPL depletion and background heat transport processes. The method utilized for calculating NSZD rates from subsurface temperature measurements requires knowledge of background temperature distribution to identify zones of elevated temperature associated with NSZD. The temperature increase from NSZD at

a given depth and time of year is calculated using **Equation 4** (Sweeney and Ririe, 2014):

$$\Delta T_{NSZD}(z,t)=T_{SZ}(z,t)-T_{BKGD}(z,t) \qquad \textbf{Equation 4}$$

Where,

$\Delta T_{NSZD}(z,t)$ = Temperature difference at depth "z" and time "t" attributable to NSZD (°C)

$T_{SZ}(z,t)$ = Temperature at depth "z" and time "t" within the LNAPL source zone (°C)

$T_{BKGD}(z,t)$ = Temperature at depth "z" and time "t" outside of the LNAPL source zone (°C)

For this study, background temperature data was collected from monitoring well S-21 to filter out temperature fluctuations in response to annual variability in radiant, solar heating at the ground surface. As described in Section 3.2.4, temperature data was collected using data loggers suspended at one meter depth intervals at wells located in the gasoline area (S-5), diesel area (S-7), and background (S-21) for a period of more than thirteen months. Additional discrete temperature data was collected from wells instrumented with data loggers and 15 nearby monitoring wells in the gasoline and diesel source areas on a quarterly basis using a thermistor.

3.6.1. Continuous Temperature Data

Plots of temperature data versus time for depths ranging from 1 to 10 m bgs at each of the wells instrumented with data loggers are presented in **Figure 48**, below. The charts also include temperature measurements recorded at ground surface using a data logger placed in the well vault at well S-7 and discrete, manual temperature measurements recorded in June 2017, October 2017, January 2018, April 2018, and July 2018 using the thermistor. Where data loggers failed, gaps in temperature data are modelled using a best-fit sinusoidal function, shown on **Figure 48** as dotted lines.

Figure 49. Summary of temperature data recorded using data loggers and thermistors in background (S-21), gasoline (S-5), and diesel area wells

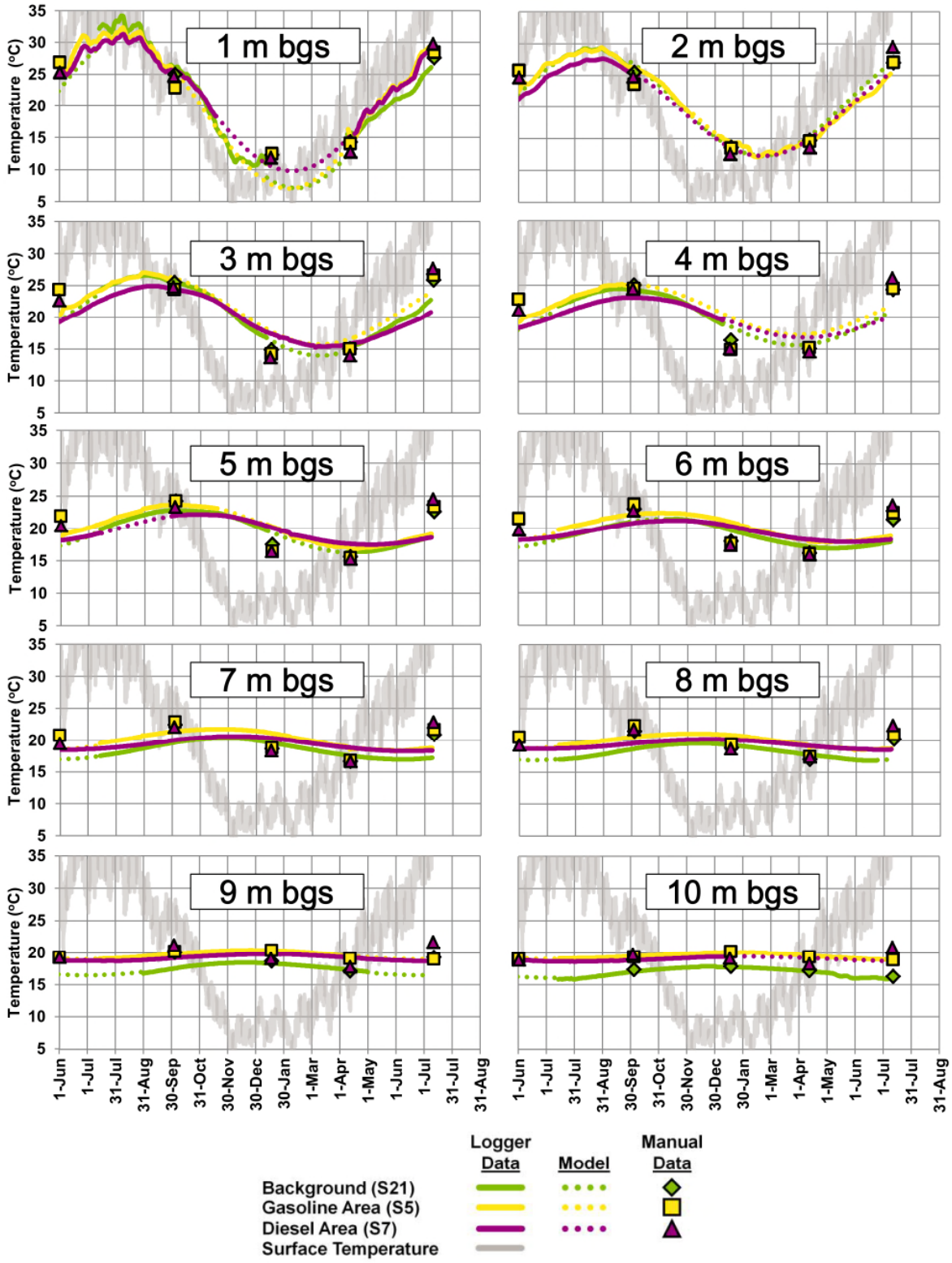

Where at least 365 days of temperature data were available, gaps in subsurface temperature were modelled using **Equation 5**:

$$T(z,t)=T_m+S\cdot\sin(\omega\cdot t)+C\cdot\cos(\omega\cdot t)=T_m+A\cdot\cos(\omega\cdot t-\varphi) \quad \textbf{Equation 5}$$

Where T_m is the mean annual soil temperature (°C), and ω is the angular frequency of the 1st harmonic in units of radians per day. Amplitude coefficients S, C, and A were determined using Fourier analysis techniques (**Equations 6**, **7** and **8**, respectively), and the phase angle (φ) was determined using **Equation 9**.

$$S=\frac{2}{365}\cdot\sum_{t=1}^{365}T_t\cdot\sin(\omega\cdot t) \quad \textbf{Equation 6}$$

$$C=\frac{2}{365}\cdot\sum_{t=1}^{365}T_t\cdot\cos(\omega\cdot t) \quad \textbf{Equation 7}$$

$$A=\sqrt{S^2+C^2} \quad \textbf{Equation 8}$$

$$\varphi=tan^{-1}\left(\frac{S}{C}\right) \quad \textbf{Equation 9}$$

Where T_t is the average temperature at depth "z" on day "t" (°C). For depth intervals where less than 365 days of temperature data were recorded, the amplitude coefficients and phase angle were estimated iteratively by minimizing residuals between model and measured temperatures using Solver in Excel.

Generally, the temperature data shown in **Figure 49** indicate:

- Temperatures measured near the base of the vadose zone/near the water table (below 8 m) in source zone wells (S-5 and S-7) are generally higher than temperatures measured at the same depth from the background location. This observation is consistent with soil gas data interpretation, indicating that biodegradation is occurring in this depth interval.
- On average, temperatures measured in the upper few meters of the subsurface (above the zone of more intense biodegradation) are similar in the background and source zone locations, which suggests that data collected from S-21 are suitable for understanding background temperature distribution resulting from seasonal variability.
- The mean annual subsurface temperature decreases with depth at all locations. The trend is most pronounced at the background location (S-21), where the mean annual temperature in the upper 4 m of the subsurface ranges from approximately 19.0 to 20.7°C and the mean annual temperature at 10 m bgs is cooler by at least 2 degrees (17.0°C).

Common models for background subsurface temperature distribution typically assume transient heat transport into and out of the subsurface through conduction as a function of periodic temperature fluctuations at the air-soil interface (de Vries, 1963; Monteith, 1973; Sweeney and Ririe, 2014). These models predict that the mean annual soil temperature is approximately constant with depth, with seasonal fluctuations in response to changes in temperature at the ground surface boundary condition. The finding that subsurface temperatures were, on average, cooler at depth indicates that conventional subsurface temperature models that predict subsurface temperatures based on a surface boundary condition alone are insufficient for modelling background subsurface temperatures at this site. The mechanism(s) responsible for the cooler temperatures at depth for this site are unclear. Historical weather data from a nearby weather station was evaluated to determine whether air temperatures were warmer on average during the time of

the study than during previous years, but no obvious warming trends leading up to the study period were identified. The site is located near the edge of an urban area with rural/agricultural land use to the south. The warmer temperatures in the shallow zone may be the result of a change to urban/paved conditions (Ferguson and Woodbury, 2007; Kooi, 2008; Benz et al., 2017). Ground surface temperatures are generally higher in paved areas than in vegetated or bare soil conditions due to differences in albedo and shading (Bodri and Cermak, 2007). It is possible that the subsurface is gradually warming in response to the historical change in land use, and temperatures at depth have not yet equilibrated to the increase in mean temperature at ground surface. Given that the site is located very close to the boundary between urban and rural/agricultural land, It is also possible that temperatures at depth have reached a steady state condition between that of the urban and neighbouring rural/agricultural areas.

3.6.2. Soil Thermal Properties

Site-specific soil thermal diffusivity values (α, defined as the ratio of the thermal conductivity to volumetric heat capacity) were estimated from the continuous temperature data at the background location using a combination of the phase lag and amplitude ratio methods (Carson, 1963; van Lier and Durigon, 2012).

Figure 50. Graphical example of phase lag and amplitude attenuation with depth used to calculate site-specific soil thermal diffusivity values.

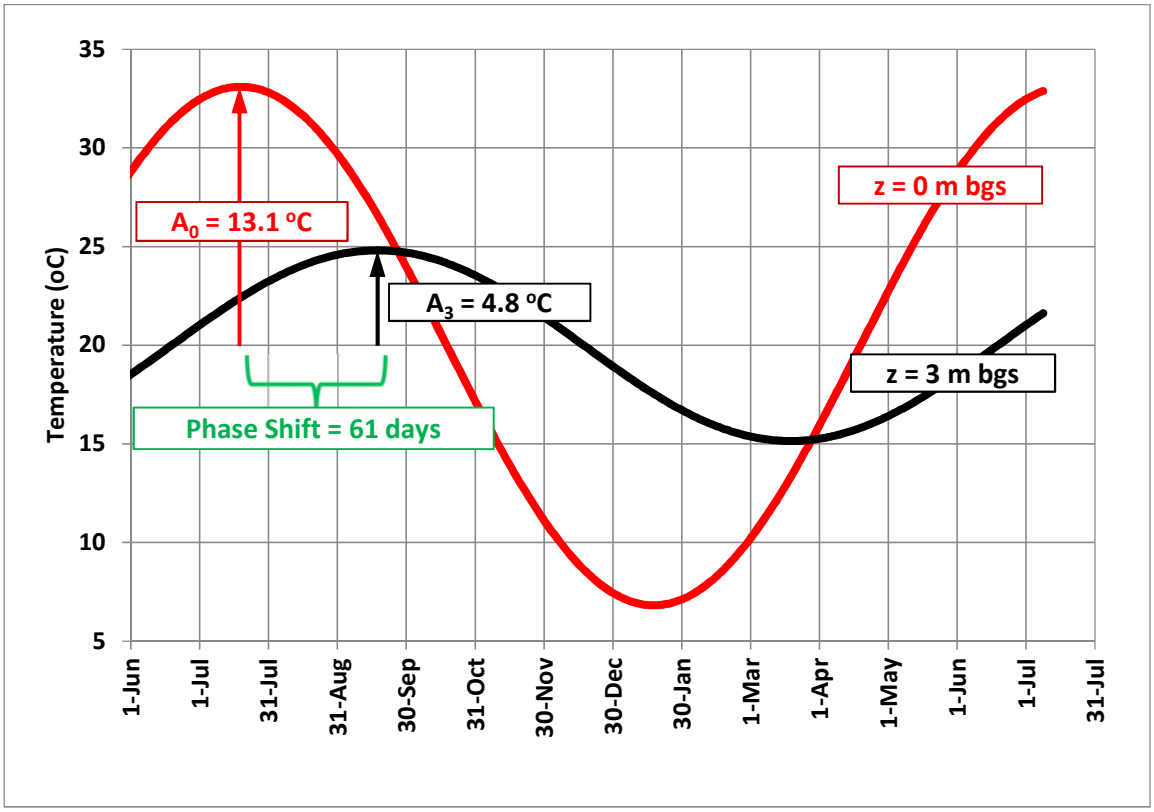

The formulas for calculating thermal diffusivity using the phase lag and amplitude ratio methods are presented as **Equations 10** and **11**, below.

$$\alpha = \frac{1}{2 \cdot \omega} \cdot \left[\frac{z_2 - z_1}{\Delta t}\right]^2$$ **Equation 10**

Where Δt is the time difference between the minimum or maximum annual temperature at depths z_1 and z_2.

$$\alpha = \frac{\omega}{2} \cdot \left[\frac{z_2 - z_1}{ln\left(A_1/A_2\right)}\right]^2$$ **Equation 11**

Where A_1 and A_2 are the amplitudes of the temperature wave (relative to T_m) at depths z_1 and z_2. A graphical example of the methods is presented in **Figure 50** (above), using data from ground surface (z = 0) and 3 m bgs collected from S-21. Thermal diffusivity values calculated from temperature data for each 1 m vertical interval of subsurface are presented in **Table 19**, below, along with thermal conductivity (K) values estimated from thermal diffusivity using an estimate of the volumetric heat capacity (C_v) of 1.44 x 10^{-6} J/m^3/K. Thermal conductivity values presented in **Table 19** represent the mean of the diffusivity values calculated using the phase lag and amplitude ratio methods.

Table 19. Site-specific thermal diffusivity estimates

Depth z (m)	Amplitude (°C)	Date of Max Temp	α (Eq. 8) (m^2/s)	α (Eq. 9) (m^2/s)	Mean α (m^2/s)	K J/m.s.K	Lithology as described in the boring logs
1	11.8	13-Aug	7.6E-07	1.5E-06	1.1E-06	1.5	Gravel in sandy-silty matrix
2	8.3	21-Aug	1.6E-06	8.3E-07	1.2E-06	1.7	More silty
3	6.2	9-Sep	9.3E-07	1.2E-06	1.0E-06	1.5	Smaller gravel and more sandy
4	4.4	27-Sep	1.0E-06	8.1E-07	9.2E-07	1.3	Gravel and fine sand
5	3.3	14-Oct	1.2E-06	1.3E-06	1.3E-06	1.8	Gravel in sandy-silty matrix
6	2.3	5-Nov	6.9E-07	7.0E-07	7.0E-07	1.0	Gravel in sandy-silty matrix
7	1.7	26-Nov	7.6E-07	9.5E-07	8.5E-07	1.2	Gravel in sandy-silty matrix
8	1.3	15-Dec	9.3E-07	2.0E-06	1.4E-06	2.0	Gravel in sandy-silty matrix (moist at 8,9 m)
9	1.0	29-Dec	1.7E-06	1.1E-06	1.4E-06	2.0	Gravel in sandy-silty matrix (water table at 9,4 m)
10	0.9	8-Jan	1.2E-06	1.3E-06	1.2E-06	1.8	Clayey silt

Discussion of temperature data analysis for the discrete, manual readings as well as for the continuous temperatures recorded using data loggers are discussed in greater detail in the following sections.

3.6.3. Manual Temperature data

The annual mean of the four manual quarterly temperature profiles registered for several monitoring wells are shown in **Figure 51**. All of the profiles have been compared against S-21 profile, considered as representative of background conditions in the subsurface.

Figure 51. Quarterly Manual Temperature Profiling Results

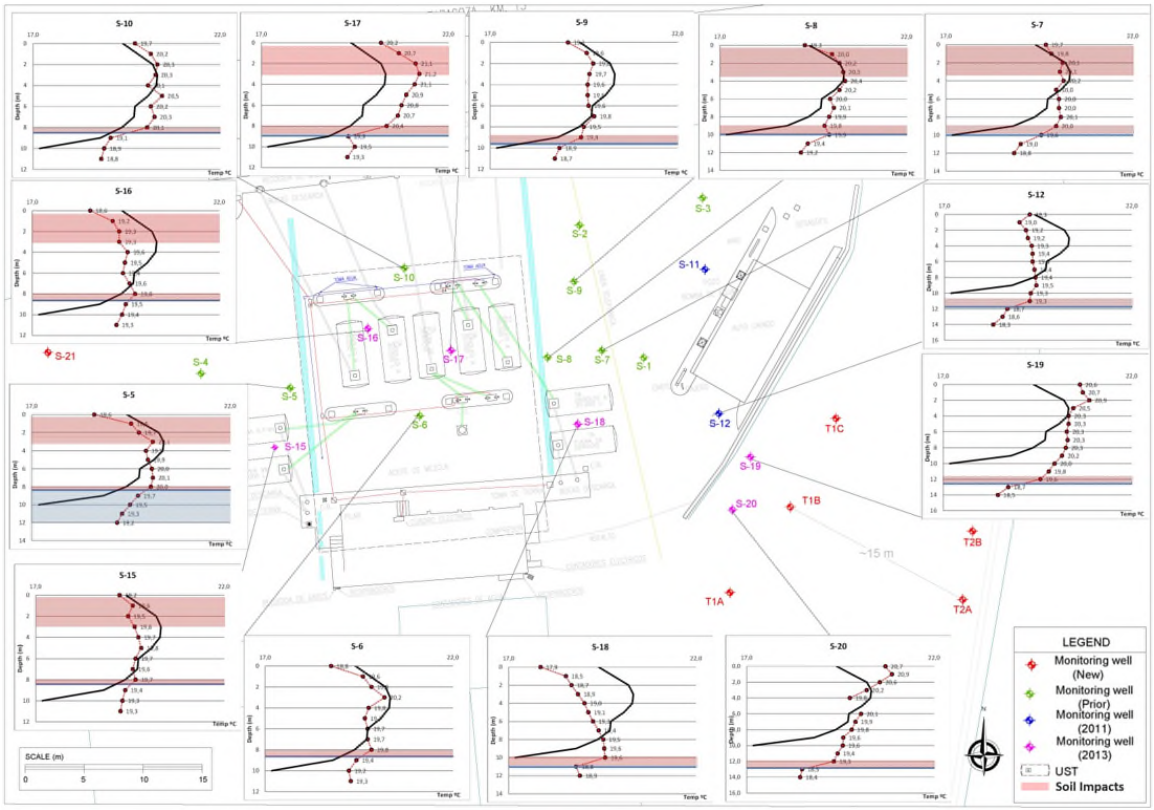

The comparison of the annual average background temperature profile and the annual average temperature profiles observed in the monitoring wells located in the source areas shows an anomalous behaviour, as higher temperatures were measured in the shallow soil column (<6 m) in the background well vs. source area wells.

There is no known hydrocarbon source in the background location that could affect the temperature profile between the surface and the depth of 6 m. The differences of solar exposition between the background and the source areas is not considered significant, since only those monitoring wells closer to buildings are affected by a diminished solar exposition. Therefore, a higher solar exposition of the background well does not explain the more elevated temperatures of the well.

Though higher surface temperatures exist within the upper portion of the vadose zone at the background well, temperatures measured in source zone locations at depths greater than 6 to 7 m (immediately above and within the LNAPL smear zone) are higher than temperatures measured in the background. On average, temperatures measured from source zone locations at a depth of 10 m bgs are 1.7 to 2.8ºC warmer than temperatures measured at 10 m bgs in the background well. This fact is consistent with biodegradation at the depth of LNAPL.

3.6.4. Methodology for Estimating NSZD Rates from Temperature Data

Using the background-corrected temperatures calculated from **Equation 12**, the upward, conductive heat flux away from the depth at which the maximum temperature difference was observed at each source zone monitoring location was calculated using Fourier's law of heat conduction (**Equation 12**):

$$q_T = K_u \cdot \left(\frac{\Delta T}{\Delta z}\right)_u + K_d \cdot \left(\frac{\Delta T}{\Delta z}\right)_d$$ **Equation 12**

Where,

q_T = Total conductive heat flux upward and downward from the depth of the maximum observed increase in temperature relative to background (watts per square meter - W/m^2)

K_u = Effective thermal conductivity of subsurface materials from depth of maximum observed increase in temperature to ground surface (watts per meter, per Kelvin - W/m/K)

K_d = Effective thermal conductivity of subsurface materials from depth of maximum observed increase in temperature to total depth of temperature measurement (W/m/K)

$\left(\frac{\Delta T}{\Delta z}\right)_u$ = Upward temperature gradient (°C/m)

$\left(\frac{\Delta T}{\Delta z}\right)_d$ = Downward temperature gradient (°C/m)

Conductive heat flux from biodegradation was estimated using thermal conductivity (K) values of 1.6 watts per meter, per Kelvin (W/m/K) based on site-specific estimates of thermal diffusivity and literature values for soil volumetric heat capacity, as described above.

Values for the upward temperature gradient were determined from differences in daily averaged source zone and background temperatures over the full study period for wells where continuous data was collected, and from average temperature values from wells where discrete, quarterly measurements were recorded. The mean temperatures were plotted and the upward slope of the temperature difference profile was calculated.

Heat flux estimates calculated from temperature gradients and thermal conductivity values were then used to estimate equivalent NAPL depletion rates based on stoichiometric relationships for the prevailing biodegradation reactions along with the heat of reaction (determined using published data for the standard enthalpy of formation, e.g., Haynes, 2012) using **Equation 13**:

$$R_{NSZD} = \frac{q_T}{\Delta H_{rxn}}$$ **Equation 13**

Where R_{NSZD} is the NSZD rate in units of grams of LNAPL per square meter, per second ($g/m^2/s$), and ΔH_{rxn} is the heat of the biodegradation reaction in joules per gram (J/g). The prevailing hydrocarbon biodegradation reactions are assumed to be methanogenesis (**Equation 14**) followed by aerobic oxidation of methane (**Equation 15**), or direct aerobic oxidation (**Equation 16**), as indicated below, where “a” and “b” represent the number of carbon and hydrogen atoms in a given hydrocarbon compound, respectively:

$$C_aH_b + \left(a - \frac{b}{4}\right) \cdot H_2O \rightarrow \left(\frac{a}{2} + \frac{b}{8}\right) \cdot CH_4 + \left(\frac{a}{2} - \frac{b}{8}\right) \cdot CO_2$$ **Equation 14**

$$\left(\frac{a}{2} + \frac{b}{8}\right) \cdot (CH_4 + 2 \cdot O_2 \rightarrow CO_2 + 2 \cdot H_2O)$$ **Equation 15**

$$C_aH_b + \left(a + \frac{b}{4}\right) \cdot O_2 \rightarrow a \cdot CO_2 + \left(\frac{b}{2}\right) \cdot H_2O$$ **Equation 16**

Using the above stoichiometric relationships and the standard heat of formation for each of the molecules involved in the reactions, the heat energy released to the surrounding formation can be calculated. The overall release of energy for either of the above pathways (**Equation 14** followed by **Equation 15**, or **Equation 16**) is equivalent, as the reactants and products are the same. A summary of molecular weights and standard heat of formation for each of the chemical compounds represented in **Equations 5** through **7** are presented below in **Table 20** (Haynes, 2012). Soil gas data (discussed in more detail below) indicate that oxygen is present near the base of the vadose zone at concentrations greater than a few vol%. This suggests that either the bulk of the depletion at this site is occurring through direct aerobic oxidation of hydrocarbons within the smear zone, or that the methanogenic zone is very thin. Based on these observations, heat inputs were estimated using values for direct aerobic oxidation only (**Equation 16**).

Table 20. Molecular weights and standard enthalpy of formation for constituents in NSZD reactions

Constituent	Molecular Weight (g/mol)	Standard Enthalpy of Formation (kJ/mol)
Hexadecane ($C_{16}H_{34}$)	226.4	-456.1
Octane (C_8H_{18})	114.2	-250.1
Water (H_2O)	18.0	-285.8
Carbon Dioxide (CO_2)	44.0	-393.5
Oxygen (O_2)	32.0	0.0
Methane (CH_4)	16.0	-74.6

Hexadecane ($C_{16}H_{34}$) was used as a representative hydrocarbon for diesel fuels (Bacha et al., 1998) to calculate NSZD rates. However, the heat released from biodegradation reactions is relatively invariant for a broad range of hydrocarbons on a mass basis, and thus selection of different representative hydrocarbons would not change the results significantly. A comparison of the heat released from oxidation (or methanogenic degradation followed by methane oxidation) for a number of aliphatic and aromatic hydrocarbon compounds is presented in **Figure 52**, below.

Figure 50. Heat of reaction for various hydrocarbon compounds

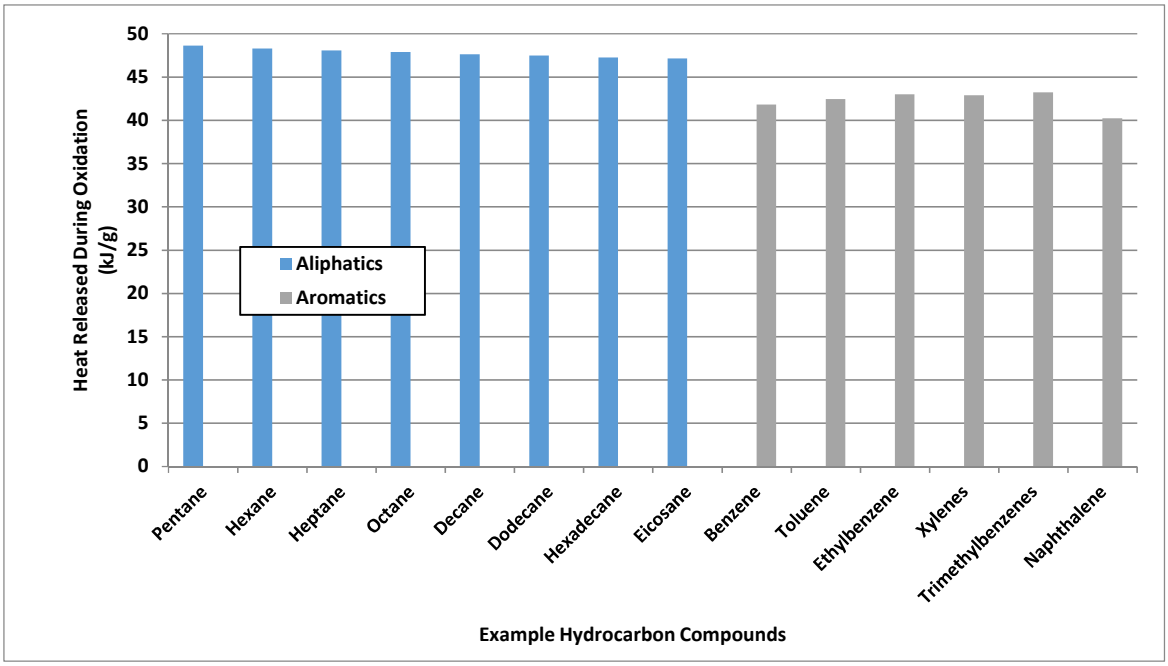

3.6.5. Results

The observation of elevated temperatures in the source zone wells provides a qualitative line of evidence that NSZD is occurring at all source zone locations included in the study. Heat flux away from zones of elevated temperature was estimated using **Equation 12** with background corrected thermal gradients and a soil thermal conductivity of 1.6 W/m/K based on site-specific estimates of soil thermal diffusivity and literature values for volumetric heat capacity. NSZD rates were calculated as described using an LNAPL density of 0.77 g/cc for the gasoline area and 0.85 g/cc for the diesel area.

The annual average increase in temperature in source zone wells (relative to the background well) were calculated using **Equation 4**. In all cases, the depth of the maximum background-corrected temperature occurred at 10 m bgs, the deepest measurement interval from the background well (S-21). Given that the maximum temperature increase was observed at the maximum depth evaluated, estimates of downward thermal gradients could not be made directly. Thus, estimates of heat flux include only the heat from biodegradation that is lost by conduction to the ground surface. Given that this approach ignores downward and lateral heat flux away from zones where heat is being generated, biodegradation rates obtained are likely conservative.

As noted above, average annual temperatures measured using the thermistor were cooler in source zone locations than at the background well within the upper 6 meters of the vadose zone. For these data, upward thermal gradients were estimated by dividing the maximum temperature difference calculated using **Equation 4** divided by the depth where the maximum annual average temperatures were observed (10 meters), as described by Warren and Bekins (2015). NSZD rates estimated from discrete, quarterly measurements range from 2,000 to 2,700 L/ha/yr, with an average value of 2,500 L/ha/yr in the gasoline area and from 1,900 to 3,200 L/ha/yr with an average value of 2,700 L/ha/yr for the diesel area.

A summary of the manual temperature profiling results are presented in **Table 21** (below).

Table 21. Summary of Manual Temperature Profiling Results

Source Zone Well ID	Annual Mean ΔT_{max} (°C)	Depth of ΔT_{max} (mbgs)	Upward Thermal Gradient (°C/m)	NSZD Rate (L/ha/yr)
Gasoline Area				
S-5	2.28	10	0.23	2,700
S-6	2.03	10	0.20	2,400
S-10	1.70	10	0.17	2,000
S-15	2.10	10	0.21	2,500
S-16	2.20	10	0.22	2,600
S-17	2.30	10	0.23	2,700
Diesel Area				
S-7	2.35	10	0.24	2,800
S-8	2.73	10	0.27	3,200
S-9	1.65	10	0.17	1,900
S-12	2.10	10	0.21	2,500
S-18	2.38	10	0.24	2,800
S-19	2.75	10	0.28	3,200
S-20	2.38	10	0.24	2,800

For the continuously recorded temperature data, the annual average temperatures recorded at each depth interval were plotted against the background temperature profile to calculate average upward thermal gradients. Temperature profiles along with fluid levels, well construction details, and results of soil screening during well installation using a photoionization detector (PID) are presented in **Figure 53**.

Figure 53. Annual mean temperature profiles recorded using data loggers in gasoline (S-5) and diesel (S-7) areas compared to background (S-21)

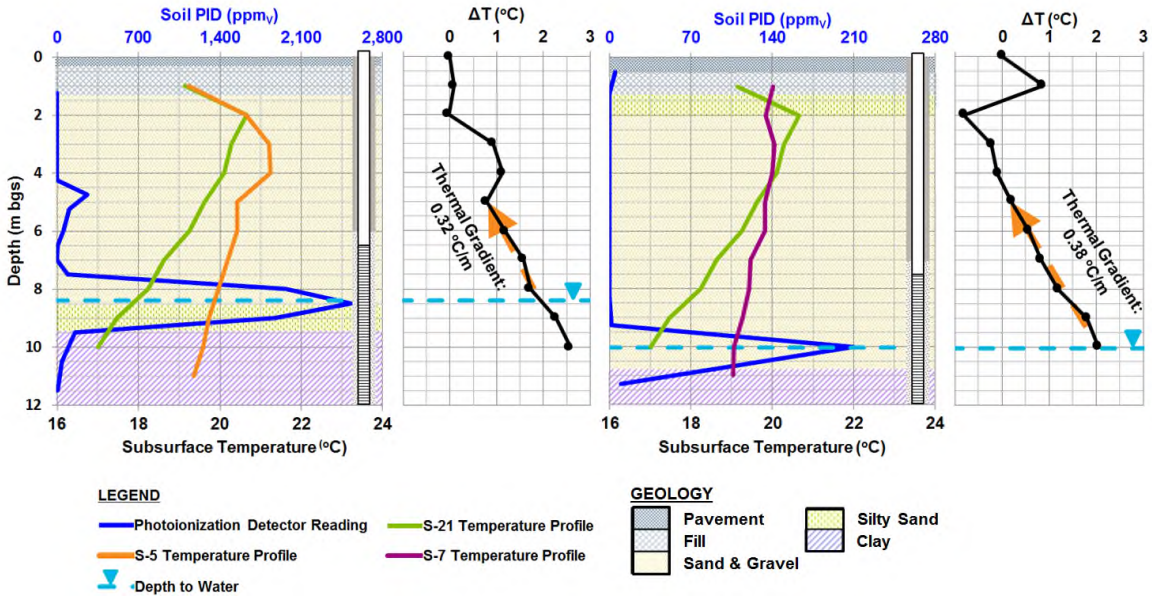

Average temperatures measured using data loggers are similar to those obtained from the quarterly snap shot measurements, with a maximum temperature increase of approximately 2.1 to 2.6°C relative to background observed at 10 m bgs. The upward thermal gradients shown on **Figure 53** are calculated over the depth range of 5 to 10 mbgs are likely representative of biodegradation occurring at the base of the vadose zone. However, temperature data from S-5 exhibits increased temperatures relative to background in the shallow vadose zone that may reflect the presence of shallow impacts, consistent with soil gas concentration gradient and CO_2 trap results from the gasoline area.

On average, continuous temperature data indicate average NSZD rates representative of the deeper hydrocarbon impacts of approximately 3,000 L/ha/yr at S-5 (gasoline area) and 3,200 L/ha/yr at S-7 (diesel area).

3.7. COMPARISON OF BIODEGRADATION RATES

The biodegradation rates have been estimated by different approaches described in detail in previous sections. These are:

- Soil gas methods, namely the rates estimated using the O_2 and CO_2 concentration gradients measured in designated multilevel soil-vapour probes and monitoring wells;
- Passive CO_2 flux traps and;
- Temperature methods based on data provided by continuous data logger sensors and manual quarterly measurement rounds using a thermistor.

The results are summarized in **Table 22**, expressed as ranges and annual average biodegradation rates provided by the different approaches at each source area and background, where applicable.

Table 22. Range of biodegradation rates estimated using different methods (L/ha/yr)

Method	Gasoline area	Diesel Area	Background
O_2/CO_2 profiles in vapor probes	85 – 490 (260)	460 – 1,500 (930)	-34 – 17 (0)
O_2/CO_2 profiles in monitoring wells	52 –2,700 (1,100)	46 – 2,900 (1,100)	-34 – 23 (0)
CO_2 traps	17,000 – 130,000 (54,000)	0-1,000 (460)	5,3 00-19,000 (12,000)
Temperature sensors	3,000	3,200	Not applicable
Temperature manual measurements	2,000 – 2,700 (2,500)	1,900 – 3,200 (2,700)	Not applicable

All methods utilized provide strong qualitative evidence that biodegradation is taking place at a significant rates at the site. While the quantitative estimates of biodegradation rates vary between methods, the results generally reflect the complexity of the processes responsible for NSZD, and the interferences that each method is subject to under the unique conditions at the site. The vertical (1-dimensional) mass and energy transport assumptions typically employed when evaluating NSZD are most appropriate when applied at sites with a consistent gas diffusion coefficient in the vadose zone, and where impacts are present at a consistent depth. By contrast, site-specific conditions include:

- pavement with abundant cracks and fissures at the ground surface,
- the presence of shallow impacts, and
- carbonate minerals in the soil matrix, which may act as a CO_2 sink.

The effects of these conditions are most evident in the soil gas concentration profiles and CO_2 trap results. The presence of shallow impacts, along with gas exchange between the atmosphere and subsurface through preferential flow pathways (e.g., cracks in the pavement) are likely responsible for the elevated NSZD rates estimated in the background and gasoline areas using the CO_2 traps and the reversal of O_2 and CO_2 concentration gradients observed between soil gas probes installed at shallow depths (approximately 1 to 1.5 m bgs), and probes installed at approximately 5 m bgs. Additionally, the low NSZD rates estimated from CO_2 traps installed in the diesel area (where shallow impacts are not present) may be the result of CO_2 reacting with carbonate minerals as it migrates upward through the vadose zone.

In general, there is relative agreement between biodegradation rates estimated for the impacts at the base of the vadose zone between the soil gas concentration and thermal gradient methods, although the rates based on O_2 and CO_2 profiles measured in designated vapour probes are lower than those provided by the rest of methods, due to the limited vertical resolution of the probes. The probes were installed at three fixed depth intervals and were not able to capture soil gas composition changes near the base of the vadose zone, where vertical soil gas concentration gradients are highest.

4. CONCLUSIONS

The main conclusions and lessons learned from this project are the following:

- A typical impervious cover at a retail station does not prevent oxygen flux in the subsurface and therefore does not stop NSZD
- NSZD measurements indicate that biodegradation processes are occurring in both source areas.
- Subsurface NSZD measurements (i.e., soil gas concentrations and temperature gradient methods) were more appropriate than the surface methods (CO_2 flux trap) at the investigated site and provided sufficient information to estimate depletion rates associated with hydrocarbon impacts at the base of the vadose zone.
- NSZD rates determined from passive CO_2 flux trap measurements for this particular site are inconsistent with the results of subsurface biodegradation rate estimation methods. However, CO_2 trap results do confirm that petroleum-derived CO_2 is being produced through biodegradation.
- While soil gas measurements, CO_2 trap results, and soil gas carbon isotope results provided evidence of lateral gas transport in the upper portion of the vadose zone, the soil gas concentration gradient method was determined to be applicable near the base of the vadose zone, where changes in soil gas composition were more representative of a vertical soil gas transport regime.
- The temperature method is less subject to interferences associated with non-1-dimensional gas transport conditions. However, interpretation of the data is affected by lateral variations in surface temperature, with the result the background well may not be a valid reference for each measurement location. Given that the amplitude of surface temperature fluctuations decreases exponentially with depth due to the diffusive nature of heat conduction (Bodri and Cermak, 2007), the method may still be applicable when the NSZD reaction zone is sufficiently deep (which is the case at this site).
- Using an annual average for the temperature method is helpful in smoothing out fluctuations and obtaining a clearer measurement of the net temperature gradient (after subtraction of the background).
- Biodegradation rates quantified by the gas and temperature methods yield comparable values.
- The use of monitoring wells for soil gas and temperature measurements provides the ability to adjust and optimize depth intervals and data density, improving quantification of NSZD rates. Readings from fixed depth intervals may miss the reaction zone and underestimate NSZD.

5. REFERENCES

1. Aelion, C.M., P. Höhener, D. Hunkeler, and R. Aravena, editors. 2010. Environmental isotopes in biodegradation and bioremediation. Taylor and Francis, Boca Raton, FL.

2. American Petroleum Institute (API). 2017. Quantification of Vapor Phase-Related NSZD Processes. Regulatory and Scientific Affairs Department, American Petroleum Institute (API), Technical Publication 4784, May 2017.

3. Askarani, K.K., E.B. Stockwell, K.R. Piontek, and T.C. Sale. 2018, Thermal Monitoring of Natural Source Zone Depletion. Groundwater Monitoring and Remediation, 38: 43-52.

4. ASTM International (2016). Standard Test Methods for Determining Biobased Content of Solid, Liquid, and Gaseous Samples using Radiocarbon Analysis, D6866-16, ASTM International, West Conshohocken, PA.

5. Bacha, J., L. Blondis, J. Freel, G. Hemighaus, K. Hoekman, N. Hogue, J. Horn, D. Lesnini, C. McDonald, M. Nikanjam, E. Olsen, B. Scott, and M. Sztenderowicz. 1998. Diesel Fuels Technical Review (FTR-2). Chevron Products Company, Chevron USA Inc., San Ramon, CA.

6. Beck, P. and Mann, B. 2010. A Technical Guide for Demonstrating Monitored Natural Attenuation of Petroleum Hydrocarbons in Groundwater. CRC CARE Technical Report No. 15. Cooperative Research Centre for Contamination Assessment and Remediation of the Environment. Adelaide, Australia.

7. Bekins, B. A., Godsy, E. M. & Warren, E. (1999) *Distribution of microbial physiologic types in an aquifer contaminated by crude oil*. Microbial Ecol. 37, 263-275.

8. Benz, S., P. Bayer, and P. Blum (2017). Global patterns of shallow groundwater temperatures. Environmental Research Letters. 12(3).

9. Bodri, L., and Cermak, V. 2007. Borehole Climatology. Elsevier Science, Ltd.

10. Carrier, W.D. 2003. Journal of Geotechnical and Geoenvironmental Engineering 129(11): 1054-56.

11. Carson, J.E. 1963. Analysis of Soil and Air Temperatures by Fourier Techniques. J. Geophys. Res. 68, 2217-32.

12. CL:AIRE, 2019. An Introduction to Natural Source Zone Depletion at LNAPL Sites. Contaminated Land: Applications in Real Environments (CL:AIRE) Technical Bulletin, TB20. https://www.claire.co.uk/information-centre/cl-aire-publications

13. Comité Euro-International du Béton (1990). CEB-FIP Model Code 1990, Bulletin d'Information, No.195, 196, Lausanne.

14. CRC CARE. 2018. Technical measurement guidance for LNAPL source zone depletion. CRC CARE Technical Report No. 44. Cooperative Research Centre for Contamination Assessment and Remediation of the Environment, Newcastle, Australia. https://www.crccare.com/publications/technical-reports

15. Davis, G.B., B.M. Patterson, and M.G. Trefry. 2009. Evidence for instantaneous oxygen-limited biodegradation of petroleum hydrocarbon vapors in the subsurface. Groundwater Monitoring & Remediation 29, no. 1: 126– 137.

16. de Jong van Lier, Quirijn & Durigon, Angelica. (2013). Soil thermal diffusivity estimated from data of soil temperature and single soil component properties. Revista Brasileira de Ciência do Solo. 37. 106-112.

17. DeVaull, G., and Rhodes, I. 2018. Estimates of Hydrocarbon NAPL Depletion from Compositional Change over Time. 26th National Tanks Conference and Exposition, September 2018, Louisville, Kentucky.

18. DeVries D.A. (1963) Thermal Properties of Soils. In W.R. van Wijk (ed.) Physics of Plant Environment. North-Holland Publishing Company, Amsterdam.

19. Ferguson, Grant & D. Woodbury, Allan. (2007). Urban heat island in the subsurface. Geophy Res Lett 34(23). Geophysical Research Letters - GEOPHYS RES LETT. 34. 10.1029/2007GL032324.

20. Galperin, Y., and Kaplan, I., Review of Microbial Processes in the Near-Surface Environment and Their Implications for the Chemical Fingerprinting of Hydrocarbon Fuels, Environmental Forensics 12:236-252, 2011.

21. Garg, S., Newell, C. J., Kulkarni, P. R., King, D. C., Adamson, D. T., Renno, M. I. and Sale, T. (2017), Overview of Natural Source Zone Depletion: Processes, Controlling Factors, and Composition Change. Groundwater Monit R. doi:10.1111/gwmr.12219

22. Haynes, W.M. 2012. CRC Handbook of Chemistry and Physics, 93rd Edition. CRC Press

23. Hua, F., and H.Q. Wang. 2014. Uptake and trans-membrane transport of petroleum hydrocarbons by microorganisms. Biotechnology & Biotechnological Equipment 28: 165– 175.

24. Interstate Technology & Regulatory Council (2009) Evaluating Natural Source Zone Depletion at Sites with LNAPL. April 2009.

25. ITRC (Interstate Technology & Regulatory Council). 2018. LNAPL *Site Management: LCSM Evolution, Decision Process, and Remedial Technologies*. LNAPL-3. Washington, D.C.: Interstate Technology & Regulatory Council. LNAPL Update Team. https://lnapl-3.itrcweb.org.

26. Johnson, P., P. Lundegard, and Z. Liu. 2006. Source zone natural attenuation at petroleum hydrocarbon spill sites: Site-specific assessment approach. Ground Water Monitoring & Remediation 26, no. 4: 82-92.

27. Kooi, H. 2008. Spatial variability in subsurface warming over the last three decades; insight from repeated borehole temperature measurements in The Netherlands. Earth & Planetary Science Letters, 270, 86-94.

28. Lundegard, P. and Johnson, P. 2006. Source zone natural attenuation at petroleum hydrocarbon spill sites – II: Application to a former oil field. Ground Water Monitoring & Remediation 26, no. 4: 93-106.

29. Lundegard, P.D., R.E. Sweeney, and G.T. Ririe (2000). Soil Gas Methane at Petroleum Contaminated Sites: Forensic Determination of Origin and Source. *Environmental Forensics*, 1:3-10.

30. Lundy, D. 2014. An Investigation of the Relationship Between Lateral Spreading and Mass Depletion of an LNAPL Body in Contact with Groundwater at the Bemidji, MN Crude Oil Release Site. In partial fulfilment of the requirements for the Degree of Doctor of Philosophy. University of Georgia, Athens, Georgia.

31. Lyman, W.J., Reidy, P.J., Levy, B. 1992. *Mobility and Degradation of Organic Contaminants in Subsurface Environments*. C.K. Smoley, Inc., Chelsea, MI.

32. Mahler, N., T. Sale, and M. Lyverse. 2012. A Mass Balance Approach to Resolving LNAPL Stability. *Ground Water* 50 (6):861-71.

33. McCoy, K., J. Zimbron, T. Sale, and M. Lyverse. 2014. Measurement of Natural Losses of LNAPL

34. Using CO2 Traps. Groundwater. doi: 10.1111/gwat.1240.

35. Meckenstock, R.U., F. von Netzer,, C. Stumpp, T. Lueders, A. Himmelberg, N. Hertkorn, P. Schmitt-Kopplin, M. Harir, R. Hosein, S. Haque, and D. Schulze-Makuch. 2014. Water droplets in oil are microhabitats for microbial life. Science 345:673-676.

36. Mohr, D.H. and P.H. Merz (1995). Application of a 2D Air Flow Model to Soil Vapor Extraction and Bioventing Case Studies. Groundwater, 433-444, May-June, 1995.

37. Monteith, J.L. 1973. Principles of Environmental Physics. Edward Arnold Pulishers, Ltd., London, England.

38. National Research Council, 1993. Ground Water Vulnerability Assessment: Predicting Relative Contamination Potential Under Conditions of Uncertainty. Washington, D.C.: National Academy Press.

39. National Research Council (NRC). 2013. Alternatives for Managing the Nation's Complex Contaminated Groundwater Sites. In *Division on Earth and* Life *Studies. National Academy of Sciences*, edited by Water Science and Technology Board Committee on Future Options for Management in the Nation's Subsurface Remediation Effort. Washington, D.C.: National Research Council.

40. Newell C.J., S.D. Acree, R.R. Ross, S.G. Huling. 1995. Light Non-Aqueous Phase Liquids. EPA-540-5-95-500, United States Environmental Protection Agency, Office of Research and Development, Robert S. Kerr Laboratory, Ada, OK, 1995.

41. Ng, G.-H.C. , B.A. Bekins , I.M. Cozzarelli , M.J. Baedecker , P.C. Bennett , and R.T. Amos . 2014. A mass balance approach to investigating geochemical controls on secondary water quality impacts at a crude oil spill site near Bemidji, MN . Journal of Contaminant Hydrology 164: 1– 15.

42. Rice, D. W., R. G. Grose, J. C. Michaelsen, B. P. Dooher, D. H. MacQueen, S. J. Cullen, W. E. Kastenberg, L. G. Everette, and M. A. Marino, 1995. California Underground Leaking Fuel Tank (LUFT) Historical Case Analyses," Report submitted to the California State Water Resources Control Board and Senate Bill 1764 Advisory Committee, Nov. 16, 1995.

43. Ririe, T.G., R.E. Sweeney, and B. Tallant (2013). Use of Temperature to Determine Rate of Biodegradation in the Vadose Zone. Presentation at the Third International Symposium on Bioremediation and Sustainable Environmental Technologies in Jacksonville, FL, Battelle Memorial Institute, June 10-13, 2013.

44. Sihota, N.J., O. Singurindy, and K.U. Mayer. 2011. CO_2-efflux measurements for evaluating source zone natural attenuation rates in a petroleum hydrocarbon contaminated aquifer. Environmental Science and Technology 45, no. 2: 482-488.

45. Subramanian, S., R.E. Sweeney, T. Ririe, and D. Tsao (2011). High Temperature Anomaly During AS/SVE Operation at a Former Refinery. Presentation at the First International Symposium on Bioremediation and Sustainable Environmental Technologies in Reno, NV, June 27-30, 2011.

46. Sweeney, R.E, and G.T. Ririe. 2017. Small Purge Method to Sample Vapor from Groundwater Monitoring Wells Screened Across the Water Table. Ground Water Monitoring and Remediation, 37 (4), 51–59.

47. Sweeney, R.E, and G.T. Ririe. 2014. Temperature as a Tool to Evaluate Aerobic Biodegradation in Hydrocarbon Contaminated Soil. Ground Water Monitoring and Remediation, 34 (3), 41–50.

48. Warren, E., and B.A. Bekins. 2015. Relating Subsurface Temperature Changes to Microbial Activity at a Crude Oil-contaminated Site. Journal of Contaminant Hydrology, 182 (2015) 183-193.

49. Whyte, L.G., Slagman, S.J., Pietrantonio, F., Bourbonniere, L., Koval, S.F., Lawrence, J.R., Inniss, W.E., and Greeg, C.W., *Physiological Adaptations Involved in Alkane Assimilation at a Low Temperature by Rhodococcus sp. Strain Q15,* Applied and Environmental Microbiology Vol. 65 No. 7, July, 1999.

50. Wiedemeier, T.H., H.S. Rifai, C.S. Newell, and J.T. Wilson. 1999. Natural Attenuation of Fuels and Chlorinated Solvents in the Subsurface. John Wiley and Sons Ltd., New York.

ANNEXES

Download the Report Annexes here.

Concawe
Environmental Science
for European Refining

Concawe
Boulevard du Souverain 165
B-1160 Brussels
Belgium

Tel: +32-2-566 91 60
Fax: +32-2-566 91 81
e-mail: info@concawe.org
http://www.concawe.eu

ISBN 978-2-87567-125-7